Investigating the role of ROS in eliciting mitochondrial retrograde response during *Drosophila* cardiogenic mesoderm specification events

Thesis

Submitted
By

Swati
PH10056

For the award of the degree of

Doctor of Philosophy

Department of Biological Sciences
Indian Institute of Science Education and Research (IISER) Mohali
Sector-81, Mohali-140306, Punjab, India

December, 2018

Dedicated to my family

Declaration

The work presented in this thesis entitled "Investigating the role of ROS in eliciting mitochondrial retrograde response during *Drosophila* cardiogenic mesoderm specification events" has been carried out by me under the supervision of Dr. Sudip Mandal at the Indian Institute of Science Education and Research (IISER) Mohali. This work has not been submitted in part or full for a degree, a diploma, or a fellowship to any university or institute. Whenever contributions of others are involved, every effort is made to indicate this clearly, with due acknowledgement of collaborative research and discussions. This thesis is a bona fide record of original work done by me and all sources listed within have been detailed in the references.

Date: Swati

Place: (Candidate)

In my capacity as the supervisor of the candidate's thesis work, I certify that the above statements by the candidate are true to the best of my knowledge.

Date: Dr. Sudip Mandal

Place: (Supervisor)

Acknowledgements

I would like to acknowledge Dr. Sudip Mandal to give me this wonderful opportunity to dive in the interesting field of developmental biology. I sincerely want to offer my gratitude to Dr. Lolitika Mandal who trained me in embryo handling and processing.

I would like to thank my lab mates who were always there to guide and cheer me up during times of failures and hardships.

I would like to offer gratitude to IISER Mohali and CSIR, India for providing me financial support and necessary facilities.

Most importantly, none of this work would have been possible without the unconditional love and support of my family. I thank God to give me the most loving and supporting partner who stood with me during all the testing times like a rock.

Swati

May, 2018

Contents

Synopsis

Introduction:

Congenital Heart Diseases (CHDs) are major cause of prenatal and neonatal mortality. These defects occur due to abnormalities during heart formation in utero. The treatments of CHDs pose a major challenge due to lack of in depth understanding of underlying factors. There are certain evidences that suggest abnormal mitochondrial function in these cardiomyopathies. A large percentage of prenatal dilated cardiomyopathies reportedly exhibit defects in mitochondrial oxidative phosphorylation. However, we still have a very little understanding of causal role played by mitochondria in CHDs. Considering the fact that heart has highest density of mitochondria followed by skeletal muscles and central nervous system, investigation of mitochondrial involvement in CHDs is a very intriguing question.

Extensive research has not been done in this area, main reason being lack of a suitable model system to answer the underlying question that whether metabolic dysfunction can directly hit the developmental programs and circuits at the specification level. Most aspects of this question remain unanswered because mitochondria fuels all the biochemical pathways in a cell and targeting mitochondria for epistasis studies is a different ball game than targeting a developmental gene. Mitochondria is a very dynamic organelle per say if we try to create a pool of dysfunctional mitochondrial population by knocking down some components of ETC, they combat this through fusion- fission mechanisms so that damaged components of mitochondria are replenished by healthy one and the whole mitochondrial network works fine for a longer time. Hence, it takes relatively more amount of time until the pool of bad mitochondria is accumulated to a level that mitochondrial function restoration is not possible for the system.

Second thing is, even in that scenario, when a bad mitochondrial population is created; system can crash completely as ATP is required to fuel each and every step of any signal transduction pathway. Therefore, it is not trivial to get an observable phenotype by mutating mitochondrial components.

The *Drosophila* embryonic heart is termed as dorsal vessel. It is a simple contractile tube which is similar to the tubular heart of early vertebrate embryo. Despite the evolutionary distance between

Drosophila and vertebrates, cardio genesis is governed by similar fundamental mechanisms. The transcription factors as well as signalling pathways involved in cardio genesis are highly conserved among *Drosophila* and vertebrates. Dorsal vessel is comprised of merely104 cardio blasts; an extremely simple organ; hence enables pinpointing any minor cardiac deformity. The anterior portion is termed aorta whereas posterior portion is termed Heart proper. Hemolymph flows from posterior to anterior of the dorsal vessel. The posterior portion has specific subset of cardio blasts that form the inflow tracts termed as Ostia. Dorsal vessel has segmental repeated pattern of cell types which is a hallmark of insects. The cardio blasts are flanked by pericardial cells which function as nephrocytes.

Drosophila can prove to be a good model system to understand cardiac development and function, which can open new doors to understand cardiomyopathies and improve their treatment.

Objectives:

The specific objective of this study was to establish a model system to study key role, if any, of complex-I of ETC in causing CHDs and to investigate whether metabolic perturbations target developmental programs during cardiogenic specifications. Further, we wanted to investigate what anomalies are created by perturbing ETC during cardiogenic mesoderm formation and what are the mediators of dysfunctional ETC to elicit retrograde response from mitochondria to nucleus.

Outcome of this study:

Establishment of a model system to study metabolic dysfunction induced congenital heart diseases in *Drosophila* embryos

In order to perturb mitochondrial complex-I activity during embryonic development, two components of complex-I of ETC; ND75 which is the largest core subunit of complex-I and ND42, an accessory subunit required for the assembly of complex-I of ETC were knocked down at different temporal and spatial windows and embryos were observed for lethality in terms of hatching rate.

We used 4 Gal4 lines Tincar**Δ**4 Gal4, Hand Gal4, Mef2 Gal4 and Twist Gal4 to knock down ND42 and ND75 from the developing mesoderm. Tincar and Hand are relatively late stage drivers whereas Mef2 and Twist are early drivers. No significant embryonic lethality was observed with Tincar, Hand and Mef2 Gal4 drivers. However severe embryonic lethality was observed in F1 generation embryos

by knocking down ND42 and ND75 with Twist Gal4. Twist Gal4 is the early mesoderm Gal4 driver. Its expression starts at stage 4 when mesoderm begins to form. Live imaging of these embryos indicate cardiac malfunction at stage 17 of embryonic development. Quantitative analysis of cardiac parameters using SOHA (Semi-automated Heartbeat Analysis) confirmed the cardiac defects with respect to different parameters for example Heart rate, Heart period, systole-diastole diameters and systole -diastole intervals. Notably, cardiac fibrosis like condition was also observed in these embryos as revealed by Pericardin. Pericardin is a type IV collagen like protein that is expressed majorly by pericardial cells, therefore marking the boundaries of cardiac tube at stage 16. Its expression was increased and mis-localized to the lumen of knock down embryos.

We therefore established *Drosophila* embryonic heart as a model system to study metabolic dysfunction induced CHDs, thereby opening new doors to investigate and unravel the unexplored aspects in this field.

ROS mediated retrograde response from mitochondria targets cell fate specification during cardio genesis in *Drosophila* embryos

We further investigated the cardiac defect in knock down embryos at cellular level and we found an intriguing cell specification defect at stage 16 of embryonic development. In wild type stage 16 embryo, cardiac tube is formed of 4 Tinman positive and 2 Seven up positive cardio blasts in each hemi segment. However, in complex-I mutant embryos, we found that this 4+2 pattern of cardio blasts is altered to 2+4 pattern. By tracking this phenotype to the earlier stages, we found that this change in cell identity initiates at stage 13 where some of Tinman positive cells begin to lose Tinman expression and ectopically begins to express Seven up. Therefore, ***identity of cells is changed due to metabolic disturbances***.

Since ND42 and ND75 are complex-I components, in order to investigate the underlying cause for these cardiac defects, ATP assay was performed as perturbing ETC at the first step might lead to ultimate end result of the ETC i.e. generation of ATP. However, we found no significant drop in ATP levels in knock down embryos relative to control. The other most prominent factor that might get altered due to complex-I malfunctioning was ROS level as hampering complex-I leads to more free electrons in the system, which reacts to oxygen to form superoxide and subsequently peroxide ions. In complex-I knockdown embryos, ROS levels were indeed found to be high as indicated by mitoSOX dye and gstD GFP reporter line. Co-immunostaining of Twist protein and gst D GFP

showed that ROS levels are only increased in the Twist expressing mesoderm cells at stage 10 of embryonic development, suggesting that knockdown of ND42/ND75 using Twist GAL4 has resulted in elevated ROS levels in mesodermal population.

We were able to establish ROS as the key mediator to elicit retrograde response from mitochondria to regulate cell fate specification since over-expression of SOD2 in the background of ND42/ND75 knockdown was able to significantly rescue embryonic lethality, cardiac malfunctioning and cell fate specification defects.

High ROS levels in the mesoderm cause severe cell number reduction in Embryonic Lymph Gland

Cellular characterization of dorsal vessel of ND42/ND75 knock down embryos revealed that Lymph Gland which is also of mesoderm origin exhibit severe reduction in cell number as observed at stage 16 of embryonic development. As compared to control that has average 22 cells per lobe, cell number is declined to average 10-12 cells per lobe in ND42/ND75 knockdown embryos. For these studies, we also focused on PINK1B9 mutants and PINK1 knockdown embryos since PINK1 that is a PTEN induced kinase is reported to phosphorylate ND42 of complex-I of ETC. Therefore, it indirectly affects complex-I of ETC. Interestingly, we found the same trend in PINK1 knockdown embryos.ROS reporter gst D GFP was high in the developing mesoderm in the background of ND42/ND75 and PINK1 knockdown. Over expression of SOD2 in these 3 knockdown backgrounds was able to significantly rescue cell number in lymph gland as well as ROS levels, establishing ROS as the key mediator to elicit this response.

Conclusion:

My research has opened a new door in the field of CHDs investigations that occur due to metabolic disturbances. I have successfully created complex-I deficit in the developing cardiogenic mesoderm that resulted in altered cardiac functionality, a model system to study underlying cause of CHDs in such conditions. A significant accomplishment in this direction is to discover that knock down of genes encoding components of complex-I of ETC lead to alteration in cell fate specification during cardiogenesis. My thesis also throws light on pivotal role of ROS in eliciting retrograde response from mitochondria to nucleus to regulate cell fate decisions. Last but not least, I have also shown the causal role of high ROS levels in regulating cell number of embryonic lymph gland. Given the high conservation of TFs and molecular mechanisms regulating cardio genesis and hematopoiesis in

Drosophila and vertebrates, the outcome of my thesis can open new doors in the field of metabolic regulation of developmental programs.

Submitted by

Swati

(PH10056)

Chapter: 1

Introduction

1.1 Congenital Heart Defects:

Congenital heart defects (CHD) are structural and functional abnormalities in heart structure that occur before birth. Approximately 8 out of 1000 newborns have CHDs ranging from mild to severe. Congenital heart defects occur due to incomplete or abnormal development of fetus heart during the early weeks of pregnancy (Peterson et al., 2014). Some CHDs are known to be associated with genetic disorders such as Down syndrome (Benhaourech et al., 2016). However, the cause of most of them is unknown. Investiga*ting* the mechanism by which these abnormalities happen during early embryonic development might have an impact on clinical management of these congenital malformations.

Symptoms of CHDs include shortness of breath, fatigue, limited ability to do exercise and abnormal sounds of heart murmur diagnosed by the physician while listening to the heart beats. Various methods used to detect CHDs are echocardiogram, electrocardiogram, chest X-ray and MRI methods (Wren et al., 2008).

1.2 Types of Congenital Heart Defects:

Congenital heart defects can be categorized into 3 main categories:

- **Heart valve defect**: In these types of CHDs, the valves that direct blood flow inside the heart may close up or leak. Therefore, the ability of the heart to pump blood is hampered. Some CHDs included in this category are Stenosis, Regurgitation, Atresia and Ebstein's anomaly
- **Heart wall defect:** In these types of defects, natural walls between different sides and chambers of the heart do not develop correctly; therefore backflow of blood is not restricted. These defects exert high pressure on the heart and result in high blood pressure. Some of the CHDs included in this category are Atrial Septal Defect, Ventricular Septal Defect and Complete Atrioventricular Canal Defect

- **Blood vessel defect:** These defects are due to the malfunctioning of arteries and veins that carry blood to the heart and back out to the body. Therefore, blood flow is blocked leading to various health complications. Some of the examples include Patent ductusarteriosus, and Truncusarteriosus.

1.3 Metabolic dysfunction induced CHDs:

There are certain metabolic factors that are known to increase the risk of having CHDs, however, no obvious cause is identified in most cases.

The primary congenital cardiomyopathies occur commonly in the cardiac muscle, with abnormal cardiac metabolism apparent soon after birth or early infancy. Abnormalities (mutations/ knock out/ failed transcription) of mitochondrial DNA and/or nuclear genes encoding proteins involved in mitochondrial oxidative phosphorylation are also evident in cardiomyopathies(Giordano, 2005).

Particularly, complex-I, III and IV of Electron Transport Chain present on the inner membrane of mitochondria are reported to be involved in various cardiomyopathies (Scheubel et al., 2002).

Metabolic pathways in the developing cardiac tube are finely tuned and disruption of maturation of these pathways can lead to cardiomyopathies in early life (Liesa et al., 2009). The bioenergetics maturation i.e. the switch from anaerobic glycolysis to mitochondrial respiration to generate ATP and mitochondrial structural evolution from smooth round cristae to well formed tubular cristae starts well before birth and con*tin*ues as the organism matures. The bioenergetics maturation in the developing heart is not very well explored. We still have very little understanding of the role of bioenergetics in cardiac development. However, it is the area of utmost relevance as bioenergetics maturation is an important part of cardiomyocyte differentiation.

The defects in mitochondrial OXPHOS have been reported to be one of the leading cause of prenatal and neonatal cardiomyopathies (Gibson et al., 2008). Most often, neonatal cardiomyopathies lead to fatal heart failure, although they may eventually progress into dilated form, improve or even regress completely (Finsterer, 2009; Lev et al., 2004). The

pathophysiological mechanisms by which these cardiomyopathies occur are complex. Complex-I deficiency is regarded as the most common defect associated with metabolic defects induced cardiomyopathies (Yaplito-Lee et al., 2007). Complex-I is the first, largest and most complicated respiratory complex of ETC in mitochondria that oxidizes NADH transferring electrons to ubiquinone. It is the primary entry point for electrons into the mitochondrial respiratory chain and thereby plays an essential role in generating mitochondrial membrane potential. Complex-I is also a major source for generating ROS. Mutations of two nuclear genes *NDUFV2* and *NDUFS2* encoding complex-I subunits have been strongly linked with early onset hypertrophic cardiomyopathies. These mutations caused a marked decrease in the amount of nuclear-encoded subunits and complex-I activity (Benit et al., 2003). Mutation in *NDUFV2* has also been linked to Parkinson's disease, an association that may illustrate the large variety of clinical expression of mitochondrial disorders(Nishioka et al., 2010).

In a lamb model of CHD with increased PBF (Pulmonary blood flow), the mechanism involved loss of carni*tin*e homeostasis due to loss of NO signaling thereby leading to pulmonary endothelial dysfunction (Sharma et al., 2013). It has also been reported that impairment of mitochondrial DNA replication facilitates heart failure in ventricular hypertrophic condition (Reddy et al., 1995).

Although the involvement of mitochondria in cardiomyopathies is known, we have a little insight into underlying components and molecular processes that orchestrate these defects. Recent advances in stem cell research and in the growing field of systems biology provide a tremendous amount of new data leading to new hypothesis and to new heart disease gene candidates that may also have potential roles during heart formation and establishment of cardiac function. Usually, these hypotheses are tested in cell-based assays that have their own particular set of limitations.

1.4Homology between *Drosophila* and vertebrate heart

Drosophila melanogaster has been proved to be a good model organism to study basic mechanisms of cardiac development, cardiac function and disease.

By looking at the tubular heart in *Drosophila* and multi-chambered heart in vertebrates, it is hard to find any similarity in terms of structure as well as function in both of them. However, if we look at the events involved in the formation of vertebrate multi-chambered heart, it is

interestingto find that many of the same signals, families of transcription factors and regulatory circuits operate during cardiogenesis in *Drosophila* and vertebrates.

1.4a *BMP and Dpp*:

Heart in vertebrates, as well as *Drosophila*, is derived from a subpopulation of mesodermal precursor cells, however, vertebrate heart is derived from ventral mesodermal cells in contrast to dorsal mesoderm cells in *Drosophila*(Bodmer, 1995). These ventral mesodermal cells become committed to cardiogenic fate in response to BMP expressed in the endoderm adjacent to the heart forming region (Andree et al., 1998; Schultheiss et al., 1997). Similarly, in *Drosophila*, BMP homolog *Dpp*from the overlying adjacent ectoderm induces cardiogenic mesoderm formation adjacent to the overlying ectoderm (Bodmer, 1995).

1.4b*Nkx2.5 and Tinman*:

Nkx2.5 is a vertebrate ortholog of *Tinman*(*Tin*) and is expressed in cardiogenic mesoderm starting from lineage specification till adulthood (Komuro and Izumo, 1993; Lints et al., 1993). Both of these genes have a very dynamic expression pattern and their expression is regulated by different enhancers during different stages of heart development (Schwartz and Olson, 1999). One of the early Nkx2.5 cardiac enhancers is activated by BMP signaling (Liberatore et al., 2002) similar to *Tin*B enhancer activation by ectodermal *Dpp* signaling in flies. Nkx2.5 and *Tinman* have structural and functional similarities. Importantly, ectopic expression of Nkx2.5 is capable of rescuing visceral mesoderm formation in *Tin* mutants.However it is incapable of compensating heart function in *tin* mutants (Park et al., 1998; Ranganayakulu et al., 1998). Nkx2.5 fails to rescue heart development due to the presence of a unique N-terminal domain in *Tin* which, when transferred to Nkx2.5, results in the chimeric protein capable of rescuing heart and visceral muscle fate (Liberatore et al., 2002).

1.4c GATA and Pannier:

Pannier is a GATA transcription factor in *Drosophila* and is activated by *Tinman*. Pannier then collaborates with *Tinman* to activate *Mef2* which is required for heart differentiation(Lovato et al., 2015). Similar to *Drosophila*, GATA and *Mef2* families of transcription factors play a crucial role in cardiomyocyte differentiation in vertebrates(Jiang and Evans, 1996). In vertebrates, three members of the GATA family are expressed in cardiac lineage: GATA 4, 5 and 6 (Jiang and Evans, 1996; Laverriere et al., 1994). GATA factors have shown to form complexes with Nkx2.5

and *Mef2* transcription factors to regulate downstream cardiac genes (Durocher et al., 1997; Lee et al., 1998b; Sepulveda et al., 1998).

1.4dHAND and eHAND:

In *Drosophila*,there is a single *Hand* gene which has been shown to be required for the formation of dorsal vessel as well as lymph gland. *Hand* expression is regulated by *Tinman* and Pannier in cardioblasts and by Serpent in the lymph gland (Han and Olson, 2005). T-box transcription factors are also shown to regulate *Hand* expression during cardiogenesis(Han and Olson, 2005). In vertebrates, d*HAND* and e*HAND* are expressed initially in the entire linear tube but are later restricted to right and left ventricular chambers (Srivastava and Olson, 2000). *HAND* in vertebrates is also shown to be regulated by GATA transcription factors (McFadden et al., 2000).

1.4e H15 and TBX5:

In *Drosophila*, H15 is expressed in cardioblasts and has been shown to be crucial for proper tube formation and cardioblasts alignment (Griffin et al., 2000). In vertebrates, The T-box transcription factor Tbx5 is expressed inthe developing heart and acts synergistically with Nkx2.5to activate the *atrial natriuretic factor* (*ANF*) and *connexin 40* genes (Bao et al., 1999; Durocher et al., 1997). Mutations in *Tbx5* in mice and humans result in severe abnormalities in posterior segments of the heart that includeatrial and ventricular septal defects and conductionabnormalities(Basson et al., 1999).

1.4f Conservation in terms of signaling pathways involved in cardiogenesis:

1) FGF signaling in mesoderm migration:

In *Drosophila*, during gastrulation, two FGF8 ligands *Pyramus* and *Thisbe* are expressed in broad domains in the ectoderm. Mesodermal cells express FGFR named *Heartless* at this stage which responds to these signals by migrating in a dorsolateral direction until they have formed a monolayer that reaches as far as the dorsal layer of (Beiman et al., 1996; Gisselbrecht et al., 1996; Gryzik and Muller, 2004; Imam et al., 1999; Michelson et al., 1998; Shishido et al., 1997; Stathopoulos et al., 2004; Vincent et al., 1998).In mammalian embryos, there is an analogous requirement of FGFR-mediated mesoderm migration. In gastrulaitng mouse embryos, FGFR1 is ocncentrated in the posterior mesoderm and is maintained in migrating mesodermal wings (Rossant et al., 1997; Yamaguchi et al., 1992).

Dpp signaling in establishment of cardiogenic mesoderm:

After mesoderm migration, *Dpp* signaling plays a very critical role in cardiogenic mesoderm determination by regulating the expression of *Tinman*, an NK homeodomian encoding gene necessary for the development of dorsal mesoderm derivatives(Frasch, 1995; Reim and Frasch, 2005). In mouse embryos homozygous for Bmp-2 null mutation, no heart is formed at all, indicating a critical role played by BMP signaling in vertebrate cardiogenesis(Schultheiss et al., 1997; Somi et al., 2004). At the stage of heart formation, when cells are located in two bilateral regions in the anterolateral part of chicken embryos, BMP4 and BMP7 are expressed by the adjacent ectoderm while BMP2 and BMP5 are expressed by adjacent endoderm (Schultheiss et al., 1997; Somi et al., 2004). The expression of these BMPs persit until and beyond the onset of Nkx2.5 expression and the fusion of cardiac precursors into the heart tube.

Wingless signaling in cardiogenic mesoderm specification:

The intersection of *Dpp* and wingless expressing domains specify cardiogenic mesoderm (Borkowski et al., 1995; Lockwood and Bodmer, 2002) in *Drosophila*. In vertebrates, temporally regulated canonical Wnt signaling involving Wnt3a and β-catenin specify cardiogenic mesoderm (Lindsley et al., 2006).

Restriction of cardiogenic mesoderm by *Notch* signaling:

Signaling through *Notch* receptor restricts the number of cardiac progenitors that are specified in the dorsal mesoderm. Eliminating *Notch* using a temperature-sensitive allele during this cardiac mesoderm specification stage results in embryos with significantly larger numbers of every cardiac cell type (Hartenstein et al., 1992; Mandal et al., 2004).*Notch* signaling has a similar restrictive effect on cardiogenic mesoderm specification in vertebrates. In *Notch* knock outs and Suppressor of Hairless activated and dominant negative versions, it has been shown that *Notch* signaling led to ES cells adopting neuroectodermal and not cardiogenic fates (Lowell et al., 2006; Schroeder et al., 2003)

1.5 An overview of cardiogenesis in *Drosophila:*

The development of *Drosophila* embryonic heart, termed as Dorsal Vessel, is a cascade of tightly regulated developmental decisions. Dorsal vessel originates from the mesoderm. Formation of mesoderm initiates with nuclear localization of maternally derived Rel domain transcription factor *Dorsal* in response to cues laid down in the oocyte (Roth et al., 1989; Rushlow et al.,

1989; Steward, 1989).At the ventral side of developing embryo, *Dorsal* activates the expression of zygotic regulatory genes *Twist* and *Snail* which are required for specification and morphogenesis of the mesoderm (Jiang and Evans, 1996; Lep*tin*, 1991; Pan et al., 1991; Thisse et al., 1991).Subsequently, mesodermal cells invaginate and spread laterally to form a monolayer beneath the overlying ectoderm. This mesoderm specification event that occurs at stage 5 of embryonic development coincides with the expression of *Tinman, Nkx2.*5 homeodomain transcription factor throughout the mesoderm. By stage 8, the mesoderm further invaginates and spread dorsally along the inside of ectoderm. At stage 9 of embryonic development, *Dpp* signaling from the dorsal ectoderm instructs only dorsal mesoderm which is in direct contact with ectoderm to retain *Tinman* expression (Fig.1.1A). At stage 11 of embryonic development, the visceral mesoderm precursors move to the interior of the embryo, leaving only the *Tin*-expressing heart precursors close to the epidermis. At this stage, low and high *Tinman* expressing regions come into the picture along with the specification of cardiac progenitors (Fig.1.1B). A subset of cardioblasts begins to lose *Tinman* expression and starts to express *Seven up* at this stage. During dorsal closure (stage 12), this subset of cardioblasts becomes absolute negative for *Tinman* expression and positive for *Seven up* expression thereby leading to cardioblast diversification (Fig.1.1C). At this stage, the distinct heart precursors begin to coalesce to form a continuous row of dorsal vessel cells on each side of the embryo. After this stage, no cell division takes place in the dorsal vessel during embryonic development. Only cardioblasts differentiation and migration towards the midline occurs which con*tin*ues till stage 17 (Fig.1.1D). At stage 17, the differentiated heart tube is located at the dorsal midline, surrounded at the anterior end by the lymph glands and ring gland(Fig.1.1E).

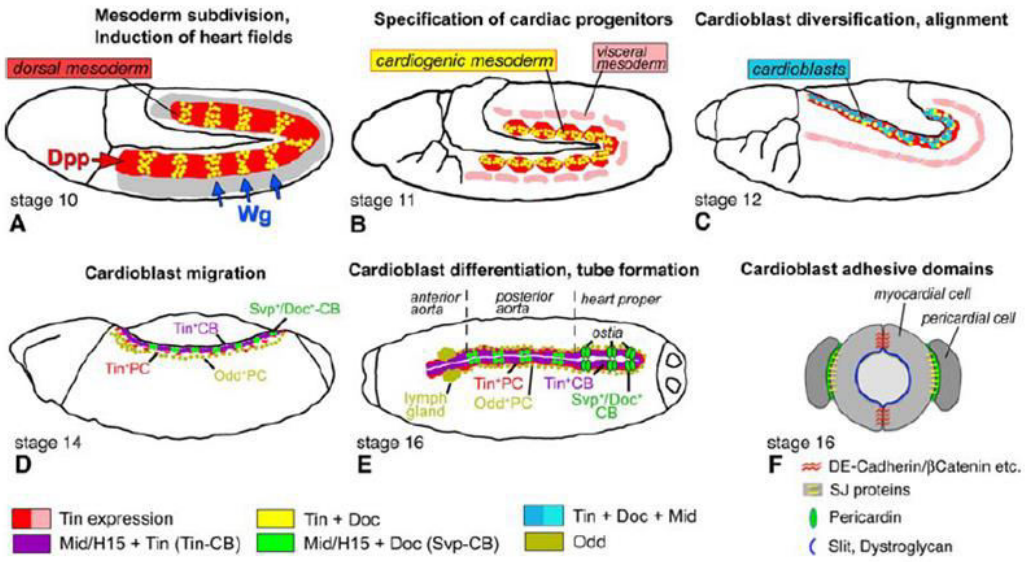

Fig. 1.1 Schematic overview of heart development in *Drosophila* embryo {Adapted from Genetic and Genomic dissection of cardiogenesis in *Drosophila* model; Pediatric Cardiology, (Reim and Frasch, 2010)}

The *Drosophila* embryonic heart is called the dorsal vessel. It is an extremely simple tubular structure formed of a total 104 cardio blasts. Pericardial cells that function as nephrocytes in *Drosophila* and supported by alary muscles that hold the dorsal vessel in place flank the dorsal vessel. Despite the evolutionary distance from vertebrates, the dorsal vessel is reminiscent of the tubular heart in the early vertebrate embryo. There are similarities in the direction of blood flow from posterior to anterior and ultrastructural similarities of cardiomyocytes(Bodmer and Venkatesh, 1998; Zaffran and Frasch, 2002). *Drosophila*embryonic heart, like the vertebrate heart tube, also has an anterior-posterior polarity, the anterior portion is termed as aorta whereas the posterior portion is termed heart proper(Cripps and Olson, 2002). The posterior portion has specialized cardiomyocytes that form the inflow tracts termed as ostia. Segmentation also applies to the dorsal vessel which is the hallmark of insects. There is a segmentally repeated pattern of cell identities along the length of the tube.

Dorsal vessel spans from T1 to A5 segments. A total of 12 cardio blasts per hemisegment in the thoracic region do not show any diversity with respect to cell identities (Fig.1.2). However, cardio blasts in abdominal segments are diversified primarily into 2 subpopulations. There is a pattern of 4+2 cardio blasts per hemisegment. The *Tinman* expressing 4 cardio blasts are muscular in nature whereas 2 *Seven up* positive cardio blasts are non-muscle cells which later differentiate to form inflow tracts termed ostia (Fig.1.2).

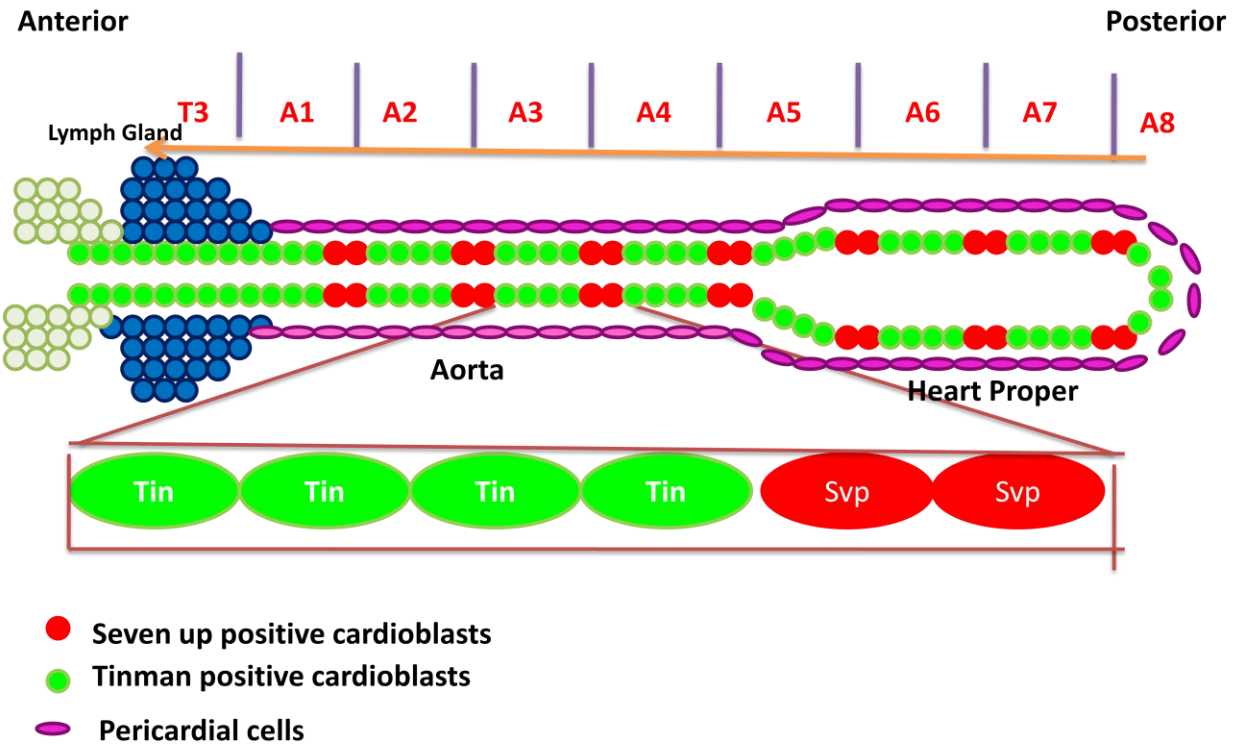

Fig. 1.2: Schematic showing cardiac tube composition and organization in stage 16 *Drosophila*embryo

1.6 Cell fate specifications during cardiogenesis:

1.6a Signaling pathways involved in mesoderm migration:

The dorsal vessel originates from the mesoderm. At the beginning of embryogenesis, mesoderm is specified in response to cues laid down in the oocyte, which results in nuclear localization of the maternally derived Rel-domain transcription factor *Dorsal* (Roth et al., 1989; Rushlow et al., 1989; Steward, 1989). *Dorsal* directly activates the expression of zygotic regulatory genes *Twist* and Snail (Jiang et al., 1991; Pan et al., 1991; Thisse et al., 1991). *Twist* and Snail encodes bHLH and Zinc-finger transcription factors respectively, which are required for specification and morphogenesis of the mesoderm (Lep*tin*, 1991). Mesodermal cells subsequently invaginate and spread to form a layer closely opposed to the overlying ectoderm. Fibroblast growth factor signaling, a pathway involved in diverse biological processes, regulates the mesodermal spreading. *Heartless* (Htl) has been identified as the FGF receptor within mesodermal cells. In Htl mutant embryos, the mesoderm does not migrate and a majority of dorsal mesoderm

derivatives are lost, including the dorsal vessel (Beiman et al., 1996; Gisselbrecht et al., 1996; Shishido et al., 1997). In heartbroken embryos, a downstream mediator of Htl, comparable phenotype has been observed (Michelson et al., 1998; Vincent et al., 1998). The FGF ligands that work through Htl are encoded by *Pyramus* and *Thisbe*, two genes expressed in epithelial cells in dynamic patterns adjacent to Htl-expressing mesoderm derivatives. *Pyramus* and *Thisbe* mutant embryos exhibit defects comparable to those seen in Htl mutants that include delayed mesodermal migration and loss of dorsal vessel (Stathopoulos et al., 2004).

1.6b Signaling pathways involved in induction of cardiogenic mesoderm:

Due to the migration of mesoderm, the most lateral cells are positioned under *Dpp* expressing cells of the dorsal ectoderm. *Dpp*, which is a member of TGF-beta superfamily, is secreted by the ectoderm. It binds to and activates its membrane receptor Thickvein, which phosphorylates Mad. Phosphorylated Mad complexes with Medea and translocate to the nucleus to activate the transcription of downstream genes (Wisotzkey et al., 1998). *Dpp* mediated signaling is the initial pathway that induces dorsal mesoderm specification. *Dpp* signaling induces the expression of *Tinman*(Fig.1.3).*Tinman* plays a crucial role in cardiac cell specification (Frasch, 1995). In the *Tin* loss of function mutants, all dorsal mesodermal derivatives are missing including the dorsal vessel, visceral muscles and a subset of dorsal body wall muscles. Numerous heart-specific genes including *Pannier*, *Mef2*, *β3 tubulin*, *Toll* and *d-SUR*has been shown to be regulated by *Tin*(Akasaka et al., 2006; Gajewski et al., 2001; Kremser et al., 1999; Wang et al., 2005). *Tin* is first expressed in the whole mesoderm being activated by *Twist*(Yin et al., 1997). After that, *Tinman* expression is maintained in the dorsal mesoderm only. *Dpp* regulates *Tinman* gene expression in the dorsal mesoderm through Smad binding sites (Xu et al., 1998). Activated Mad binds to its recognition site in the *tin*-D enhancer element which is downstream of the *Tinman* gene. *Tinman* also binds to its consensus sites in the regulatory module. Thus the synergistic activity of *Tinman* and Mad are required for expression of *Tinman* in dorsal mesoderm. The *Tinman* expression is lost from the rest of the mesoderm which is not underneath the *Dpp* secre*tin*g ectoderm. Thus *Tinman* pan-mesodermal expression provides the dorsal mesodermal cells the potential to interpret *Dpp* signaling. Subsequently, within the dorsal mesoderm, *Tinman* and *Dpp* signaling activate expression of pannier the function of which is required for the

specification of cardiac progenitor cells (Fig.1.3) (Alvarez et al., 2003; Gajewski et al., 2001; Klinedinst and Bodmer, 2003).

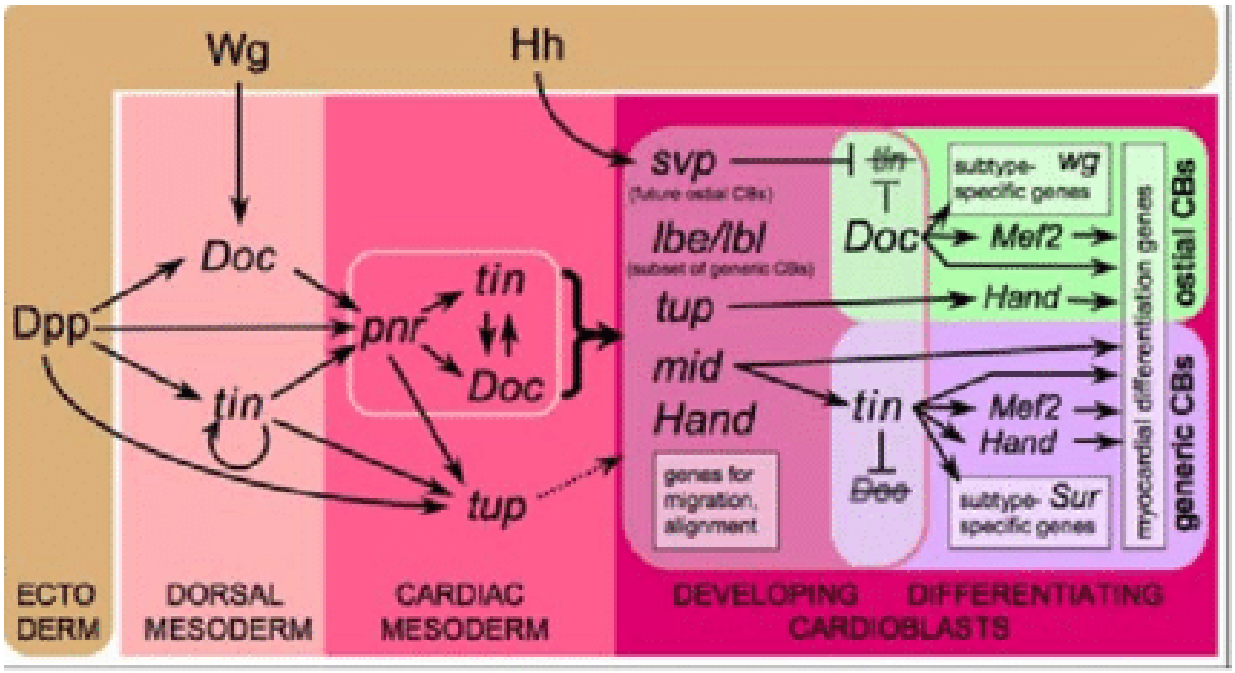

Fig.1.3 Regulatory interactions within the *Drosophila* cardiogenic mesoderm.Arrows and bars indicate positive or negative regulation respectively.

*Dpp*loss-of-function mutation causes a complete loss of cardiac and visceral mesoderm cells. Conversely, ectopic *Dpp* signaling induces ectopic heart development within the ventralmost region of the mesoderm (Yin and Frasch, 1998; Zaffran and Frasch, 2002).

Based on these results, it was concluded that *Dpp* signaling is essential for the delineation of the dorsal mesoderm within the mesoderm. However, *Dpp* is not sufficient for this process since ectopic signaling does not instruct other parts of the mesoderm to differentiate into cardiac tissue, except for the ventral-most domain. Thus it was proposed that there must be another signaling pathway in addition to *Dpp* that promotes cardiogenesis(Yin and Frasch, 1998; Zaffran and Frasch, 2002).

Wingless (Wg) is another signaling component demonstrated to be essential for heart development. Wg induces the specification of cardiogenic mesoderm from the dorsal mesoderm. It is secreted from transverse stripes of ectodermal cells that intersect with the dorsal *Dpp* expression domain. Dorsal mesodermal cells that receive *Wg* have the potential to induce

cardiogenic progenitors, while other cells become specified as visceral mesoderm primordia. In Wg loss-of-function embryos, progenitors of the dorsal vessel do not form indicating a critical requirement for this secreted molecule in heart formation (Lawrence et al., 1995; Wu et al., 1995).

Wingless signaling activates its downstream transcriptional regulator *Pangolin* (Park et al., 1996). *Pangolin* has three target genes i.e. *Sloppy-paired (Slp) 1, 2 and even-skipped* (Lee and Frasch, 2000). *Slp* inhibits the expression of *Bagpipe*, which functions in the specification of visceral muscle lineage from the dorsal mesoderm and maintains the expression of *Wg* in ectoderm which is crucial for *Wg* to exert its subsequent function in heart development (Jagla et al., 1997; Lee and Frasch, 2000) (Fig.1.4)

Wingless pathway also targets *even-skipped* that specifies a subtype of pericardial cells. The enhancer element of *even-skipped* has pan binding sites which together with mad and *Tinman* regulates *even-skipped* expression (Halfon et al., 2000; Knirr and Frasch, 2001). *Wingless* signaling also selectively regulates *Doc* genes but the mechanism of activation is not known (Reim and Frasch, 2005).

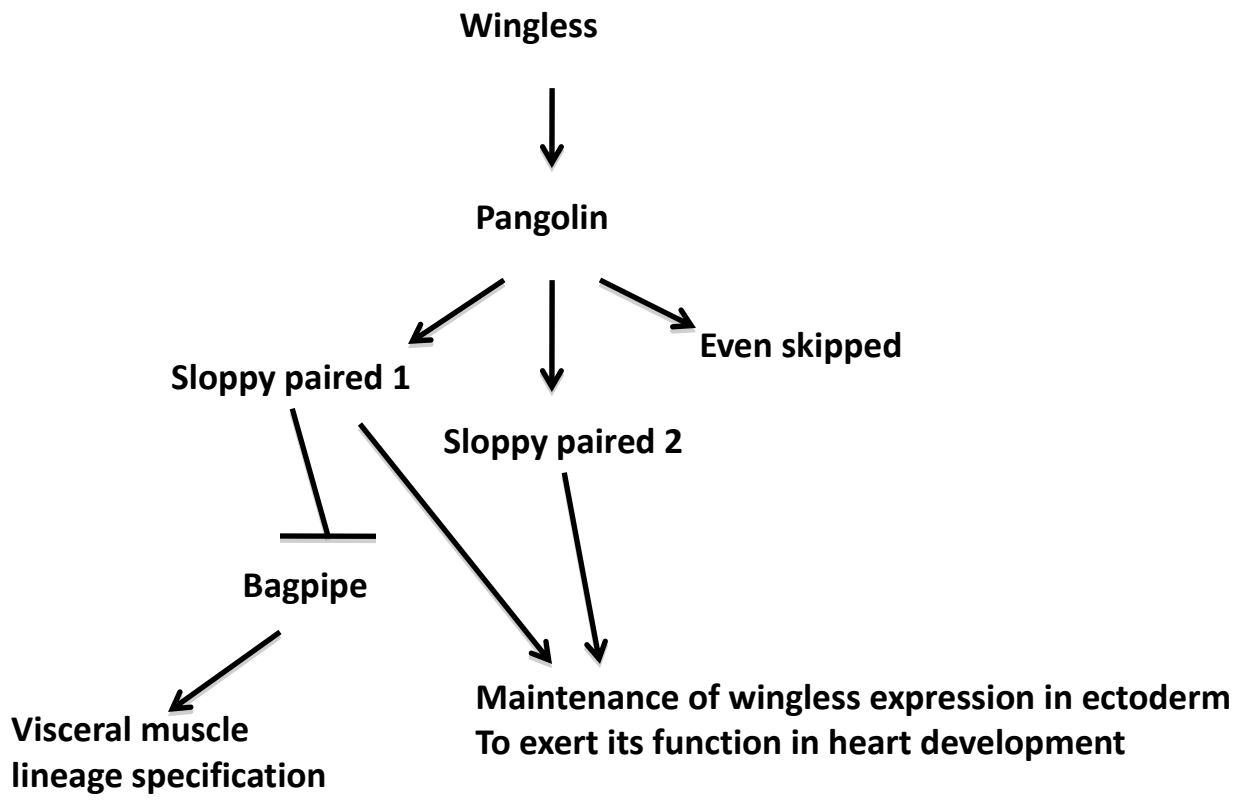

Fig.1.4 Line diagram showing wingless signaling during cardiogenesis in *Drosophila* embryo

1.6c Signaling pathways involved in restriction of cardiogenic progenitors:

Notch is another signaling which is vital to lineate cardiogenic mesoderm from dorsal mesoderm. Notch has a dual function in *Drosophila* heart development: to limit the cardiac progenitors and to control the lineage decisions in the specification of cardioblasts(Zaffran and Frasch, 2002).

The phenotypes relevant to both Notch (N) functions were observed using the Nts^1 allele. ShiftingNts^1 embryos to a restrictive temperature at 6–8 h of embryo development resulted in the supernumerary cardio blast and pericardial cell formation. In contrast, shifting embryos at 8–10 h of development failed to generate an increase in cell populations, but the relative number of these two cardiac cell types changed as more cardioblasts were formed at the expense of pericardial cells. The mutation of the N ligand Delta caused the same early phenotype of increased cardioblasts and pericardial cells(Carmena et al., 2002; Hartenstein et al., 1992; Mandal et al., 2004; Zaffran et al., 1995).

In the dorsal mesoderm, Notch shows its known function of lateral inhibition i.e. it restricts the specification of cardiogenic mesoderm (Mumm and Kopan, 2000). Notch signaling in dorsal mesoderm leads to distinct cardiac progenitors from a population, these progenitors will then give rise to cardioblasts and pericardial cells. Subsequently, N functions in controlling lineage decisions in the specification of cardioblasts from defined heart precursors; here notch plays a role in asymmetric cell fate determination (cardioblast vs. pericardial cell). Therefore in N mutants, only one type of cell, the cardio blasts are generated at the expense of pericardial cells (Han and Bodmer, 2003; Ward and Skeath, 2000).

After specification, cardioblasts align and meet at the dorsal midline as two continuous rows where they start the process of differentiation to form the functional heart. Like *Dpp* and *Wg*, *Hedgehog (hh*) is secreted by the ectoderm and interpreted by the neighboring cells. The *Hh* is expressed in cell stripes adjacent to *wingless*-expressing cells and maintains wingless expression, hence contribu*tin*g to the induction of cardiogenic mesoderm (Park et al., 1996).

Second, *Hh* signaling controls *Seven up* expression, thus it indirectly regulates the differentiation of a subset of cardioblasts within the dorsal vessel (Ponzielli et al., 2002).

1.6d Migration and alignment of cardioblasts and pericardial cells at the dorsal midline

Post-cardioblast alignment, the two rows migrate dorsally toward each other. Migrating cardioblasts contact the ectoderm layer adjacent to its leading edges and rely on this association for movement (Rugendorff et al., 1994). Thus genes involved in dorsal closure may indirectly control cardioblast migration. However, there are a few genes known to be expressed in heart and required for cardioblast migration. One example is *Pericardin*(*Prc*), which encodes a collagen-like component of the extracellular matrix (Chartier et al., 2002). *Pericardin* is produced by pericardial cells at the beginning of the dorsal closure process, becoming concentrated at the basal surface of cardioblasts that are in close proximity to overlying ectodermal cells as dorsal closure proceeds. In *Prc* mutant embryos, migration, as well as assembly of cardioblasts, is disrupted. Based on its expression pattern and mutant phenotype, *Prc* is likely to mediate the coordinated migration of dorsal ectodermal sheets and associated cardioblast rows. Additional molecular components of this migration process need to be identified and studied as to their relationship to *Prc* (Chartier et al., 2002).

1.6e Role of Slit and Robo in proper migration and alignment of cardioblasts and pericardial cells:

Dorsal closure leads to the zipping up of two open sides of the embryo that are formed due to germ band retraction during stage 12 of embryonic development. From stage 13 onwards, differentiating cardioblasts and pericardial cells from each side of the embryo con*tin*ue to migrate towards the dorsal midline. The proper migration and positioning of cardioblasts and pericardial cells towards the dorsal midline involve adhesion between relevant cells, appropriate polarization of cardioblasts, contact between membrane domains and cell shape changes (Medioni et al., 2008).

Slit/ *Robo* signaling plays a key role in this final phase of heart morphogenesis (Kramer et al., 2001; Wong et al., 2002). *Slit* is expressed only by cardioblasts and accumulates at the dorsal midline; *Robo* is expressed by both cardioblasts and pericardial cells and *Robo*2 is expressed only by pericardial cells (Qian et al., 2005; Santiago-Mar*tin*ez et al., 2006).

Misexpression studies revealed that normal *Robo* and *Robo*2 expression and function is required for correct localization of *Slit* and its receptors which ultimately determines correct migration, alignment, and positioning of both cardioblasts and pericardial cells.Mutant embryos with *Slit* or *Robo* loss of function exhibit delayed the migration of cardioblasts and pericardial cells towards the midline. The cardioblasts and pericardial cells in these embryos fail to form two continuous rows of cells at the midline (Vanderploeg et al., 2012).

After dorsal closure, when two rows of cardioblasts from each side of the embryo come in close contact with each other at the dorsal midline, each cardioblast first becomes constricted along with its dorsal domain and comes in contact with its contralateral counterpart thereby forming a pair (Fig.1.5A and B)). The cells in this pair now adopt a crescent shape, thereby allowing the ventral domains of cardioblasts to join and thus form a tube enclosing a lumen (Fig.1.5D and E).In wild type embryos, cell adhesion proteins E-cadherin and β-catenin are specifically localized at the membranes along with constricted dorsal domain and ventral domain whereas *Slit* and *Robo* are concentrated at the luminal domain. In embryos lacking *Slit* function, the initial constriction of cardioblasts along their dorsal junction domains does not occur whereas in embryos lacking both *Slit* and *Robo*, E-cadherin and b-catenin are mislocalized into the presumptive luminal domain, thereby preven*tin*g luminal encapsulation (Qian et al., 2005; Raza et al., 2017; Santiago-Mar*tin*ez et al., 2006).

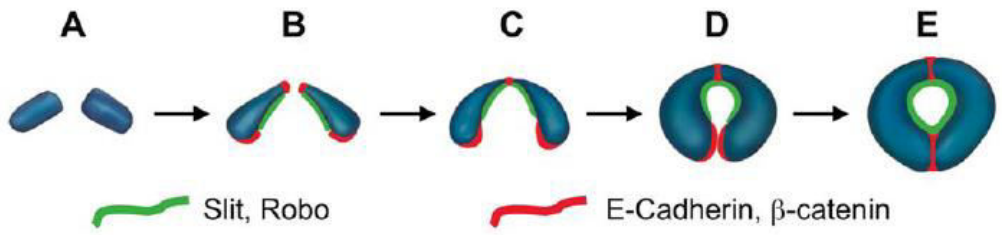

Fig.1.5 Schematic representation of two cardioblasts showing temporal sequence of events during lumen formation in Drsophila cardiac tube {Adapted from (Medioni et al., 2008; Santiago-Mar*tin*ez et al., 2006)}

1.7 Challenges in Genetic analysis of mitochondrial perturbations

Extensive research has not been done in this area, the main reason being establishmentof a suitable model system to answer the underlying question that whether mitochondrial dysfunction can directly hit the developmental programs and circuits at the cell specification level.Most aspects of this question remain unanswered because mitochondria fuels all the biochemical pathways in a cell and targeting mitochondria for epistasis studies is a different ball game than targeting a developmental gene. Mitochondria is a very dynamic organelle per se if we try to create a pool of dysfunctional mitochondrial population by knocking down some components of ETC, they combat this through fusion-fission mechanisms so that damaged components of mitochondria are replenished by healthy one and the whole mitochondrial network works fine for a longer time. Hence, it takes relatively more amount of time until the pool of bad mitochondria is accumulated to a level that mitochondrial function restoration is not possible for the system.

Second thing is, even in that scenario, when a bad mitochondrial population is created; the system can crash completely as ATP is required to fuel each and every step of any signal transduction pathway. Therefore, it is challenging to get an observable phenotype by mutating mitochondrial components.

1.8 Mitochondria and retrograde signaling:

Mitochondrial retrograde signaling is a pathway of communication from mitochondria to the nucleus in normal and pathophysiological conditions. There are multiple factors involved in retrograde signaling that sense and tansmit mitochondrial signals to regulate changes in nuclear gene expression. Retrograde signaling by mitochondria is most extensively worked out in yeast

(Liu and Butow, 2006; Parikh et al., 1987). In yeast, mitochondrial dysfunction leads to a decrease in intracellular ATP concentration which activates the RTG (retrograde) pathway through rtg1-rtg3 activation leading to altered expression of various genes like CIT1(encoding mitochondrial citrate synthase), CIT2 (peroxisomal citrate synthase), PYC1(pyruvate carboxylase), ACS1(acetyl coAsynthetase), ACO1(aconitase) and DLD3(D-lactate dehydrogenase) ensuring that sufficient glutamate for biosynthetic pathways is available in cells with reduced respiratory capacity (Liao and Butow, 1993; Liao et al., 1991).In mammals, mitochondrial dysfunction results in a drop in membrane potential leading to high intracellular calcium. An increment in calcium levels leads to activation of various calcium-dependent kinases and phosphatases like calcineurin, PKC, CamKIV, JNK and MAPK through transcription factors like ATF2, CEBP, NFAT, CREB, Egr1, CHOP and NF-KB (Butow and Avadhani, 2004; Srinivasan et al., 2010) impairing various cellular processes associated with activation of these transcription factors.

In yeast and in C.elegans, YME1, and SPG7, the mitochondrial-derived peptides are shown to be involved in the activation of retrograde signaling. In D. melanogaster and in C.elegans, it has been shown that the disruption of different complexes of ETC leads to activation of mtUPRs together with attenuation of the IIS (Insulin Signaling) pathway (Liu et al., 2011).ROS has been shown to be part of mtUPR induced by knockdown of CCO1(a subunit of mitochondrial cytochrome oxidase) in C.elegans(Lee et al., 2010).

Apart from the peptides generated by degradation of existing mitochondrial proteins, a number of short open reading frames (SORF) in the mtDNA can give rise to biologically active peptides such as humanin which provides cytoprotection and affects metabolism. The mitochondrial sORF derived peptides are potent and evolutionary conserved signals and are able to affect various physiological processes (Caricasole et al., 2002; Hashimoto et al., 2001; Niikura et al., 2004) that include insulin sensitivity and metabolic homeostasis.

In *Drosophila*, it has been shown that mutation in NDUFS1/*ND75* which is a component of complex-I of Electron Transport Chain leads to life span extension by attenuation of insulin/ insulin-like growth factor(IIS) signaling (Owusu-Ansah et al., 2013). Interestingly, this increase in life span is suppressed by forced expression of catalase or glutathione peroxidase thereby uncovering a pivotal role ofH_2O_2 in the signaling pathway. Another study in D. melanogaster

presents evidence for the activation of mtUPR (mitochondrial unfolded protein response) along with attenuation of IIS pathway in a mutant defective for coenzyme Q synthesis (Liu et al., 2011). The main outcome of mtUPR activation in D. melanogaster has been reported to be an increased life span (Copeland et al., 2009). It has been identified that mutation in complex-I subunit *Pdsw* or *complex-IV subunit cytochrome c oxidase Va (CoVa)* causes cell cycle arrest in the developing *Drosophila* eye (Owusu-Ansah et al., 2008). Further mechanistic insight revealed that loss of *Pdsw* leads to complex-I inhibition leading to high ROS levels which control the expression of *p27* homolog cell cycle regulator *dacapo* via *c-Jun N-terminal kinase* and transcription factor *FoX*o(Mandal et al., 2010). Loss of CoVa leads to defective complex-IV activity and causes decreased expression of cyclin E through activation of AMP kinase and transcription factor p53(Mandal et al., 2005).In contrast to the previous conception that mitochondrial retrograde signaling is a cell-autonomous phenomenon, recent studies have revealed that mitochondrial dysfunction in one tissue can generate a systemic signal that can affect cells in distant parts. Mild inhibition of complex- I activity in muscle causes increased expression and secretion of *ImpL2* (an ortholog of *human insulin-like growth factor-binding protein 7, IGFBP7*), which systemically inhibits insulin receptor pathway and increases lifespan in *Drosophila*(Owusu-Ansah et al., 2013). Muscle-specific mitochondrial dysfunction has been shown to give rise to *TGF-β*-mediated retrograde response in adipose tissue (Song et al., 2017). The mitochondrial retrograde response has also been observed in *Drosophila* CNS where neuron-specific overexpression of mitochondrial transcription factor TFAM or knockdown of a subunit of complex-V causes defects in neuronal dysfunction, reduced redox potential and decreased number of presynaptic mitochondria and active zones (Cagin et al., 2015). In these models, transcriptomic analysis of the larval nervous system suggests HIF-1A to be an important regulator of mitochondrial retrograde response. Strikingly, knockdown of HIF-1A alleviates reduced neuronal function in the *Drosophila* Leigh syndrome model and Parkinson's model of mitochondrial dysfunction (Cagin et al., 2015).

1.9Signal transduction by reactive oxygen species:

ROS has long been considered as purely harmful molecules, although recent evidence suggests that ROS regulates diverse intracellular signaling pathways thereby regulating various physiological parameters ranging from the response to growth factor stimulation to the generation of an inflammatory response. Nearly a century ago, Child and colleagues had

correlated redox gradients in developing embryo to regional differentiation of blastomeres. In 2004, Wong et al showed that H_2O_2 production on the surface of sea urchin egg is used as a part of enzymatic reaction which results in the development of a protective shell around the young fertilized egg (Wong et al., 2004). This was a piece of strong evidence that proved ROS can be purposefully made and harnessed to regulate physiological processes. In contrast, there are various studies that suggest ROS can cause and even accelerate various pathological conditions such as age associated muscle degeneration, neurodegenerative disorders and cardiomyopathies. Hence, redox signaling seems to act as an important regulator of physiological and pathophysiological outcomes from life's inception to its end (Balaban et al., 2005).

Complex-I and complex III are the major producers of ROS in the Electron Transport Chain where electrons derived from NADH and FADH2 react with oxygen to form superoxide ions by one electron reaction and hydrogen peroxide by two electron reactions. The viewpoint about ROS was changed with the observation that for growth factors like PDGF and EGF, ligand binding stimulates ROS production burst and inhibition of this ROS burst halts normal RTK signaling (Bae et al., 1997; Sundaresan et al., 1995).

Further studies established a family of Tyrosines and phosphatase as intracellular targets of oxidants (Lee et al., 1998a; Salmeen et al., 2003). These effects of ROS are modulated in large part through covalent modification of specific cysteine residues present in the redox-sensitive target proteins.

There are varied examples in which mitochondrial oxidants appear to participate in signaling events. These examples include regulation of HIF1 alpha during low oxygen conditions (Brunelle et al., 2005; Guzy et al., 2005; Mansfield et al., 2005), regulation of autophagy through direct regulation of Atg4 activity (Scherz-Shouval et al., 2007), regulation of inflammatory response through formation of NLRP3 inflammasome(Bulua et al., 2011; Nakahira et al., 2011; Zhou et al., 2011). Apart from phosphatases, there are other signaling molecules such as p21ras (Clavreul et al., 2006; Lander et al., 1995) and certain 14-3-3 isoforms (Kim et al., 1988) which are direct targets of reactive oxygen and nitrogen species.

In *Drosophila* hematopoietic progenitors, moderately high levels of ROS have been shown to trigger differentiation while low levels impair differentiation; therefore establishing a signaling role of ROS in hematopoietic cell fate(Brunelle et al., 2005; Frei et al., 2005; Guzy et al., 2005;

Kaelin, 2005). Mitochondrial ROS reportedly triggers a pathway mediated by Rho effector ROCK that influences tissue patterning and homeostasis through the regulation of mitochondrial morphology and tissue tension (Muliyil and Narasimha, 2014). Studies in *Drosophila* have evidenced that stabilization of HIF-α under hypoxic condition leads to transcriptional activation of *Scylla* and *Charybdis,* that can inhibit cell growth by negatively modula*tin*g the Tsc-TOR pathway (Reiling and Hafen, 2004). Since the hypoxic condition can also lead to the production of mitochondrial ROS, it raises the plausible involvement of ROS in limi*tin*g cell growth (Brunelle et al., 2005; Frei et al., 2005; Guzy et al., 2005; Kaelin, 2005). Mitochondrial ROS has been shown to modulate cell cycle progression through the upregulation of Dacapo(Owusu-Ansah et al., 2008).

1.10 ROS as a retrograde response in pathological conditions:

Mitochondria act both as producers and sensors of elevated ROS levels. Most of the cellular ROS is generated by Electron Transport Chain machinery present on the inner mitochondrial membrane. An increase in ROS levels above a threshold can damage components of ETC resulting in mitochondrial respiratory stress (Kirkinezos and Moraes, 2001). The mitochondrial DNA is present in close proximity to Electron Transport Chain components making it susceptible to damage by malfunctioning ETC. Therefore when ROS levels elevate above the capacity of the antioxidant defense system, it can potentially cause mitochondrial DNA damage (Yakes and Van Houten, 1997).

Mitochondrial ROS mediated retrograde signaling is reported to be a causative factor in many pathophysiological conditions (Formen*tin*i et al., 2012).

A recent report by Fan et al showed that in mouse cell lines, mitochondrial heteroplasmic DNA mutation results in oxidative stress and increased production of ROS which provides a survival advantage to these cells (Fan et al., 2012; Wallace and Fan, 2009). Another evidence of ROS mediated retrograde signaling under pathological conditions is provided by mitochondrial localization of the adaptor protein Shc, p66 which regulates ROS production. By silencing this gene, an increase in the life span of mice has been reported (Migliaccio et al., 1999).In lung injury, alveolar epithelial cells develop hypoxia, resulting in mitochondrial ROS production and

activation of HIF-1α gene targets. This results in cellular reprogramming; leading to aberrant tissue repair, lung dysfunction and pulmonary fibrosis (Zhou et al., 2009).

In *Drosophila*, experiments performed have raised the possibility of ROS involvement in affec*ting* presynaptic mechanisms of neurotransmitter release (Milton and Sweeney, 2012). ROS induces synapse overgrowth by upregulation of presynaptic JNK/AP-1 signaling pathways and Fos expression (Milton et al., 2011; Milton and Sweeney, 2012; Sanyal et al., 2002). In other studies, mild disruption in mitochondrial function has been shown to cause synapse loss via ROS production (Mast et al., 2008).

In *Drosophila* larvae, ROS cause smaller synaptic varicosities and dendritic arbors leading to reduced synaptic input sites (Zwart et al., 2013). Neuronal ROS signaling operates via redox-sensitive protein DJ-1b, a homolog of vertebrate PARK7. Oxidation of DJ-1b increases inhibitory interactions with PTEN thereby leading to disinhibition of PI3Kinase signaling which is a known regulator of synaptic terminal growth (Cuesto et al., 2011; Jordan-Alvarez et al., 2012; Kumar et al., 2005; Mar*tin*-Pena et al., 2006). These findings suggest that ROS exert pathological effects on synaptic plasticity, memory, and cognition.
A recent study by Bodmer et al has shown that in flies, significant elevation or reduction of ROS causes cardiac dysfunction (Lim et al., 2014). In this particular paper, authors showed that manipula*ting* ROS in pericardial cells could regulate heart function in a paracrine manner. In pericardial cells. ROS activates a p38MAP kinase-dependent signaling cascade which affects myocardial cell function (Lim et al., 2014).In the Hun*ting*ton disease fly model, oxidative stress induced by the accumulation of poly-Q aggregates has been shown to cause increased arrhythmia and cardiac dilation (Melkani et al., 2013). Overexpression of superoxide dismutase, an antioxidant enzyme rescued the poly-Q induced cardiomyopathy.In another report, overexpression of antioxidant enzyme catalyse suppressed age-induced arrhythmia (Monnier et al., 2012).

1.11 Regulation of cell fate by ROS:

ROS are highly reactive reduced forms of molecular oxygen, such as the superoxide radical anion (O2_-) and hydrogen peroxide H2O2. Under physiological conditions, ROS are

naturallyproduced by the respiratory chain during OXPHOS. Although ROS exert oxidative damage on lipids, proteins, and DNA, they also act as secondary messengers and depending on the nature and level of production have been shown to be involved in the regulation of stem cell self-renewal, pluripotency, and differentiation (Maryanovich and Gross, 2013). Stimulating or inhibiting ROS production has been shown to favor or prevent mESCs differentiation into cardiomyocytes(Ateghang et al., 2006; Buggisch et al., 2007; Sauer et al., 2000; Schmelter et al., 2006). mESCs simultaneously treated with antioxidants and cyclosporin A, an inhibitor of the mitochondrial permeability transition pore (MPTP) results in increased mitochondrial biogenesis and ROS generation that synergistically favors cardiomyocyte differentiation (Cho et al., 2014) providing a solid evidence for role of ROS in regulation of early differentiation .

ROS regulates the proliferation and differentiation of rat neural progenitors, with proliferat*in*g neural progenitors displaying low levels of ROS in comparison with differentiated neuronal and astrocytic counterparts (Tsatmali et al., 2005). A recent study shows that rapid burst of superoxide radical anions called superoxide flashes, which are highly reactive reduced forms of molecular oxygen, were involved in regulating the self-renewal and differentiation of mouse embryonic neural progenitor cells (NPCs). Mitochondrial superoxide scavengers or MPTP inhibitors reduce the frequency of superoxide flashes and enhance NPC proliferation (Hou et al., 2012).

In contrast, increased superoxide flashes are necessary for the differentiation of mouse NPCs into cortical neurons, and inhibi*tin*g mPTP or scavenging mitochondrial ROS impairs differentiation (Hou et al., 2012). In a mouse model of adult hippocampal neurogenesis, a peak in mitochondrial abundance and ROS levels was observed in a highly proliferative, intermediate progenitor state, but not in undifferentiated neural stem cells or postmitotic neurons (Walton et al., 2012). Although these differences might depend on the embryonic or adult status of the NPCs, data suggest that the involvement of ROS in neurogenesis might be limited only to a specific stage of cell differentiation. In hMSCs, mitochondrial complex III-derived ROS, independent of OXPHOS, are required for the expression of PPARg and initiation of the adipogenic transcriptional program. Mitochondria-targeted antioxidants such as mitoCP prevent both the adipogenic differentiation and the associated increase in ROS, whereas addition of exogenousH_2O_2 to mitoCP-treated hMSCs rescues adipogenic differentiation (Tormos et al.,

2011). Similarly, hypoxia stimulates adipocyte differentiation by enhancing the production of mitochondrial ROS. On the other *Hand*, both exogenous H_2O_2 and oligomycin-dependent inhibition of mitochondrial activity inhibit the osteogenic differentiation of hMSCs. These data suggest that mitochondrial OXPHOS is required for osteogenic differentiation and excessive ROS hamper osteogenic differentiation (Chen et al., 2008). Beyond their role in MSC differentiation, mitochondrial ROS are also involved in MSC senescence. The treatment of mouse MSCs with transforming growth factor b1 induces their senescence. This effect is, at least partly, mediated by the generation of mitochondrial ROS, suggesting that maintaining low levels of mitochondrial ROS is necessary to preserve MSC stemness(Wu et al., 2014).

The involvement of ROS in function of Hematopieitic Stem Cells (HSCs) has also been established and recently reviewed (Kohli and Passegue, 2014; Maryanovich and Gross, 2013).mHSCs with low ROS levels are more quiescent and display increased self-renewal potential compared with HSCs displaying higher ROS levels, which are prone to exhaustion upon serial transplantations (Jang and Sharkis, 2007). The negative impact of ROS on mHSC self-renewal is mediated by the activation of p38 MAPK and mammalian target of rapamycin(mTOR) pathways, with studies showing that inhibi*tin*g either of these pathways restores the long-term reconstitution ability of HSCs with high levels of ROS (Ito et al., 2006). In contrast, ROS triggered the differentiation of *the Drosophila* population of hematopoietic progenitors resembling mammalian myeloid progenitors through the activation of c-Jun N-terminal kinases, leading to activation of *Forkhead* box O and inhibition of the activity of polycomb group of genes(Owusu-Ansah and Banerjee, 2009). Similarly, increasing ROS in AKT1/AKT2 double-deficient mHSCs, which show lower ROS levels, rescue the defects in differentiation (Nooter et al., 1978). Thus, low levels of ROS are necessary to preserve the quiescence of HSCs and increased ROS levels favor HSC differentiation.

1.12 ROS in cardiogenesis

Dysfunction of mitochondrial electron transport chain can cause heart malformations and embryonic death (Ingraham et al., 2009; Larsson et al., 1998), suggesting the mitochondrial function is essential to cardiac function in the embryo.

Since ROS can modify protein post-translationally by amino acid oxidation, hydroxylation or nitration, their targets are redox-sensitive cysteine residues in proteins involved in calcium

*Hand*ling, contractile proteins, as well as proteins, involved in various signaling pathways(Burgoyne et al., 2012; Knock and Ward, 2011). Cardiac contractility is directly affected by redox modulation of calcium *Hand*ling proteins e.g. calcium-calmodulin kinase II (CaMKII), ryanodine receptor on sarcoplasmic reticulum and sarcoplasmic reticulum ATPase (SERCA) (Burgoyne et al., 2012; Steinberg, 2013). There are certain reports which suggest that oxidation of these contractile proteins by ROS hampers contractility, although recently some modifications have been identified that increase cardiac contractility. We have a very limited understanding of how ROS modulates cardiac function because most of these studies have been carried out in vitro where it is not possible to observe simultaneous oxidative modifications of different contractile proteins (Steinberg, 2013).

The second group of proteins that are affected by redox modifications is protein kinases and phosphatases. Phosphorylation of Tyrosine by Tyrosine kinase is very important for control of vascular tone. Oxidative modifications result in the inhibition of Tyrosine phosphatases (PTP 1A, PTP1B, and PTEN) leading to abrupt constriction of smooth muscles (Knock and Ward, 2011). Other proteins involved in the regulation of vascular tone and cardiomyocyte contraction are PKA (Camp-dependent Protein Kinase A) and PKG (cGMP-dependent protein kinase G)whichare also susceptible to redox modifications (Steinberg, 2013).

The third group of proteins that are very important in cardiovascular cell signaling is MAPKs (Mitogen-Activated Protein Kinases). MAPKs are indirectly activated by ROS via ROS sensitive kinases Src, PKC, ras and MAPK kinase kinase (Zhang et al., 2003). MAPK activation has been shown in cardiac hypertrophy, cardiac remodeling after myocardial infarction and atherosclerosis (Esposito et al., 2001).

Recently, ROS has been shown to be a connecting link between redox-sensitive transcription factor NF-KB and HIF-Ialpha thereby implicating a new signaling pathway in cardiovascular pathology.

In pulmonary artery smooth muscle cells, reactive oxygen species generated either by exogenous H2O2 or by a NOX4-containing NADPH oxidase stimulated by thrombin activated or induced NF-kappaB and HIF-1alpha. The reactive oxygen species-mediated HIF-1alpha induction occurred on the transcriptional level and was dependent on NF-kappaB. This report implicates a new signaling pathway in cardiovascular pathology (Bonello et al., 2007)

It is well established that ROS is an important modulator of intracellular pathways namely mitogen activated protein kinase cascades and Akt pathways in the adult heart impacting on cardiomyocyte growth and stress response (Sugden and Clerk, 2006). ROS has also been shown to promote the differentiation of ES cells into cardiomyocytes in vitro (Puceat, 2005).

ROS can induce the expression of various cardiac-specific genes and transcription factors such as GATA4, Nkx2.5, and *Mef2* in mouse ES cells (Buggisch et al., 2007). In contrast, cardiac gene expression is inhibited in neonatal rat cardiomyocytes treated with H2O2 (Torti et al., 1998). In the context of embryonic heart, it has been proposed that balance between oxidative stress and the anti-oxidant enzyme is critical for embryogenesis and the loss of oxygen radical scavengers lead to neonatal dilated cardiomyopathy (Wallace and Fan, 2009) as demonstrated in mouse models.

In *Drosophila*, it is recently reported that under physiological conditions, pericardial cells of adult heart which are high in ROS can elicit a downstream D-MKK3-D-p38 MAPK signaling cascade that acts on cardiomyocytes to regulate their function (Lim et al., 2014).

The redox balance is thought to play a critical role in cardiac fibrosis (Xia et al., 2011). Fibrosis triggered by increased mechanical load or local tissue injury typically involves increased Renin-angiotensin-aldosterone system and TGF-beta signaling. TGF-beta promotes the transformation of interstitial fibroblasts into myofibroblasts. ROS is reported to activate TGF-beta and to promote transcription of profibrotic factors such as connective tissue growth factor. These factors are produced not only within fibroblasts but also by cardiomyocytes under stress. TGF-β–induced mesangial cell proliferation also involves ROS dependent calcineurin activation, raising the possibility that a similar mechanism may operate in cardiac fibroblasts(Xia et al., 2011). AngII induced fibroblast expression of endothelin-1, which is profibrotic, involves redox activation of AP-1 (REF).

Excessive TGF-β is involved in the onset of excess tissue fibrosis in various diseases (Zhao et al., 2008). Collagen synthesis and degradation coexist in the heart and their balance determines cardiac collagen volume. Collagen degradation involves Matrix MetalloProteases (MMPs) and their activity is controlled by TIMPs (Tissue Inhibitor of Metalloproteinases). TIMPs function as an important regulatory brake on MMP activity by inhibition of the active species, thereby suppressing collagen degradation. TIMP expression is tightly controlled at the transcription

level, which is induced by TGF-β. In one study, in AngII-treated rats, oxidative stress is reported to be high with a significant increase in the gene expression of TIMP-I and TIMP-II at sites of cardiac fibrosis, suggesting that collagen degradation is suppressed. Thus, in the model of hypertension, the imbalance of cardiac collagen synthesis and degradation results in cardiac fibrosis (Zhao et al., 2008). This study suggests that oxidative stress induces cardiac fibrogenesis by up-regulating TGF-β1 syntheses, which, in turn, triggers fibrogenic molecular and cellular events in hypertensive heart disease.

Although the complex role of redox signaling during cardiomyogenesis is not well understood, it would be imperative for understanding the pathogenesis of prenatal and postnatal cardiac diseases if the underlying molecular mechanisms could be unraveled. In this direction, Hom et al, 2011 have added an elegant finding that embryonic cardiomyocytes are influenced by mitochondrial maturation, the closure of MPTP (Mitocohndrial Permeability Transition Pore) results in reduced ROS levels and thus inducing differentiation.

Much of the evidence is derived from in-vitro differentiation of stem cells demonstrating that disruption of mitochondrial respiration impairs the ability of pluripotent stem cells to differentiate into cardiomyocytes and to maintain stemness. It has been reported that the ablation of mitofusin 1 and 2 impairs differentiation of mouse ESCs into cardiomyocytes and arrests embryonic mouse heart development, indicating a key role played by mitochondrial morphology in cardiomyocyte differentiation (Kasahara et al., 2013). ROS has been implicated in the stimulation of ES-cell-derived cardiomyogenesis and neonatal cardiac cell proliferation. In contrast, high levels of ROS can delay cardiac differentiation suggesting these cardiogenic effects to be concentration-dependent.

1.13 Gene analyzed for this study:

1.13a Pericardin:

In *Drosophila*, *Pericardin* is one of the four identified collagen-like proteins; the other three are Collagen IV alpha2 (Viking, Vkg), Cg25c (Dcg1), and Multiplexin. The precursor protein of *Pericardin* consists of 1713 amino acids. It harbors an N-terminal signal peptide as well as a long repeat region separated into a collagen-like domain and a non-collagen-like domain. The collagen-like domain contains 26 atypical and several typical $(Gly\text{-}X\text{-}Y)_n$ repeats. At the C-terminus, there is a single potential Integrin-binding site (RGD) (Chartier et al., 2002; Sellin et

al., 2009; Volk et al., 2014). Unlike ubiquitously distributed Collagen IV, *Pericardin* assembles specifically within distinct matrices: these include the matrix of the heart tube, the surface of pericardial cells and oenocytes, and the cap cells of chordotonal organs.

Lack of *Pericardin*, or its ECM adapter protein Lonely heart (Loh), causes heart failure upon aging (Rotstein and Paululat, 2016; Sellin et al., 2009).During development, *Pericardin* is synthesized and secreted by different tissues. During embryogenesis, *Pericardin* is secreted by pericardial cells; later, in first and second instar larvae, the main source of *Pericardin* secretion is the adipocytes. After biosynthesis, secretion, and release into the hemolymph, *Pericardin* specifically assembles at the outer surface of the cardiac tube and incorporates into the meshwork formed by typical structural components of basement membranes such as Collagen IV, Perlecan, andNidogen(Drechsler et al., 2013).

Pericardin secretion is affected by adipocyte-specific knock-down of small GTPase*Sar1* expression thus affec*tin*g the formation of a proper heart ECM in *Drosophila* (Sellin et al., 2009). Mislocalization or loss of *Pericardin* expression leads to loss of heart integrity whichultimately results in heart failure and heart collapse. These findings demonstrate that proper Pericaridin assembly in the larval heart is essential for organ integrity (Wilmes et al., 2018).

1.13b*Tinman*:

Tinman (tin) is a homeodomain protein with several CAX repeats. It is first expressed in the mesoderm primordium and this expression requires mesoderm determinant *Twist.*

Tinman has a dynamic pattern of expression. Initially, it is expressed in the entire trunk mesoderm, then its expression is refined to the dorsal mesodermal domain and finally *tin* expression becomes restricted to heart progenitors.

Each phase of *Tinman* expression is driven by a discrete enhancer element, 4 in total which determines the expression pattern of *Tinman*at a different phase of embryonic development and is subject to different regulatory inputs. These elements are located downstream of the transcription start site. The earliest *tin* expression in the entire trunk mesoderm is regulated by *Twist* dependent enhancer element *tin*B.

A second enhancer element *tin*D regulated by *Dpp* activates *tin* expression in the dorsal portion of the mesoderm. A third element, *tin*C is active in the dorsal vessel which activates expression from stage 12 on, in four out of six cardioblasts per hemisegment. Finally, an element A (about

500 bp), located in the 5' portion of the first intron, activates *tin* in the anterior tip of the head (Yin et al., 1997; Zaffran et al., 2006).

Embryos mutant for *Tinman* gene does not form heart primordial. Fusion of anterior and posterior endoderm is also impaired. Many of the somatic wall muscles develop but abnormally. Ubiquotous expression of *Tinman* in *Tinman*mutant embryos partially restores formation of heart cells and visceral mesoderm. *Tinman* is one of the earlies gene required for heart development in *Drosophila(Bodmer, 1993).*

1.13c Seven up:

The protein *Seven up* is an orphan nuclear receptor and belongs to steroid receptor superfamily. *Seven up* is required for the development of four out of eight photoreceptors that develop in each ommatidium of the eye. Studies have shown that *Seven up* function requires Ras signaling to function (Begemann et al., 1995; Kramer et al., 1995). Most of the work exploring the function of this gene has been done in the context of photoreceptor development and the growth of the malpighian tubules. In the Malpighian tubules, there is strong evidence that *Seven up* is a downstream target gene of EGFR signaling (Kerber et al., 1998).

Seven up gene encodes two transcripts *Svp* type I and *Svp* type II. *Seven up* type I encodes a protein with both a DNA-binding domain and a ligand binding domain (LBD)*, and Seven up* type II diverges from type I in the middle of the LBD. During cardiogenesis, *Seven up* is initially activated in the cardiac mesoderm and then restricted to the inflow tracts forming cells in the dorsal vessel. Using bioinformatics tool, a 1007-bp enhancer of *Seven up* was identified. This enhancer is initially activated by *Tinman* via *Twist* through a conserved 3' enhancer.(Ryan et al., 2007). Though *Seven up* is activated by *Tinman* in the cardiogenic mesoderm, its expression soon becomes mutually exclusive with *Tinman* expression from stage 12 onwards.

Complete loss of function of *Svp*(svp^{e22} or svp^{AE127}) resulted in embryonic lethality. Embryo development of these embryos proceeds till stage 16 but they lack any muscular movements and these embryos never hatch and eventually die. The cardiac tube has been shown to develop normally and delayed cardiac mascular activity was observed. However, ostial cells exhibit a delay in their shape remodeling and look more like *tin*-positive cardioblasts.Ostial cells reportedly do not function as evident from the lack of their opening and closing (Ponzielli et al., 2002).

Hh signaling has been shown to be instrumental in the specification of *tin*- and *Seven up*-cardioblasts by inducing the expression of *Seven up* in cardioblasts which, in turn, leads to the repression of *tin*(Ponzielli et al., 2002).

Mef2:

Mef2 (Myocyte enhancer factor 2) is expressed in the presumptive heart and skeletal muscle precursors. *Mef2* expression is dependent on *Twist*(Cripps et al., 1998). *Mef2* expression is complex and dynamic in embryos. *Mef2* is first evident in the late cellular blastoderm stage and continues to be expressed throughout the mesoderm during mesoderm invagination . At mid-germband extension, *mef2* expression is reduced in the ventrolateral mesoderm but maintained in the dorsal region. During germ band retraction, expression increases in visceral mesoderm and in somatic muscle precursors (Postigo et al., 1999). Certain reports suggest the role of *Zfh1* in regulating *Mef2* expression patterns in muscle precursors (Postigo et al., 1999). *Mef2* is required for continuous differentiation of muscle cells but not for their initial specification (Ranganayakulu et al., 1995). *Mef2* protein has a N-terminal MADS box and consists of 516 amino acids. *Mef2* is a direct transcriptional target of *Tinman* and Pannier in cardioblasts(Gajewski et al., 2001). Lame duck (lmd) has been shown to activate *Mef2* in fusion-competent myoblasts via enhancer I-E in *Drosophila* embryos (Duan et al., 2001). In adult *Drosophila* myoblasts, transcription of *Mef2* has been shown to be induced by steroid hormone ecdysone(Lovato et al., 2005).

Hand:

Hand gene family is highly conserved among*Drosophila* and vertebrates and encodes basic helix-loop-helix (bHLH) transcription factors that play a crucial role in cardiac and vascular development. In *Drosophila*, *Hand* is expressed in cardioblasts, pericardial cells, and lymph glands; the three major cell types that form the circulatory system . *Hand* has been reported to be required for heart and lymph gland formation (Han et al., 2006). The homeodomain proteins Pannier and *Tinman* directly regulate *Hand* in cardioblasts and pericardial cells while serpent regulates *Hand* expression in the lymph gland (Han et al., 2006). One additional family of transcriptional factors that have been shown to regulate *Hand* expression is the T-box family whose members are Dorsocross 1, 2 and 3 (Han et al., 2006)..

1.14 Objectives of present work:

Mitocohndria provides ATP to fuel every signaling pathway inside the cell. Therefore, it was quite intuitive to know whether it would affect developmental decisions made by nucleus. To answer this question, I chose *Drosophila*cardiogenesis because of simplicity of model, easy genetic manipulations and well explored circuitry of cardiogenic specifications.

The specific questions that I asked for my study are:

1) Whether mitochondrial perturbations can affect the development of the heart in *Drosophila*embryo; thereby attempt*in*g to establish *Drosophila* embryonic heart as a model to study metabolic dysfunction induced CHDs.
2) If so, investiga*tin*g the cardiac defects in terms of functionality, structural and cellular characterization.
3) Even though mitochondrial dysfunction has been associated with CHDs, the mechanistic basis is not known. This study aimed to study the underlying factors to exert these defects during embryonic development.

Chapter: 2

Materials and Methods:

2.1 Fly culture

The flies were reared on standard cornmeal food containing maize powder and sucrose as carbohydrates sources, yeast as the protein source, propionic acid and nepagin as preservatives and antifungal agent, respectively and agar for solidification. All fly stocks were grown at 25^{o}C (if not otherwise mentioned) in standard bottles/vials.

2.2 Fly Stocks and Genotypes

Most of the *Drosophila* stocks were procured from Bloomington Drosophila Stock Center and whenever required new lines were generated by crossing or recombining with appropriate lines.

1) ***w^{1118}***: These flies carry the recessive white mutation on the first chromosome. As a result, the homozygous mutants are white eyed. They were used as an experimental control, in most cases.

2.2. a GAL4 driver lines:

2.2d.1. ***y^{1}w*' P{Gal4-twi.2XPE}2*** (Schubiger, G. (1997.3.14). 2xPE-1 GAL4): This transgenic line has Gal4 insertion downstream of *Twist* enhancer. It expresses GAL4 in a ventral stripe 12-14 cells wide at the cellular blastoderm under the control of the *Twist* proximal element. This transgenic insertion is on the second chromosome. This fly stock is homozygous viable although there may be a segregating cyo. This fly stock was obtained from the Bloomington stock center. (# 2517)

2.2d.2. ***Mef2gal4 y[1] w[*]; P{w[+mC]=GAL4-Mef2.R}3*** (Schnorrer, F. (2009.5.11): This transgenic line has Gal4 insertion downstream of *Mef2* enhancer. It expresses Gal4 in the muscle cells. It is on the 3rd chromosome. This fly stock is homozygous viable. It was obtained from the Bloomington stock center (#27390)

2.2d.3. ***Tin C delta 4 Gal4:*** (Lo PCH, Frasch M., 2001): this transgenic line has subdeletion in 3' end of tin car enhancer. It expressed Gal4 in the *Tinman* positive cardioblasts. It is on the 3rd chromosome and homozygous viable. It was a kind gift from Manfred Frasch.

2.2d.4. ***Hand Gal4:*** (Han and Olson, 2005): This transgenic line expresses GAL4 under the control of the HCH enhancer. This fly line is homozygous viable and is on the 3rd chromosome. This stock was a gift from Eric Olson.

2.2d.5. ***w^{1118}; P{Gal4-da.G32}2; MKRS/TM6B, Tb^1*** (Wodarz, A. et al., 1995): This transgenic line expresses Gal4 under the control of *daughterless* (*da*) promoter. The *daughterless* promoter drives GAL4 expression ubiquitously in the fly through development. This fly line is homozygous viable. This transgenic insertion is on the second chromosome. This stock was obtained from the Bloomington Stock Centre (# 8641).

2.2b UAS responder lines:

2.2c.1. ***w^{1118}; P{UAS-GFP.nls} II***: This transgenic fly stock expresses cDNA of Green Fluorescence Protein tagged with Nuclear Localizing Signal downstream to UAS. Generated in Prof. Bruce Edgar's lab, this fly stock is homozygous viable. The transgene is present on the second chromosome. The stock was obtained from the Bloomington Stock Centre (#6294).

2.2c.2. ***w^{1118}; P{UAS-Cat.A}*** *(*Missirlis, et al., 2001)**:** This transgenic fly stock expresses cDNA of gene Catalase downstream to UAS. When activated by gal4 proteins, it expresses peroxide scavenging enzyme Catalase. The transgene is present on the second chromosome and is homozygous viable. The stock was obtained from Bloomington Stock Centre (#24621).

2.2c.3. ***w^{1118}; P{w[+mC]=UAS-Sod2.M}UM83*** *(*Missirlis, et al., 2003)**:** This transgenic fly stock expresses cDNA of gene Superoxide Dismutase II downstream to UAS. When activated by Gal4 proteins, it expresses superoxide scavenging enzyme *SOD2*. The transgene is present on the second chromosome and is homozygous viable. The stock was obtained from the Bloomington Stock Centre (#24494).

2.2c Mutant lines:

2.2c.1. **w^{1118}; P{w[+mc]=EP}ND-42 [G4500]/ TM6C, Sb[1] :** (Bellen et al, 2011): This fly line is a loss of function allele of *ND42* generated under Gene Disruption Project by TE mobilization using P element construct P{EP}. This

mutant fly line is balanced by TM6C, Sb on the 3rd chromosome. This line was obtained from the Bloomington Stock Centre. (# 30085)

2.2c.2. PINK1^{B9}/ FM7RFP: (Park et al, 2006): This mutant fly line is a loss of function allele of *PINK1* generated by imprecise excision of the insertion resulting in deletion of 570 bp of *PINK1* sequences.

2.2d GFP insertion lines:

***2.2da w^{1118}; P {GstD1-GFP.S}II* :** (Sykiotis and Bohmann, 2008) This transgenic fly line has an insertion on the second chromosome which expresses GFP under enhancer region of *GstD1* gene. It is used as the reporter for high ROS in the cell. This line was a kind gift from D. Bohman.

2.2db E(spl)mβ1.5-CD2 (de Celis et al, 1998): In this transgenic line, a 1.5 Kb genomic Psp14061 fragment containing the E(spl)HLHmb promoter and transcription start site derives Rnor/CD2 expression. It is used as a notch reporter line.

2.2dc HandGFP; Sco/Cyo: (Han and Olson, 2005): This transgenic line expresses GFP under the control of HCH enhancer. This fly line is homozygous viable and is on the 3rd chromosome. This stock was a kind gift from Eric Olson.

2.2dd HAND C GFP (Sellin et al, 2006)*: In this transgenic line, 1611 bp of Hand genomic sequence is fused upstream of EGFP tagged with a nuclear localization signal. It was a kind gift from Achim Paululat.*

2.2de **Zcl 1700** (Morin et al, 2001): This transgenic line is an insertion line stock derived by TE mobilization using the protein trap construct P (PTT-GA). The construct carries a w^{+mc} mini white visible marker and an Avi/GFP vital fluorescent protein marker. This fly line expresses GFP under the control of Trol and is homozygous viable. It is on the first chromosome.

2.2df w^{1118}; **SvpGFP/ cyo** (Rebecca Spokony insertion line): This transgenic fly line is an insertion line generated under Rebecca Spokony insertion lines project to create

GFP insertion lines. It expresses GFP under the control of *Seven up* and balanced by Cyo on 2nd chromosome. It marks *Seven up* positive cardio blasts in the dorsal vessel.

2.2e UAS RNAi LINES:

The different UAS-*RNAi* fly lines used in this study were obtained from the Bloomington Stock Centre, Indiana, US

These lines were generated under the Transgenic *RNAi* Project (TRiP) of Harvard University, USA (Dietzl et al; 2007). These transgenic RNAi fly lines were generated by using the Valium (Vermillion-AttB-Loxp-Intron-UAS-MCS) vector based on phiC31 site-specific integration (Ni et al; 2007).

2.2e1 y^1 sc^* v^1; UAS-ND42 RNAi^{HMS00798}: These transgenic flies express short hairpin RNA for *RNAi* of *ND42* under the control of UAS in VALIUM 20 vector. This transgenic construct is homozygously viable on the third chromosome. This stock was obtained from the Bloomington Stock center (32998).

2.2e2 y^1 v^1; UAS ND42 RNAi^{HM05104}: These transgenic flies express short hairpin RNA for *RNAi* of *ND42* under the control of UAS in VALIUM 20 vector. This transgenic construct is homozygously viable on the third chromosome. This stock was obtained from the Bloomington Stock center (28894).

2.2e3 y^1 v^1; UAS ND-75 RNAi$^{JF02791:}$ These transgenic flies express short hairpin RNA for *RNAi* of *ND75* under the control of UAS in VALIUM 20 vector. This transgenic construct is homozygous viable on the third chromosome. This stock was obtained from the Bloomington Stock center (27739).

2.2e4 *y^1 sc^* v^1; UAS-ND75 RNAi^{HMS00853}*: These transgenic flies express short hairpin RNA for *RNAi* of *ND75* under the control of UAS in VALIUM 20 vector. This transgenic construct is homozygous viable on the third chromosome. This stock was obtained from the Bloomington Stock center (33910).

2.2e5 P{KK107641} VIE-260B: These transgenic flies express short hairpin RNA of *ND42* under the control of UAS. This transgenic construct is homozygous viable and is on the second chromosome. This stock was obtained from the Vienna *Drosophila* Resources Center (110787).

2.2e6 P{KK108222} VIE-260B: These transgenic flies express short hairpin RNA of *ND75* under the control of UAS. This transgenic construct is homozygous viable and is on the second chromosome. This stock was obtained from the Vienna *Drosophila* Resources Center (100733).

2.2e7 y^1v^1; UAS PINK1 $RNAi^{JF1203}$: These transgenic fly lines express short hairpin RNA of *PINK1* under the control of UAS in the Valium 1 vector. This transgenic construct is homozygous viable and is on the third chromosome. This stock was obtained from the Bloomington Stock Centre (31262).

Table2.1 Detailed genotypes of fly lines analyzed for this study

To screen different Gal4 drivers that can induce embryonic lethality
w; Tinc^4Gal4/+; UAS X RNAi (X RNAi: GFP RNAi, ND42 RNAi, ND75 RNAi) *w; Hand Gal4/+; UAS X RNAi* *w; Mef2 Gal4/+; UAS X RNAi* *yw; Twist Gal4/+; UAS X RNAi*
For structural and functional characterization of embryonic heart
Hand GFP/+; Twist Gal4/+; +/+ *Hand GFP/+; Twist Gal4/+; UAS-ND42 $RNAi^{HMS00798}$/+* *Hand GFP/+; Twist Gal4/+; UAS-ND75 $RNAi^{HMS00853}$ /+* *Trol GFP/+; Twist Gal4/+; +/+* *Trol GFP/+; Twist Gal4/+; UAS-ND42 $RNAi^{HMS00798}$/+* *Trol GFP/+; Twist Gal4/+; UAS-ND75 $RNAi^{HMS00853}$ /+*
For Cellular characterization of embryonic heart
yw; Twist Gal4/Svp GFP; +/+ *yw; TwistGal4/SvpGFP; UAS-ND42 $RNAi^{HMS00798}$/+*

yw; TwistGal4/SvpGFP; UAS-ND75 RNAi^{HMS00853}/+
For the detection of ROS in complex-I knockdown embryos
yw; Twist Gal4 gstD GFP/+; +/+ *yw; Twist Gal4 gstD GFP; UAS-ND42 RNAi^{HMS00798}/+* *yw; Twist Gal4 gstD GFP; UAS-ND75 RNAi^{HMS00853}/+*
To isolate mitochondria of Complex I knock down larvae
w; da-Gal4/+; UAS-GFP/+ *w; da-Gal4/+; UAS-ND42-RNAi^{HMS00798}/+* *w; da-Gal4/+; UAS-ND75-RNAi^{HMS00853}/+*
To investigate whether ROS is the causal factor for metabolic dysfunction induced cardiac defects
yw; TwistGal4/ UAS SOD2; +/+ *yw; TwistGal4/ UAS SOD2; UAS-ND42-RNAi^{HMS00798}/+* *yw; TwistGal4/ UAS SOD2; UAS-ND75-RNAi^{HMS00853}/+* *Hand GFP/+; Twist Gal4/UAS SOD2; +/+* *Hand GFP/+; Twist Gal4/UAS SOD2; UAS-ND42 RNAi^{HMS00798}/+* *Hand GFP/+; Twist Gal4/UAS SOD2; UAS-ND75 RNAi^{HMS00853}/+* *Trol GFP/+; Twist Gal4/UAS SOD2; +/+* *Trol GFP/+; Twist Gal4/UAS SOD2; UAS-ND42 RNAi^{HMS00798}/+* *Trol GFP/+; Twist Gal4/UAS SOD2; UAS-ND75 RNAi^{HMS00853}/+* *yw; Twist Gal4 gstD GFP/UAS SOD2; +/+* *yw; Twist Gal4 gstD GFP/UAS SOD2; UAS-ND42 RNAi^{HMS00798}/+* *yw; Twist Gal4 gstD GFP/UAS SOD2; UAS-ND75 RNAi^{HMS00853}/+* *yw; Twist Gal4/+; svp^{AE127}/+* *yw; TwistGal4/UAS SOD2; svp^{AE127}/ UAS-ND42 RNAi^{HMS00798}* *yw; TwistGal4/ UAS SOD2; svp^{AE127}/UAS-ND75 RNAi^{HMS00853}*

To investigate the effect of high ROS levels on cell number in embryonic lymph gland in PINK1 knockdown embryos
yw; Twist Gal4/ Twist Gal4.; +/+ *yw; TwistGal4/+; UAS PINK1 RNAi^{JF01203}/+* *yw; Twist Gal4 gstD GFP/+; +/+* *yw; Twist Gal4 gstD GFP; UAS PINK1 RNAi^{JF01203}/+* *yw; Twist Gal4 gstD GFP; UAS PINK1 RNAi^{JF01203}/+* *yw; Twist Gal4 gstD GFP/UAS SOD2; +/+* *yw; Twist Gal4 gstD GFP/UAS SOD2; UAS PINK1 RNAi^{JF01203}/+* *yw; Twist Gal4 gstD GFP/UAS SOD2; UAS PINK1 RNAi^{JF01203}/+*

2.3 Fly rearing for embryo collection:

For embryo collection, flies are acclimatized to the plate conditions by transferring them to food plates overnight at 25 degrees Celsius (for *RNAi* experiments, flies are reared at 29 degrees Celsius). The next day, synchronized egg collections are set on fruit plates and enriched for desired stages.

2.4 Embryo fixation:

Embryos from the synchronized collection were transferred from plate to a mesh using a small paintbrush by squirting distilled water over the plate. A quick wash of distilled water was given to the embryos to remove unwanted debris and yeast paste. After that, embryos were dechorionated by treating them with 50 percent sodium hypochlorite solution (bleach) for 2 minutes. Bleach was removed by thoroughly washing embryos with distilled water for 3*10’ (3 washes, 10 minutes each).

In the meantime, a fixative (PEMS+4% formaldehyde + heptane) was prepared in the ratio of 7:1:7 in the scintillation vial. Embryos were incubated in the fixative for 40 minutes on a nutator. After fixation is over, the lowermost layer of fixative solution which is comprised of heptanes is removed and replaced by an equal volume of methanol. The resulting two membrane solution is shaken vigorously to facilitate removal of the vitelline membrane. The devitellinized embryos are settled down and are collected with the help of a dropper in a fresh Eppendorf tube. Again, the lowermost layer is removed and methanol of equal volume of the leftover solution is added further and the same process is repeated until all devitellinized embryos are harvested.

After collecting embryos in the Eppendorf tube, methanol is replaced by absolute ethanol and after a quick wash of 5 minutes with ethanol; these embryos are either used for immunostaining or are stored in absolute ethanol at -20 degrees for future use.

2.5 Immunostaining of *Drosophila* embryos:

Embryos stored in ethanol at -20 degrees are brought to room temperature by keeping at RT for 15 minutes.

Ethanol in the embryos is replaced by 0.1%PBT and is rocked at a nutator for 2 minutes at RT.

Embryos are given 3 subsequent 0.1% PBT washes, 10 minutes each at nutator, RT.

After PBT washes, embryos are incubated in a blocking solution (10X NGS in 0.1%PBT) for 1 hour at nutator, RT.

Blocking solution is removed and primary antibody made in 10X NGS in 0.1%PBT is added, embryos incubated in primary antibody overnight at 4 degrees kept at nutator.

The primary antibody is replaced by 0.1%PBT for a 2-minute quick wash at nutator, RT.

3 subsequent washes with 0.1%PBT of 10 minutes each is given to the embryos at nutator, RT.

Embryos are incubated in a blocking solution (10X NGS made in 0.1%PBT) for 40 minutes at a nutator, RT.

The secondary antibody is prepared in 10X NGS and embryos are incubated in the secondary antibody overnight at a nutator, 4 degrees C. From this step onwards, the vial containing embryos is to be covered with aluminum foil to prevent photobleaching of secondary antibody.

After secondary antibody incubation, embryos are quick washed with 0.1%PBT for 2 minutes at a nutator, RT.

Subsequent 3 washes with PBT of 10 minutes each are given at nutator, RT.

After the staining, PBT is replaced by DAPI Vectashield and embryos are mounted in DAPI Vectashield to observe under fluorescence or confocal microscope.

Immunofluorescence images were captured in the Laser Scanning Confocal Microscope (LSM 780, Carl Zeiss). Optical sectioning was done using line mode in the confocal microscope. Images were analyzed and processed using the software Fiji.

2.6a Live Imaging of *Drosophila* Embryos:

All collections were kept at 29 degrees since GAL4 induced RNAi knockdown efficiency is maximum at this temperature. Synchronized egg laying was set for stage 17 embryo collection. Embryos were harvested as mentioned earlier in a mesh and dechorionated using sodium hypochlorite solution. After treating with bleach, embryos were thoroughly washed with distilled water (4 washes of 10 minutes each) to completely remove bleach as it can interfere with the fluorescence signal.

After washings, distilled water was replaced with 1X PBS in the mesh containing embryos. With the help of a fine paintbrush, the embryos of stage 17 were transferred from mesh to halocarbon oil placed on the glass slide. A bridge was made using nail paint on both sides of the halocarbon oil drop containing embryos and after nail paint is dried, a coverslip is placed on the bridge on such a level that embryo is only stabilized and not mashed with the coverslip.

Live imaging was performed in the fluorescence microscope (model name and number) using FITC filter at 20x magnification and analyzed using SOHA (Semi-automated Heart Beat Analysis) software.

2.6b Semi-Automated Heartbeat analysis of Drosophila embryos:

SOHA (Semi-automated heartbeat analysis) software was used to analyze a number of contraction-relaxation parameters in Drosophila embryonic heart. SOHA incorporates a unique set of movement detection algorithms that automatically and precisely detect and measure beat to beat contraction parameters captured in live movies, therefore providing both analytical and statistical power. The resulting output provides detailed information related to pacemaker activity and contraction-relaxation parameters including M-mode, heart rate, systolic interval and diastolic intervals, systolic and diastolic diameters and fractional shortening.

Before analyzing these parameters in knockdown embryos relative to control, these different parameters are briefly defined as follows:

1. M-mode: represents the vertical movement of heart tube edges (y-axis) over time (x-axis)
2. Heart period: is measured as the interval between the start of one diastole and the beginning of the next.
3. Systolic interval (SI): SI is the duration for which cardiac tube stays in the systolic (contraction) phase.
4. Diastolic interval: (DI): is the duration for which the heart stays in the diastolic (relaxation) phase.
5. Systolic diameter: represents the contracted state of the heart tube.
6. Diastolic diameter: represents the relaxed state of the heart tube.

2.7 Immunological detection of Proteins:

2.7a Primary antibodies:

2.7a1 Mef2: This rabbit polyclonal nuclear antibody marks precursors of all three muscle types in embryos i.e. visceral, cephalic and cardiac muscles. It's working dilution is 1:1000. It was a kind gift from H.Nguyen.

2.7a2 Anti β- galactosidase: (Promega, Z3781) this mouse monoclonal purified antibody is against the β-galactosidase protein of *E.coli.* The working dilution is 1:100.

2.7a3 **Anti-GFP mouse:** (Monoclonal Anti-Green Fluorescence Protein GFP Antibody, Mouse Sigma, G6539) this is a mouse monoclonal antibody that recognizes GFP. This antibody was used at working dilution 1:100 for immunostaining.

2.7a4 **Pericardin:**(Developmental Studies Hybridoma Bank, Iowa, EC11) This mouse monoclonal antibody marks extracellular matrix surrounding the pericardial cells and *Seven up* positive cardio blasts from stage 10 of embryogenesis onwards. It also marks ring gland and oenocytes. Its working dilution is 1:3.

2.7a5 **Twist:** This rabbit polyclonal antibody was a kind gift from Maria Leptin. It marks the entire mesoderm population from stage 5 onwards. Its working dilution is 1:1000.

2.7a6 **Seven up:** This rabbit polyclonal antibody marks a subset of cardiac progenitors from stage 11 onwards which later on differentiate into non-contractile inflow valve-forming cells in the cardiac tube. Its working dilution is 1:500.

2.7a7 **Tinman:** This rabbit polyclonal antibody marks the entire mesoderm at stage 9 but later restricted only to cardiogenic precursors. It was a kind gift from Manfred Frasch. Its working dilution is 1:1000.

2.7a8 **Zfh1:** This rabbit polyclonal antibody marks all types of pericardial cell populations at stage 16 of embryonic development. It also marks the lymph gland and circulating hemocytes at stage 16 of embryonic development. Its working dilution is 1:1000.

2.7a9 **Even skipped:** (Developmental Studies Hybridoma Bank, Iowa, 3C10): This mouse monoclonal antibody deposited by Goodman C., marks a subset of pericardial cells surrounding the cardiac tube at stage 16 of embryonic development. Its working dilution is 1:10.

2.7a10 **Odd**: This rabbit polyclonal antibody was a kind gift from Skeath. This antibody marks a subset of pericardial cells surrounding the cardiac tube at stage 16 of embryonic development. Odd also marks the lymph gland at this stage. Its working dilution is 1:1000.

2.7a11 **Antennapedia:** (Developmental Studies Hybridoma Bank, Iowa, 4C3:) This mouse monoclonal antibody, deposited to the DSHB by Brower, D. marks nuclei of cells of the thoracic embryonic epidermis and several segments of the central and peripheral

nervous system. In this study, this antibody is used to mark the niche of the lymph gland which is located in the T3 segment. Its working dilution is 1:5.

2.7b Secondary antibodies for immunostaining:

The different secondary antibodies, used to detect the primary antibodies, were as follows.

2.7b1 Cy^{TM3}-Conjugated affinipure goat anti-mouse (Jacksons Immuno Research Laboratories, USA # 115-166-062). This affinity purified secondary antibody conjugated with cyanine Cy^{TM3} dye (absorption maxima/ emission maxima is 550 nm/ 570 nm) was used at a dilution of 1:600 to detect primary antibodies raised in mouse.

2.7b2 (FITC)-Conjugated affinipure goat anti-mouse (Jacksons Immuno Research Laboratories, USA # 115-095-166). This affinity purified secondary antibody conjugated with Fluorescein FITC dye (absorption maxima/ emission maxima is 492 nm/ 520 nm) was used at a dilution of 1:600 to detect primary antibodies raised in mouse.

2.7b3 Cy^{TM3}-Conjugated affinipure donkey anti-rabbit IgG (H+L) (Jacksons Immuno Research Laboratories, USA # 711-165-152). This affinity purified secondary antibody conjugated with cyanine Cy^{TM3} dye (absorption maxima/ emission maxima is 550 nm/ 570 nm) was used at a dilution of 1:600 to detect primary antibodies raised in rabbit.

2.7b4 (FITC)-Conjugated affinipure donkey anti-rabbit (Jacksons Immuno Research Laboratories, USA # 115-095-166). This affinity purified secondary antibody conjugated with Fluorescein FITC dye (absorption maxima/ emission maxima is 492 nm/ 520 nm) was used at a dilution of 1:600 to detect primary antibodies raised in rabbit.

2.7c Stains:

2.7c1 DAPI (4',6-diamidino-2-phenylindole dihydrochloride, Molecular Probe, India # ZB1130). This is a blue fluorescent dye that binds to A-T rich region in dsDNA

thereby use to stain nuclei in alive as well as fixed tissues. Its absorption maxima/ emission maxima is 351nm/ 461nm. The working dilution was 1µg/ml.

Embryos after secondary antibody treatment were washed with 1X PBS for 5'X3. Then, embryos were incubated in DAPI solution (1µg/ml) in 1X PBS for 30 minutes at room temperature. After incubation, embryos were washed with 1X PBS and observed after mounting in vectashield.

2.8 Statistical analysis of lumen diameter of cardiac tube in stage 16 Drosophila embryos:

In order to measure lumen diameter of cardiac tube marked by TrolGFP, cardiac tube was subdivided into anterior aorta and posterior heart proper region. In both of these parts of the cardiac tube, 5 points of measurements were taken from each segment. Average of these measurements was calculated to infer readings for each sample.

2.9 MitoSOX dye labeling of *Drosophila* embryos:

Embryos were transferred from the fruit plate to the sieve with the help of a paint brush. Embryos were treated with bleach for 2 minutes to remove chorion. After that, they were given 4 washes of 10 minutes each with distilled water for complete removal of bleach. Embryos were dehydrated with 100% isopropanol for 40 seconds followed by pat drying to remove isopropanol. After that, embryos were treated with hexane for 4 minutes followed by pat drying to remove hexane. Embryos were washed using 1X Ringer's solution containing 0.1%BSA for 2 minutes on a shaker. Sieve containing embryos was soaked in msox solution (1:5000 in 1X PBS). Volume was kept to a level that all embryos get immersed in the dye solution. They were incubated in the dye for 25 minutes. Embryos were washed off with Ringer's solution for 2 minutes on a shaker. Embryos were mounted in halocarbon oil and imaged under the confocal microscope.

2.10 ATP Assay:

ATP assay was performed as from fat bodies of control and mtAcp1 knock down fat bodies. Fat bodies were dissected in 1X PBS and homogenized in ATP assay Lysis buffer ( ). The samples were boiled at 95^0C for 5 minutes and diluted 1:1000 in dilution buffer provided in ATP luminescence kit HSII (Roche). The further assay was performed as instructed by the kit's

manual in Luminometer (Promega). A standard curve was generated and ATP concentrations were calculated. The ATP concentration was normalized with protein concentration.

2.11 Mitochondria Isolation:

Mitochondria isolation was performed by MitoIso Kit (Sigma) according to the manual's instruction. Larvae were washed and homogenized in 1X Extraction Buffer A with 0.1 mg/ml. Homogenate was centrifuged at 600 X *g* for 5 minutes at 4^0C. The supernatant was centrifuged at 11,000 X *g* for 10 minutes. The pellet was resuspended in 1X Extraction Buffer A and recentrifuged as above. The pellet was resuspended in 1X Storage Buffer and stored at -20^0C.

2.12 Complex I Assay:

The isolated mitochondria samples were thawed at room temperature. 3 µl of purified mitochondrial were 150µl of prepared colorimetric complex I activity assay buffer (1X PBS, 3.5 g/l BSA, 0.2 mM NADH, 0.24 mM KCN, 60 µM DCIP, 70 µM decylubiquinone, 25 µM antimycin A). NADH: ubiquinone oxidoreductase activity as a drop in DCIP absorbance was recorded at 600 nm (on Epoch microplate spectrophotometer (BioTek, USA)) for 180 sec at the interval of 30 sec. Rotenone insensitive activity was measured as the difference in DCIP reduction in the presence of rotenone (2 µM) in the assay buffer. The Rotenone sensitive NADH: ubiquinone oxidoreductase activity was normalized with citrate synthase activity.

2.13 Citrate synthase Assay:

Mitochondrial samples were diluted to 10 fold in storage buffer. 5 µl diluted mitochondria sample was added to 150 µl of a previously prepared colorimetric citrate synthase activity assay buffer (50 mM Tris (pH 8.0), 0.1 mM 5, 5'-dithiobis- (2-nitrobenzoic acid) (DTNB), 0.3 mM acetyl-CoA, 1 mM oxaloacetic acid). Citrate synthase activity was measured as an increase in DTNB absorbance at 412 nm using a microplate spectrophotometer [at an interval of 30 sec for 180 sec]

2.14 RNA isolation from embryos on Column

An appropriate number of (200 embryos/.) synchronized embryos were collected and dechorionated using sodium hypochlorite (bleach). Embryos were thoroughly washed with

distilled water to remove bleach. Dechorionated embryos were homogenized in trizol (Invitrogen) and extracted with 200µl of chloroform (Sigma). Further purification was performed by using the RNeasy Mini Kit (Qiagen) as instructed. 25 minutes incubation at 37^0c was given with RNase free 2U DNase (Qiagen-79254) in RDD buffer to remove residual DNA. The RNA pellet was dissolved in nuclease-free DEPC treated water (Sigma).

Quantitation of RNA was performed by using a Nanodrop spectrophotometer.

2.15 cDNA Synthesis

cDNA was synthesized using the Verso cDNA synthesis kit (Molecular Probe # AB1453A) following the manufacturer's recommended protocol. 500 ng of RNA was used for cDNA synthesis. RNA was incubated with a cDNA reaction mix at 42˚C for 30 min and then kept on 95˚C for 2 min. c-DNA mix was prepared using 5X RT buffer, 500µM dNTP mix, Oligo dT, and random Hexamer primer mix, RT Enhancer to remove contaminating DNA and Verso enzyme mix which acted as reverse transcriptase for c-DNA manufacture. c-DNA mix was added to the RNA and the reaction was mixed properly by pipetting and short spin. This mixture was then incubated at 42˚C for the first 30 min. The reaction was terminated by incubating at 95˚C for the last 2 min cDNA samples were stored at -20˚C.

Preparation of Reaction Mixture:

Constituents	Final Concentration	Volume (µl) For 1 reaction
Water, nuclease-free		Volume makes up to 20µl
5 X RT Buffer	1X	4
dNTPs Mix (500µM)	50 µM	2
RT Enhancer	1.5 mM	1
RNA Primer	1X	2
Verso Enzyme Mix	1 unit	1
RNA (500ng/µl)	500ng	1-5µl
Total		20

2.16 RT PCR

PCR amplification reactions were carried out in a final volume of 20 µl. The reaction mixture was prepared by adding reagents in the following sequence: PCR water; 10X Taq Buffer; dNTPs mix; $MgCl_2$; Forward Primer; Reverse Primer; and Taq Polymerase.

Preparation of PCR Reaction Mixture:

The amplification reaction consisted of 40 cycles with initial denaturation at 94˚C for 5 min, followed by 39 cycles of denaturation at 95˚C for 30 sec, annealing at 59˚C (Variable for a different set of primers) for 30 sec and extension at 72˚C for 30 sec. The reaction was terminated after the final extension for 10 min at 72˚C. 10µl of PCR products were loaded on 1% agarose gel along with 50bp DNA ladder as the marker to check the amplification.

Constituents	Final Concentration	Volume (µl) For 1 reaction
PCR water		15.8
20 X Taq Buffer	1X	1.0
dNTPs Mix (10mM)	0.2mM	0.4
Forward Primer (10µM)	1µM	0.4
Reverse Primer (10µM)	1µM	0.4
Taq Polymerase (3 unit/ µl)	0.6 units	0.2
DNA (500ng/µl)	500ng	1
Total		20

2.17 Real-Time PCR

The transcript level of different genes was compared by quantitative RT- PCR on RNA isolated from 50-60 late third instar larval imaginal discs of each genotype by using standard TRIzol method. Real-time qRT PCR was performed using the SYBR green mix Biorad on the Biorad CFX96 instrument, following the instructions provided in the manual. After setting up the reactions with SYBER Green, plate form was made on instrument and reaction was set up at

95^0c for 15 sec and 59^0c for 15 sec and 72^0c for 15 sec for 40 reactions. The melting curve was performed from 95^0c to 72^0c for 5 min, to analyze Tm of the amplicon. Expression analysis was performed on the instrument using ΔΔCt method.

Expression level was normalized to Act level and then compared with respect to W^{1118}. Primers were designed from NCBI. We specifically designed primers from the exon-exon junction to avoid any misinterpretation from DNA contamination. The specificity of primers was checked with primer blast.

The following primer sequences were used:

S.No.	Gene Name	Primer Sequence
1.	***Rp49***	TAAGCTGTCGCACAAATGGC TCTGCATGAGCAGGACCTC
2.	***PINK1***	GCTCAGCAAGGATGAAC AAATCCGCTGCATAGACGAC
3.	***ND42***	GAGGCCGATATTCACAACA GGGAGCATTGAACCAGACAT
4.	***ND75***	GTACCCGGCACCACTGTC AGCAGAATCTGGGTATCTCCAC

Chapter 3

Establishment of a model system to study metabolic dysfunction induced congenital heart diseases in *Drosophila* embryos.

3.1 Introduction

There are accumulating pieces of evidence that suggest that mitochondrial dysfunction plays a key role in early cardiac defects (Neubauer, 2007). There are reports which suggest that impairment of mitochondrial DNA replication and mitochondrial DNA deletion precedes heart failure in children with CHDs. Based on these reports, the relationship between mitochondrial biogenesis and risks of CHDs are indicated (Karamanlidis et al., 2010). There is a need to develop a model system for in depth analysis of mitochondrial associated CHDs.

In the current study, we are trying to establish *Drosophila* embryonic heart as a model system to study CHDs so that an association between metabolic dysfunction and CHDs can be questioned on the cellular level. *Drosophila* embryonic heart has emerged as one of the most attractive model systems to study cardiac defects due to its simplicity and easy genetic manipulations. Additionally, most of the transcription factors and signaling pathways involved in cardiogenesis are highly conserved in *Drosophila* and vertebrates despite their evolutionary distance.

To achieve tissue specific knockdown of mitochondrial genes, we have employed two well-established genetic tools

a) Gal4-UAS system:

The Gal4-UAS system was demonstrated by Fischer et al (Fischer et al., 1988) and later developed by Andrea Brand and Norbert Perrimon in 1993 (Brand and Perrimon, 1993). This system is the most frequently used genetic tool that allows the expression of the desired

transgene in a spatiotemporal manner (Fischer et al., 1988). This bipartite system taken from the yeast consists of transcriptional factor Gal4 and upstream activating sequence UAS (St Johnston, 2002). The sequence encoding Gal4 protein can be cloned downstream to the desired promoter. In another fly, a transgene of interest is cloned downstream to UAS. By crossing these two fly lines, the gene of interest is expressed in the desired cell type at the specified developmental time regulated by the Gal4 protein expressing promoter region in F1 progeny. Hence, targeted expression of a gene can be obtained using this tool (Fig. 3.1). A number of tricks have been used in order to refine this approach in order to achieve higher spatial a nd temporal resolution. The temperature sensitive Gal4 repressor $Gal80^{ts}$ can be co-expressed so that Gal4 –induced expression is active only during periods when the flies are shifted to 30 degreeC (McGuire, Mao, and Davis, 2004).

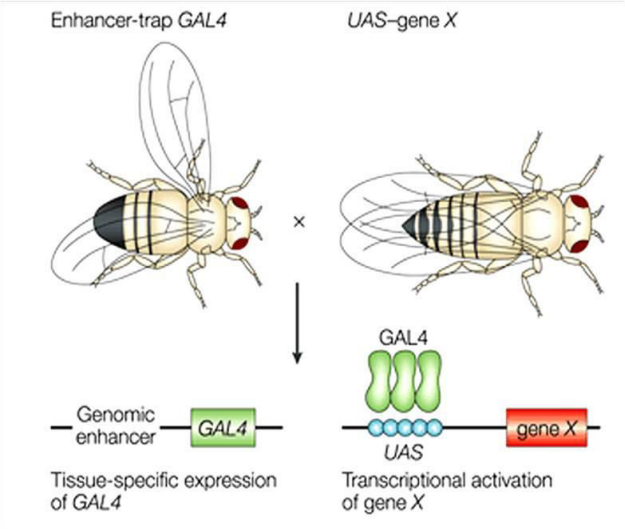

Figure 3.1: Schematics of Gal4- UAS system for targeted expression of desired transgene in spatiotemporal manner. (St Johnston, 2002)

b) *RNAi in Drosophila:*

There are many genes whose mutations are embryonic lethal; therefore it is not feasible to study the role of these genes during embryonic development due to the lack of an observable phenotype. *RNAi* mediated knockdown strategy can be employed in such a scenario for targeted knockdown of a particular gene in a tissue or organ-specific manner.

Mechanism of RNAi mediated knockdown

As shown in Figure 3.2, long double-stranded RNA (dsRNA) molecules are cleaved by Dicer into small fragments (around 20 nucleotides) known as small interfering RNAs (siRNA) (Fire et al., 1998). One of the two strands is degraded and another, acting as a guide strand forms the RNA-induced silencing complex (RISC). The guide strand, present within the RISC, binds to the complementary sequence on mRNA; this causes degradation of the targeted mRNA molecule (Fig. 3.2). This RNAi mediated gene silencing method is very robust and specific, therefore both in *vitro* as well as *in vivo* studies; it is one of the widely used tools to knock down genes. However, in case of mismatched miRNA or target sequence, non cleavage repression known as translational inhibition takes place.

Certain modifications in RNAi knockdown strategy are possible e.g. using the Gal4-UAS system, a spatiotemporal knockdown of a gene can be performed using its specific RNAi.However, there are certain drawbacks of this technique including variability of knockdown efficiency, off-target effects, and failure to identify regulatory domains of a protein(Sledz and Williams, 2005).

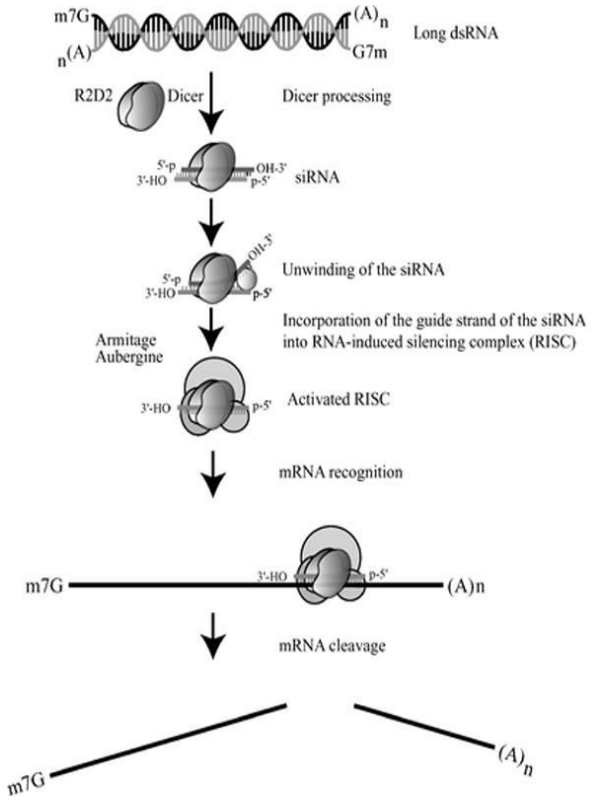

Figure 3.2: Schematic representation of the pathway for *RNAi* mediated gene silencing in *Drosophila {* Modified fromAnnual review of medicine, The silent revolution: RNA interference as basic biology, research tool, and therapeutic,***(Dykxhoorn and Lieberman, 2005)}***

Complex-I is reported to be most commonly affected in CHDs. Therefore, for this project, we chose UAS-dsRNA expressing lines for two genes *ND42* and *ND75* that encode different components of complex-I of ETC (Fig.3.3).

***ND42*:**

ND42 (NADH dehydrogenase (ubiquinone) 42 kDa subunit) is a supernumerary subunit of complex-I of ETC which is critical for assembly of complex-I subunits. It encodes an ortholog of human NDUFA10,a subunit of complex-I of the mitochondrial electron transport chain (NADH:ubiquinone reductase). It has been reported that *ND42* acts genetically as a suppressor of some *PINK1* phenotypes such as flight and climbing defects (Pogson et al., 2014). In *Drosophila PINK1* mutants, transgenic over expression of *ND42* was able to rescue flight and climbing

defects as well as mitochondrial disruption in flight muscles.*PINK1* has been shown to regulate complex-I of ETC by phosphorylation of *ND42* subunit at Ser250 (Pogson et al., 2014).

ND75:

ND75 is the core subunit of mitochondrial membrane respiratory chain NADH dehydrogenase (Complex- I). Complex I functions in the transfer of electrons from NADH to the respiratory chain. This is the largest subunit of complex I and it is a component of the iron-sulfur (IP) fragment of the enzyme. It may form part of the active site crevice where NADH is oxidized. Its human homolog is NDUFS1.

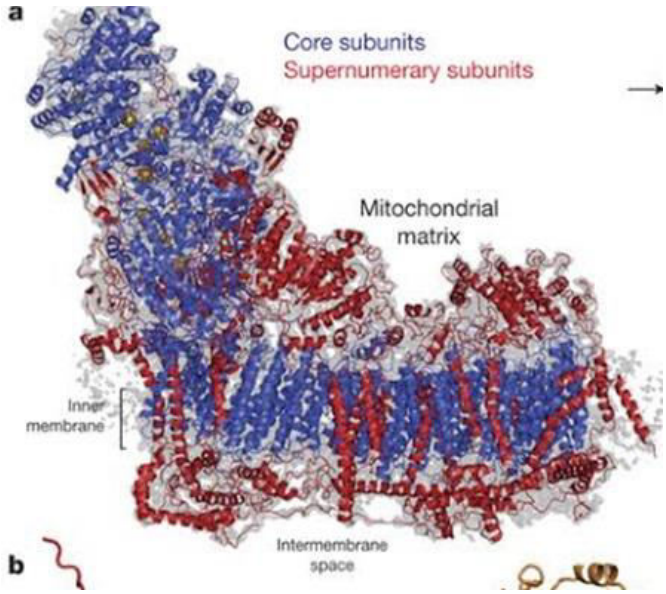

Figure 3.3: Structure of complex-I of ETC{Adapted from (Zhu et al., 2016)}

3.2 Different Gal4 lines used

In order to determine whether mesoderm specific knockdown of nuclear gene encoding complex-I components have any detrimental effect on survival rate in F1 generation, different Gal4 lines were used to induce*ND42*/75 knockdown in the developing mesoderm.Following is the description of the genes that were used to drive Gal4:

***Twist*:**

Twist is a member of helix-loop-helix protein family (Boulay et al., 1987; Thisse et al., 1988).*Twist* along with snail determine the development of mesoderm in Drosophila by regulating transcription of other genes(Wieschaus et al., 1984). Embryos mutant for *Twist* exhibit abnormal gastrulation and absence of mesodermal derivatives(Grau et al., 1984; Simpson, 1983). Transcription of *Twist* is regulated by maternally derived transcription factor Dorsal. *Twist* expression start in the blastoderm at stage 4 of embryonic development (Fig.3.4). *Twist* expressing regions give rise to different derivatives of mesoderm. Low *Twist* expressing regions give rise to visceral mesoderm whereas high *Twist* expressing regions give rise to somatic muscles. The dorsal crests of the *Twist* expressing mesodermal cells give rise to cardiac progenitors (Dunin-Borkowski and Brown, 1995). It has been shown that Notch is a key player in regulating *Twist*. Notch/ Su(H) regulates *Twist* directly as well as indirectly by activating proteins that repress *Twist*. Hence the patterning of *Drosophila* meosdermal segments depends on *Notch* regulated change in activities of network of bHLH transcriptional regulators which in turn regulate mesodermal cell fate(Tapanes-Castillo and Baylies, 2004). Therefore, *Twist*Gal4 is expected to drive RNAi induced knockdown from stage 5 or stage 6 of embryonic development since it takes some time for Gal4 protein to form and function. It will lead to *ND42*/*ND75* knockdown in all the *Twist* expressing regions of developing mesoderm.

Mef2:

As discussed in chapter 1, *Mef2* (Myocyte enhancer factor 2) is expressed in the presumptive heart and skeletal muscle precursors. *Mef2* expression is dependent on *Twist*(Cripps et al., 1998). *Mef2* expression is complex and dynamic in embryos. *Mef2* is first evident in the late cellular blastoderm stage and continues to be expressed throughout the mesoderm during mesoderm invagination (Fig.3.4)..*Mef2*Gal4 is expected to induce *RNAi* mediated knockdown of complex-I components in the developing mesoderm from stage 7 onwards in *Mef2* expressing mesodermal derivatives.

Hand:

In *Drosophila*, *Hand* is expressed in cardioblasts, pericardial cells, and lymph glands; the three major cell types that form the circulatory system (Fig.3.4). *Hand* Gal4 will drive RNAi induced

knockdown of complex-I components from stage 13 onwards in cardioblasts as well as pericardial cells.

Tincar:

Tincar is a transmembrane protein with multiple hydrophobic regions. Whole mount in situ hybridization revealed that *tincar* transcripts start to express at stage 15 of embryonic development ina subset of cells of the dorsal vessel (Fig.3.4). It was named *tincar* because of its specific expression in *Tinman* expressing cardioblasts only. *Seven up,* which is a negative regulator of *Tinman* in cardioblasts, also negatively regulates*tincar* expression. It has also been suggested that *Tinman* is involved in the activation of *Tincar*(Hirota et al., 2002).

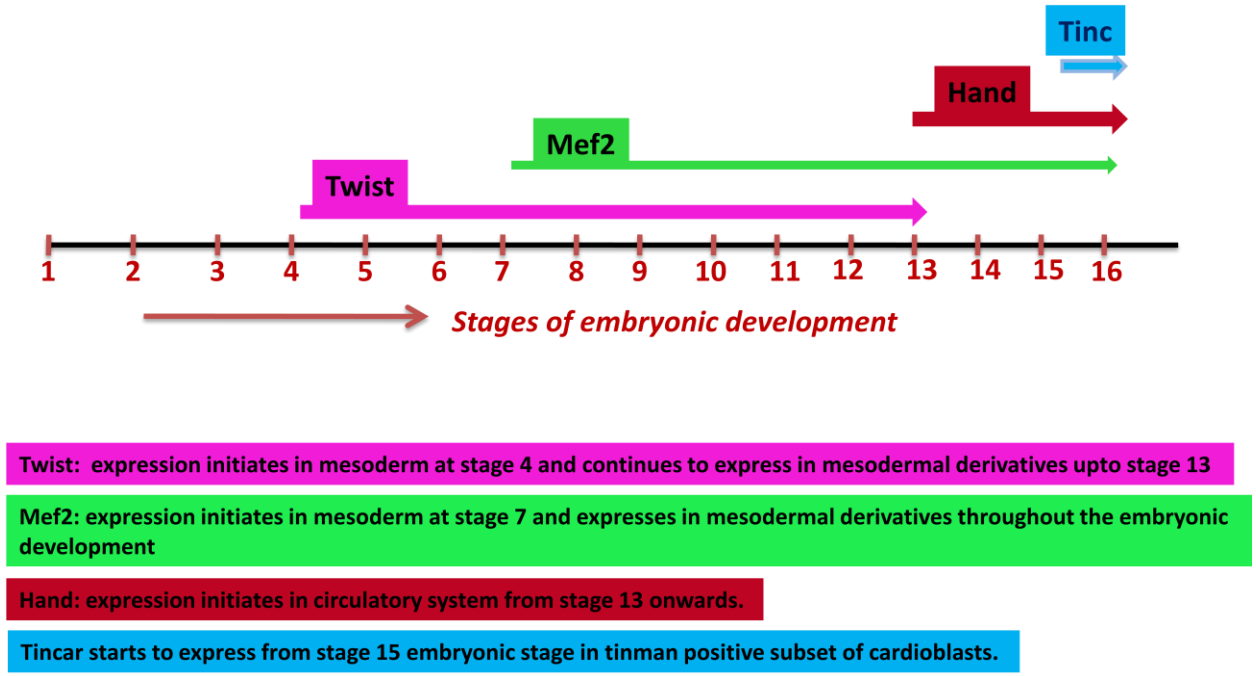

Figure 3.4: Schematic showing spatiotemporal expression of Gal4 drivers.

3.3 Results:

3.3.1 Ubiquitous Knockdown of genes encoding *ND42* and *ND75* in *Drosophila* embryo leads to decline in Complex- I activity of ETC:

By knocking down *ND42* and *ND75* using *DaughterlessGal4 (DaGal4)* which is a ubiquitous Gal4 driver, it was found that complex-I activity is declined to significant levels. In case of

DaGal4/+; UAS ND42dsRNA/+, an average of 66% complex-I activity is left whereas in case of *DaGal4/+; UAS ND75dsRNA/+*, an average of 40% activity is left (Fig. 3.5B). qRT PCR analysis revealed a drastic decline in fold change transcript levels of *ND42* and *ND75* in case of *DaGal4/+; UAS ND42dsRNA/+*, and *DaGal4/+; UAS ND75dsRNA/+*, knockdown embryos respectively(Fig. 3.5A).

3.3.2 Knockdown of ND42/75 by TincarGal4, HandGal4, and Mef2Gal4 drivers doesn't affect the hatching rate of embryos significantly:

In the synchronized embryo collection batches of *TincarGal4/+; UAS GFPdsRNA/+* which served as positive control, average 87 % embryos were hatched. In case of *tincarGal4/+;UAS ND42dsRNA/* +and *tincarGal4/+;UAS ND75dsRNA*/+ embryo collections, 86% and 84% embryos were hatched respectively, thereby suggesting no significant change ($p>0.1$) in hatching rate of knockdown embryos compared to control (Fig.3.5C).

In the synchronized embryo collection batches of *HandGal4/UAS GFPdsRNA* which served as positive control, average 87% embryos were hatched. In case of *HandGal4/UAS ND42dsRNA* and *HandGal4/UAS ND75dsRNA* embryo collections, 79% and 82% embryos were hatched respectively, inferring no significant change ($p>0.1$) in hatching rate of knockdown embryos compared to control (Fig.3.5C).

In the synchronized embryo collection batches of *Mef2Gal4/+;UAS GFPdsRNA/+*, average 85% embryos were hatched, whereas in case of *Mef2Gal4/+;UAS ND42dsRNA/+* and *Mef2Gal4/+;UAS ND75dsRNA*/+ embryo collections, 75% and 76% embryos were hatched respectively, inferring approximately 10% reduction ($p>0.01$) in hatching rate of knockdown embryos compared to control (Fig.3.5C).

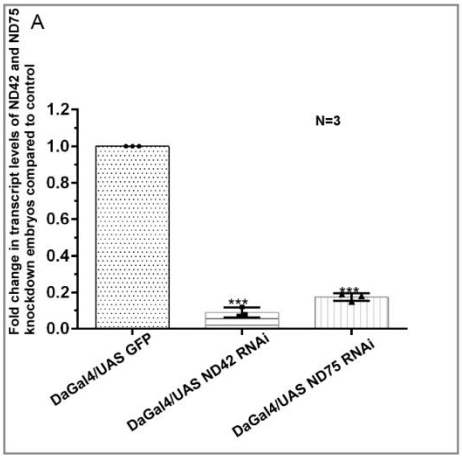
A
Fold change in transcript levels of ND42 and ND75 knockdown embryos compared to control
1.2
1.0
0.8
0.6
0.4
0.2
0.0
N=3
***
***
DaGal4/UAS GFP
DaGal4/UAS ND42 RNAi
DaGal4/UAS ND75 RNAi

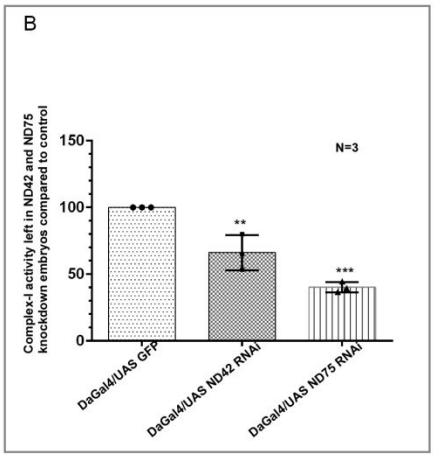
B
Complex-I activity left in ND42 and ND75 knockdown embryos compared to control
150
100
50
0
N=3
**
***
DaGal4/UAS GFP
DaGal4/UAS ND42 RNAi
DaGal4/UAS ND75 RNAi

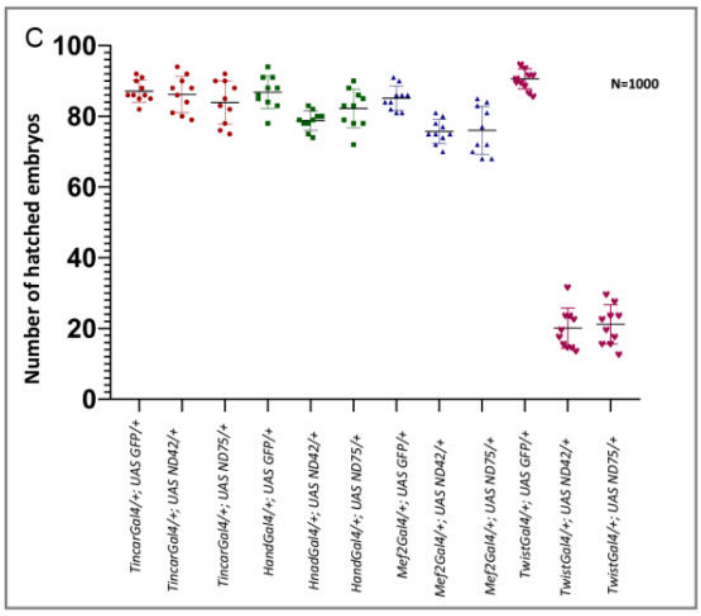
C
Number of hatched embryos
100
80
60
40
20
0
N=1000
TincarGal4/+; UAS GFP/+
TincarGal4/+; UAS ND42/+
TincarGal4/+; UAS ND75/+
HandGal4/+; UAS GFP/+
HnadGal4/+; UAS ND42/+
HandGal4/+; UAS ND75/+
Mef2Gal4/+; UAS GFP/+
Mef2Gal4/+; UAS ND42/+
Mef2Gal4/+; UAS ND75/+
TwistGal4/+; UAS GFP/+
TwistGal4/+; UAS ND42/+
TwistGal4/+; UAS ND75/+

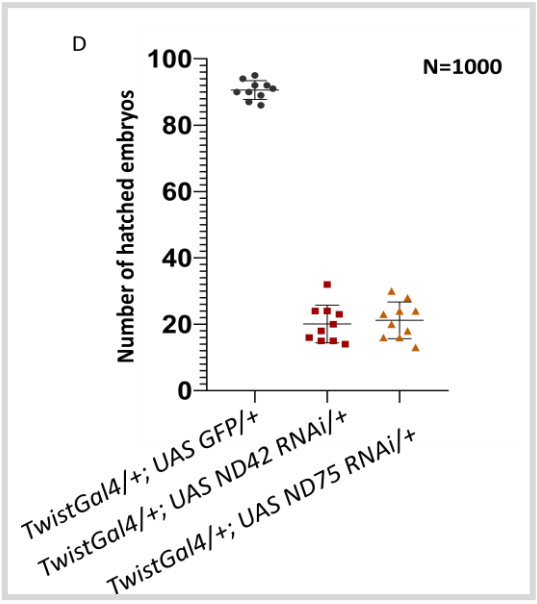
D
Number of hatched embryos
100
80
60
40
20
0
N=1000
TwistGal4/+; UAS GFP/+
TwistGal4/+; UAS ND42 RNAi/+
TwistGal4/+; UAS ND75 RNAi/+

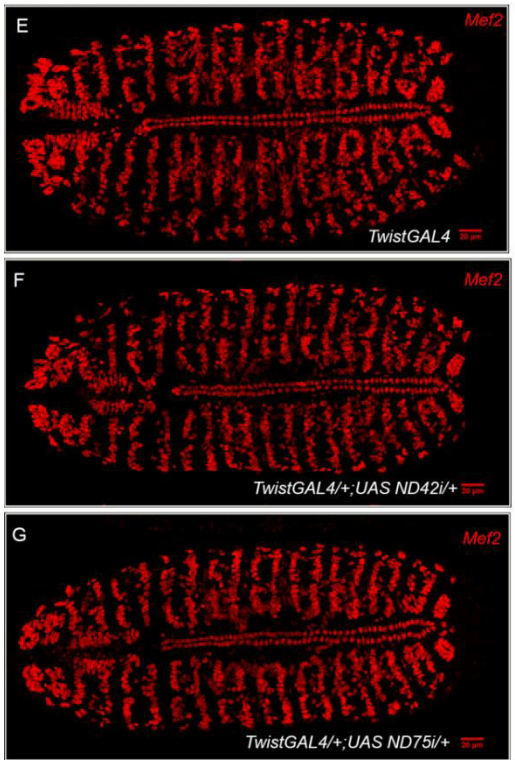

Fig. 3.5. Knockdown of ND42 and ND75 using different mesoderm drivers imparts varying degrees of embryonic lethality. qRT PCR showing fold change in transcript levels of *ND42* and *ND75* compared to control by knocking down these complex-I components using DaGal4 in stage 16 embryos **(A**).The decline in Complex-I activity by knocking down *ND42* and *ND75* using DalGal4 in larvae **(B).** Statistical analysis of hatching rate of embryos in UAS GFP, UAS *ND42*RNAi and UAS *ND75*RNAi backgrounds using 4 different Gal4 drivers) showing no significant change in hatching rate with tin car delta4 gal4, *Hand* Gal4 and *Mef2* Gal whereas around 80 percent reduction in hatching rate with *Twist*Gal4/+;UAS*ND42*dsRNA/+ and *Twist*Gal4/+;UAS *ND75*dsRNA/+ compared to *Twist*Gal/+;UAS GFP/+ (n=1000) **(C).**Drastic reduction (80%) in hatching rate of*ND42* and *ND75* knockdown embryoswhen driven by *Twist*Gal4 **(D**). No severe change in the number or alignment of mesoderm populations in knockdown embryos (b,c)compared to control (a) **(E).**

3.3.3 Mesodermal specific knockdown of complex-I components using *Twist Gal4* driver drastically reduce hatching rate of embryos:

In the synchronized collection batches of *Twist Gal4*/+;*UAS GFP dsRNA*/+, average 87 percent embryos were hatched, whereas in *DaGal4/+; UAS ND42dsRNA/+* and *TwistGal4DaGal4/+; UAS ND75dsRNA/+*, only 20% and 21% embryos were hatched respectively ($p<0.0001$) (Fig.3.5D, 3.6A). These results infer that knocking down complex-I components using *Twist*Gal4 as a driver, there is a drastic reduction in hatching rate of embryos.

The remaining 80 percent unhatched embryos were followed for the next 24 hours confirming there was no late hatching and all of them were non-viable. The hatched population of larvae, when followed for further development, was found to go up to pupal stage but flies never emerged and they underwent pupal death.

From these results, it was clear that knock-down of complex-I encoding components by using very early driver *Twist*Gal4 was detrimental to the survivability of embryos to a significant level. However, 20 percent of the total population still managed to surpass the lethality.

3.3.4 No gross defect in the mesodermal population of stage 16 knockdown embryos:

Stage 16 is the second last stage of embryonic development and the final stage at which standard embryo immunostaining protocol works. In stage 17, the cuticle is well formed; therefore most of the antibodies do not work due to the inability to penetrate the cuticle. Therefore, immunostaining with the *Mef2* antibody was carried out at stage 16 of embryonic development. *Mef2* (myocyte enhancing factor 2) antibody marks nuclei of all the skeletal muscles, pharyngeal muscles as well as all the cardio blasts that constitute the cardiac tube. We did not find any gross defect in cell alignment or change in cell number marked with *Mef2*in which KNOCKDOWN embryos?? knockdown embryos compared to the control. Hence, at stage16, we could not pinpoint the reason behind lethality associated with knockdown of complex-I components as embryos just before hatching seems to be perfectly normal in morphology as indicated by DAPI staining and devoid of any deformity in mesodermal derivatives suggested by *Mef2*immunostaining (Fig. 3.5E,F and G)

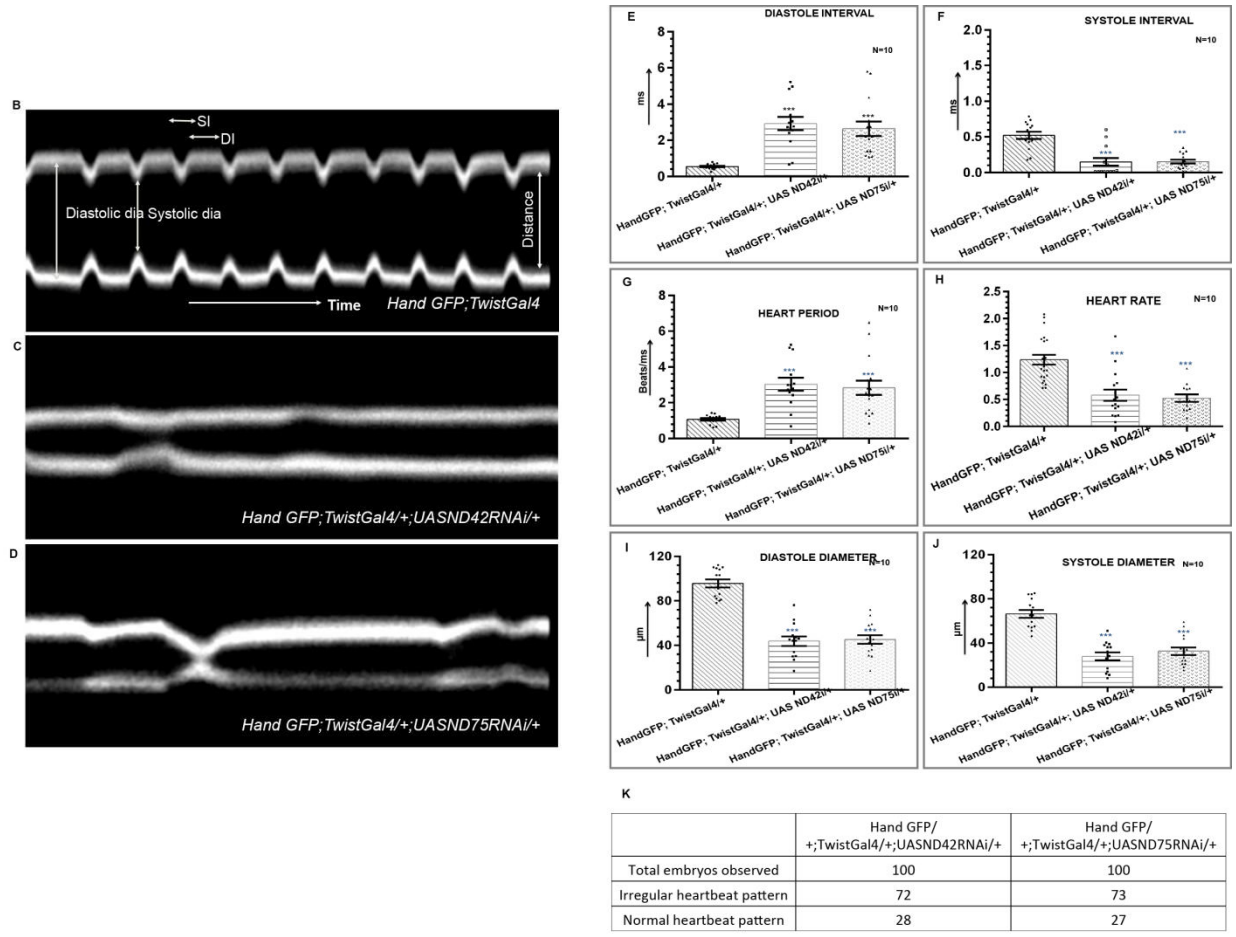

K

	Hand GFP/ +;TwistGal4/+;UASND42RNAi/+	Hand GFP/ +;TwistGal4/+;UASND75RNAi/+
Total embryos observed	100	100
Irregular heartbeat pattern	72	73
Normal heartbeat pattern	28	27

Fig. 3.6 Knockdown of ND42 and ND75 from developing mesoderm leads to cardiac malfunctionM-mode representing movement of heart wall w.r.t. time shows a drastic change in *ND42* (C) and *ND75* (D) knockdown embryos compared to regular M-mode pattern in control (B). Measurement of various cardiac parameters using SOHA (Semi-automated heartbeat analysis) shows an increase in diastole interval and decrease in systole interval in knockdown embryos compared to control (E, F) increase in heart period (G), decrease in heart rate(H) and decrease in systole-diastole diameters (I, J) compared to control. K. Quantitative analysis of the number of embryos showing irregular heartbeat pattern vs normal heartbeat pattern (n=100)

3.3.6 M-mode indicates cardiac arrhythmia in knockdown embryos:

M-mode represents the vertical movement of heart tube edges (y-axis) over time (x-axis)

We used the heart proper region in the cardiac tube of stage 17 *Drosophila* embryos to generate M-mode since the beating originates in the heart proper region and then propagated through the rest of the tube. M-modes were made from the same portion in control and knockdown embryos.

A) Wild type M-mode shows regular heart contractions as evidenced by periodic movement of heart edges along time (Fig. 3.6B)
B) *ND42* and *ND75* knockdown embryos show aberrations in their M-modes, primarily characterized by prolonged relaxations and very rare and less robust contractions(Fig. 3.6C, 3.6D)

3.3.6a *Increase in the heart period of stage 17 wild type, ND42, and ND75 knockdown embryos.*

Heart period is measured as the interval between the start of one diastole and the beginning of the next.The heart period is significantly increased in both *ND42* and *ND75* knockdown embryos compared to control. The heart period of *TwistGal4/+; UAS ND42dsRNA/+* embryos is 3.2ms compared to the heart period 1.2 ms in control. The heart period of *TwistGal4/+;UAS ND75dsRNA/+* knockdown embryos is increased to 3.1ms (*P=0.000103 and 0.00058 respectively for *ND42* and *ND75* knockdown embryos, by t-test) (Fig. 3.6G) Data are mean +_ SE. Increase in heart period indicates prolonged systole-diastolic phase i.e. heart spends more time to complete one systole-diastole cycle compared to the control.

3.3.6b *Diastolic interval is increased in ND42 and ND75 knockdown embryos*

Diastolic interval (DI) is the duration for which the heart stays in the diastolic (relaxation) phase.The diastolic interval of *ND42* knockdown embryos was 3.1 millisecond compared to 0.6ms in control (*P= 5.15E-05 by t-test). In the case of *ND75* knockdown embryos, the diastolic interval was increased to 2.8 ms (*P= 0.000121 by t-test) (Fig. 3.6E). Increased diastolic interval indicates heart remains in relaxation phase for a longer time in case of *ND42*/*ND75* knockdown embryos compared to control.

3.3.6c *Systolic interval was reduced in ND42 and ND75 knockdown embryos*

Systolic interval (SI) is the duration for which cardiac tube stays in the systolic (contraction) phase.The systolic interval of *ND42* knockdown embryos was decreased to 0.21ms compared to

the systolic interval of 0.6ms in control embryos (*P= 3..26E-05, by t-test). In the case of *ND75* knockdown embryos, the systolic interval was reduced to 0.22 ms (*P= 4.41-E06, by t-test) (Fig. 3.6F). Reduction in systolic interval suggests that heart contraction phase is shorter in knockdown embryos compared to control.

3.3.6d Knockdown embryo exhibit significantly reduced diastolic diameter.

The diastolic diameter of *ND42* knockdown embryos was 43.73 microns compared to 95.52 microns in control (*P= 9.08E-10) whereas the diastolic diameter of *ND75* knockdown embryos was significantly reduced to 45.19 microns (*P=3.84E-10) (Fig. 3.6I).

3.3.6e Reduced systole diameter in ND42 and ND75 knockdown embryos:

The systolic diameter of *ND42* knockdown embryos was significantly reduced to 27.77 microns compared to the systolic diameter of 66.38 microns in control whereas the systolic diameter of *ND75* knockdown embryos is reduced to 32.65 microns (*P =4.45E-08 and P= 3.12E-07 respectively in *ND42* and *ND75* knockdown embryos, by T-test) (Fig. 3.6J)

3.3.7 Lumen constriction revealed by TrolGFP in ND42 and ND75 knockdown embryos: In order to reconfirm the results mentioned in section 3.3.6d and 3.3.6e which stated that systolic and diastolic diameters were reduced in *ND42*/*ND75* knockdown embryos, *Trol GFP* was used as a marker to determine the status of the lumen of the cardiac tube at stage 16 of embryonic development.

Trol (Terribly Reduced Optic Lobes) is the heparin sulfate proteoglycan and the vertebrate protein Perlecan homolog in *D. melanogaster*. It is expressed in the basement membrane of embryonic tissues. In the dorsal vessel at stage 16 of embryonic development, it marks the lumen of the cardiac tube as well as the outer boundaries of the cardiac tube and alary muscles.

Inner lumen diameter, as well as the outer diameter of the cardiac tube, was measured in the *TrolGFP* background in control and knockdown embryos. Quantification was done by taking 10 measurements at different points, each for aorta and heart proper region and then averaged to give a mean value for Aorta and Heart proper region.

Confocal imaging of *TrolGFP* marked control and knockdown embryos indicates that there is a constriction in the lumen of the cardiac tube in *ND42*knockdown embryos (Fig.3.7B) compared

to control (Fig. 3.7A). A similar lumen constriction was observed in *ND75* knockdown embryos (Fig.3.7C).

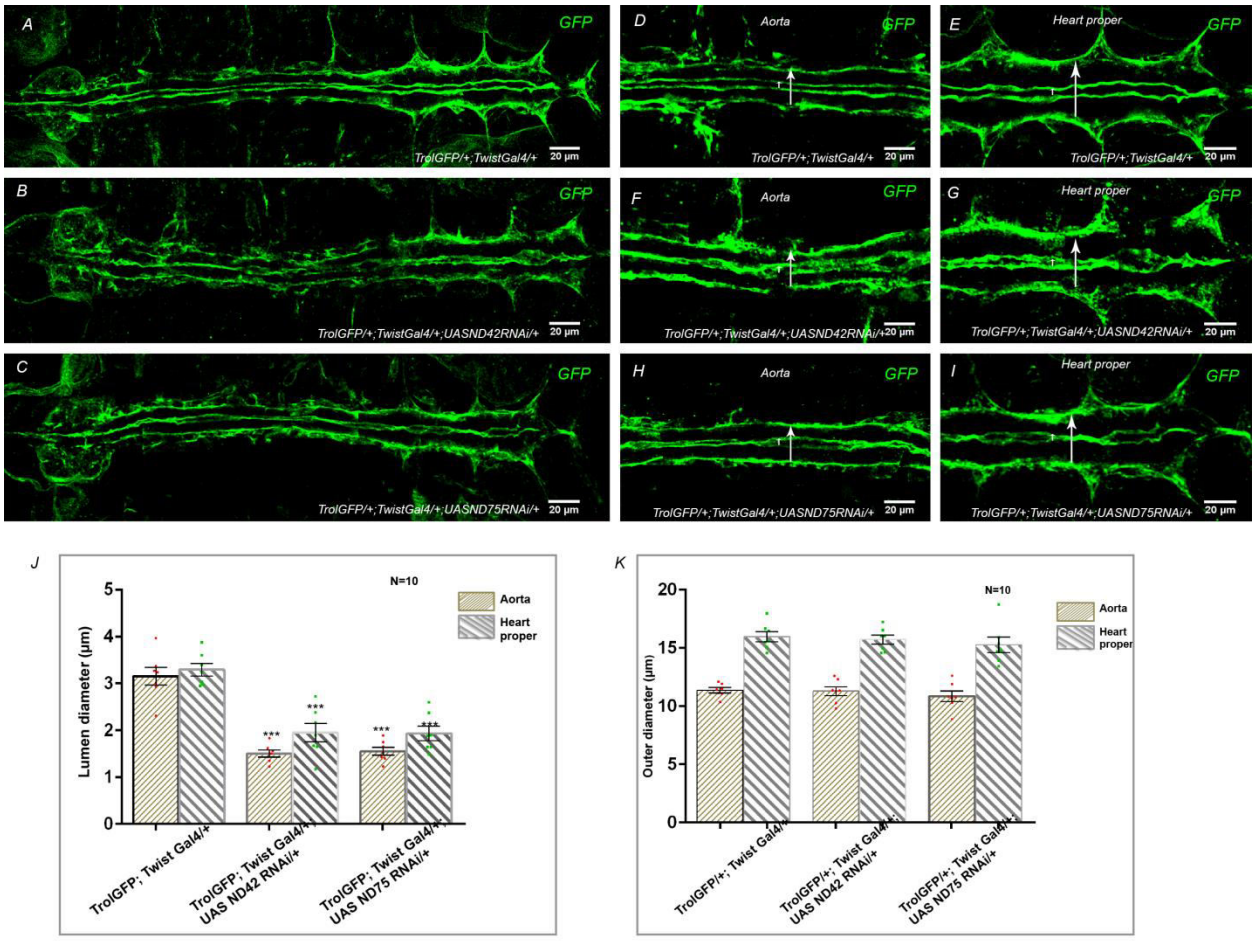

Fig. 3.7 Luminal constriction in knockdown embryos. Wild type stage 16 embryos stained for TrolGFP which is present in the basement membrane and used to mark the lumen and outer wall of the cardiac tube **(A).** In *TwistGal4/+; UAS ND42dsRNA/+*,and*TwistGal4/+; UAS ND75dsRNA/+*,knockdown embryos, the lumen is notably constricted compared to control.in the cardiac tube; TrolGFP used to mark the lumen of the cardiac tube **(B, C**). Zoomed in images of the same embryos shown on the left clarifying lumen constriction in *ND42* and *ND75* knockdown embryos in the aorta as well as heart proper regions (**D, I**). Statistical analysis showed a significant reduction in lumen diameter in knockdown embryos compared to control (n=10)**(J**) No significant change in outer diameter of the cardiac tube in knockdown embryos compared to the control **(K**).

Detailed quantitative analysis confirmed that the inner lumen is significantly constricted in *ND42*(Fig.3.7J) and *ND75* knockdown embryos (Fig. 3.7K) with *P value< 0.0001, by T-test. In

control embryos at stage 16, the average lumen diameter in the Aorta region is 3.15 microns and in the Heart proper region, the lumen diameter is 3.29 microns. In *TwistGal4/+; UAS ND42dsRNA/+*knockdown embryos, aorta and heart proper lumen diameter is significantly reduced to 1.5 microns and 1.95 microns respectively. In *TwistGal4/+; UAS ND75dsRNA/+*knockdown embryos, aorta and heart proper lumen diameter is significantly reduced to 1.55 microns and 1.93 microns respectively (Fig. 3.7 J).

Quantitative analysis of the outer diameter of the cardiac tube revealed no significant change in knockdown embryos compared to control. In control embryos at stage 16 of embryonic development, the outer diameter in Aorta and Heart proper region is 11.36 microns and 15.97 microns respectively. In *ND42* knockdown embryos, outer lumen diameter in Aorta region was measured 11.29 microns and in the heart proper region was measured as 15.71 microns with no significant change compared to control. In *TwistGal4> UAS ND75 dsRNA*, aorta measures 10.8 microns and the heart proper region measures 15.26 microns, again no significant change compared to control.(Fig. 3.7K).

3.3.8 Increased and mislocalized*Pericardin* in the lumen of the cardiac tube of *ND42/ND75* knockdown embryos:

*Pericardin*is a type-IV collagen-like protein expressed by pericardial cells and a subpopulation of cardioblasts. It is concentrated at the basal surface of cardioblasts and around the pericardial cells in close proximity to the dorsal ectoderm and is absent from the lumen (Chartier et at,2002). *Pericardin* marks the boundaries of the cardiac tube as well as alary muscles.

Interestingly, in *ND42* (Fig.3.8B) and *ND75* (Fig.3.8C) knockdown embryos,immunostaining with *Pericardin*antibody revealed an excessive *Pericardin* deposition around the cardiac tube compared to control embryos at stage 16 of embryonic development (Fig.3.8A). The *Pericardin* expression is mislocalized in the luminal region and seems to be diffused rather than concentrated around the pericardial cells in wild type embryos.

qRT PCR for *Pericardin*of stage 16 embryos revealed increased *Pericardin* transcript levels in *ND42* and *ND75* knockdown embryos. In the case of *ND42* knockdown embryos, the *Pericardin*transcript reportedly increased to 4 folds compared to control. In the case of *ND75*

knockdown embryos, there were 5 fold changes compared to the same stage control embryos (Fig.3.8D).

These two results suggest that increased *Pericardin* accumulation is the result of more *Pericardin* transcript produced by the pericardial cells

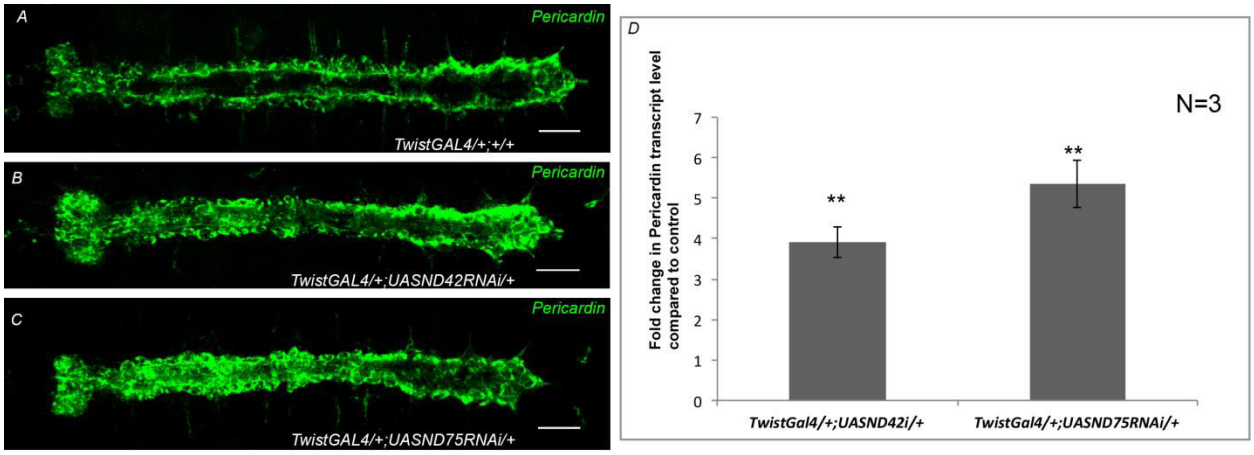

Fig. 3.8. Increased and mislocalizedPericardin (type-IV collagen-like protein) around cardioblasts in complex-I knockdown embryos Wild type stage 16 embryo immunostained for *Pericardin* which is secreted by pericardial cells, thereby marking boundaries of the cardiac tube **(A).** The increase in *Pericardin* expression can be seen along with its mislocalization in the lumen of *ND42* and *ND75* knockdown embryo at stage 16 of embryonic development **(B, C**). *Pericardin* transcript levels in stage 16 embryo are increased 4 fold and 5 fold in *ND42* and *ND75* knockdown embryos at stage 16 of embryonic development as revealed by qRT PCR(n=3) (**D**).

3.4 DISCUSSION

Congenital heart diseases due to metabolic dysfunction pose a major challenge due to poor understanding of underlying factors and lack of suitable model systems to study early cardiac defects (Juurlink, 2010; Juurlink et al., 2009; Singh et al., 2007). By taking advantage of advancements in live imaging techniques, easygenetic manipulations and given the fact that *Drosophila*cardiogenesis shares high conservation with vertebrates in terms of transcription factors and signaling pathways involved, I have investigated metabolic dysfunction induced CHDs in *Drosophila* embryos.

The first challenge of this study was to search for a strategy to induce mitochondrial perturbations in such a manner that an observable phenotype could be obtained. By employing

RNAi strategy for targeted knockdown of genes encoding complex-I components *ND42* and *ND75* of the electron transport chain, we were able to screen out the Gal4 driver which could induce mitochondrial dysfunction in a spatiotemporal manner so that hatching rate of embryos is hampered.

Cardiac malfunctioning in complex-I knockdown embryos:

Cardiac functionality is severely affected by knocking down complex-I components of ETC from the mesoderm. It implies that the dysfunctional mitochondrial population is accumulated to a sufficient level up to stage 16 of embryonic development in the cardioblasts. With *Mef2* staining, we could not see any severe defect in terms of misalignment of cardiac tube. However, in terms of function, the heart period and systole-diastole diameters are significantly altered. These results indicate the importance of mitochondrial health for the cardiac tube to initiate its first beat and suggest the critical role metabolic dysfunction can play in congenital heart diseases.

The lethality associated with complex-I knockdown in embryos was shown to be specific to *ND42* and *ND75* knockdown as no lethality was observed with knockdown of GFP from the developing mesoderm using *Twist* Gal4 driver. The functionality of the cardiac tube was severely hampered by knocking down complex-I components of ETC from the developing mesoderm. Since the average number of embryos that exhibit embryonic lethality was in concordance with an average number of embryos exhibiting cardiac malfunctioning, it was inferred that embryonic lethality was due to cardiac malfunctioning during embryonic development.

It was surprising to observe that despite the severe effect on cardiac functionality in knockdown embryos, we don't see any severe change in the alignment of cardioblasts as inferred by *Mef2* immunostaining. Cardiac tube was formed in place with no drastic misorientaiton of cardioblasts.Neither is there any abrupt increase in the total number of cardioblasts as previously shown for Notch mutant embryos. However, we see a drastic increase in *Pericardin* which is also an ECM component. These results suggest that metabolic dysfunction imparts very specific effects with respect to genes that are affected. It is quite possible that *Pericardin* transcription is sensitive to the metabolic status of the pericardial cells,that is why the altered metabolic status of the cell induced high *Pericardin* expression.

Not much is known about the regulation of *Pericardin* expression in embryos. In larval stages of *Drosophila* life cycle, *Pericardin* secretion has been shown to be affected by adipocyte-specific knock-down of Sar1 expression thus affecting the formation of a proper heart ECM in Drosophila (Sellin et al., 2009).

The relevance of elevated Pericardin in the context of cardiac pathology:

Pericardin is a type IV collagen-like component of the *Drosophila* extracellular matrix. It is predominantly expressed by pericardial cells and to a lesser extent by *Seven up* positive cardioblasts(Chartier et al., 2002).It is highly concentrated in the dorsolateral part of the heart which is in close contact with the ectoderm and has been shown to coordinate movements of the heart and ectodermal cells. In wild type embryonic heart, *Pericardin* expression is concentrated at the basal surface of cardioblasts and around the pericardial cells(Chartier et al., 2002).

By knocking down complex-I components of Electron Transport Chain from the developing cardiogenic mesoderm, a significant increase in *Pericardin* expression is seen as evident from immunostaining with *Pericardin* and real-time quantification of *Pericardin* transcript. Previous studies of adult *Drosophila* heart in high sugar diet conditions have shown deterioration of heart function accompanied by increased *Pericardin* accumulation thereby creating fibrosis-like conditions (Na et al., 2013).

Cardiac fibrosis is characterized by the net accumulation of extracellular matrix proteins in the cardiac interstitium and results in both systolic and diastolic dysfunctions. Elevation in components of ECM is a hallmark of cardiac fibrosis as reported in various model systems as well as human cell lines(Tian et al., 2017).

A collagen network is very important for the heart because it provides tensile strength as well as elasticity to allow the heart to operate normally in terms of systolic and diastolic functions. Collagen turnover is of utmost importance to maintain the balance between degradation and synthesis of collagen and imbalance of this turn over leads to excess collagen accumulation which ultimately leads to cardiac fibrosis. Renin-angiotensin-aldosterone system (RAAS) has been shown to regulate this dynamic collagen turn over and intervention of this system can prevent the process of fibrosis(Weber and Brilla, 1991).TGF-β is another very important signaling pathway that is elevated in cardiac fibrosis and operates via activation of ALK

signaling. Therefore targeting ALK5 has been shown to block certain steps of cardiac fibrosis(Chen et al., 2006; Leask and Abraham, 2004; Massague, 1998).

Possible explanations for unaltered *Mef2* expression in the cardiac tube of knockdown embryos:

Mef2 expression starts at stage 5 of embryonic development in the developing mesoderm. No apparent change in *Mef2* expression was found in complex-I knockdown embryos at stage 16 of embryonic development. Regulation of *Mef2* expression is a complex- process since *Mef2* has multiple phases of expression which are controlled by a complex array of cis-acting regulatory modules that are responsive to different genetic signals. The initial widespread expression of *Mef2* is under the control of *Twist* dependent enhancer. After that, dorsal mesoderm restricted expression is mediated through *Dpp* responsive regulatory module. *Mef2* expression in cardioblasts is dependent on at least two enhancers; the activity of one of these enhancers could be under control of *Tinman*. Therefore, *Mef2* expression pattern isa result of multiple geneticinputs during different phases of development (Nguyen, 1999), therefore it is very hard to comment which of these regulations are affected or not affected in this particular case.

In complex-I knockdown embryos, ROS induced increase in *Pericardin* expression is yet another example of modulation of ECM components by elevated ROS levels. The intermediate factors involved in inducing elevation in *Pericardin*expressoin have not been explored. As suggested by literature, ectodermal Dpp signaling may be involved, but this aspect needs further exploration. It is not known either how ROS is regulating *Pericardin* expression. We have attempted to establish a model system to answer all these questions *in vivo* so that mechanistic basis of regulation of developmental signals by ROS could be understood.

Chapter 4

ROS mediated retrograde response from mitochondria targets cell fate specification during cardiogenesis in *Drosophila* embryos

4.1 Introduction

In my previous chapter, I have established *Drosophila* embryonic heart as a model to understand metabolic dysfunction induced CHDs. My next objective was to investigate the underlying factors responsible to exert these cardiac defects. Metabolic defects have long been reported to be responsible for early cardiac defects however the intermediate factors are not very well understood. By taking advantage of easy genetic manipulations, genetic analysis tools and very well explored cardiogenesis in *Drosophila*, we wanted to pinpoint the underlying factors responsible for metabolic dysfunction induced CHDs.

Only structural and functional aspects of cardiac defects were explored, but since we are knocking down *ND42* and *ND75* from early mesoderm, it means there must be something wrong with cardiac specifications events which lead to the ultimate result of cardiac malfunctioning. Hence, we further performed cellular characterization of the cardiac tube of these embryos at stage 16 of embryonic development.

Investigating the cardiac phenotype at the cellular level will give an answer to the spatial and temporal basis of the initiations of events that ultimately lead to cardiac malfunctioning. These studies will open the door to the transcription factors and signaling pathways that are involved in

imparting these defects. Hence, the mystery of the mechanistic basis of metabolic dysfunction induced CHDs can be solved.

4.1.1 Reactive Oxygen Species:

Reactive oxygen species spans various molecules derived from oxygen which accepts extra electrons and can oxidize other molecules (Cross et al., 1987). A single electron reduction of oxygen (O2) results in the formation of superoxide (O2-) radicals. Superoxide dismutase can convert two superoxide molecules to one molecule of no-radical hydrogen peroxide and one water molecule. Hydrogen peroxide can accept another electron from free Fe2+ by the Fenton reaction to become a hydroxyl radical (HO•). These are three primary forms of ROS that have different reactivities and can have different effects on cellular physiology (Fig.4.1A)

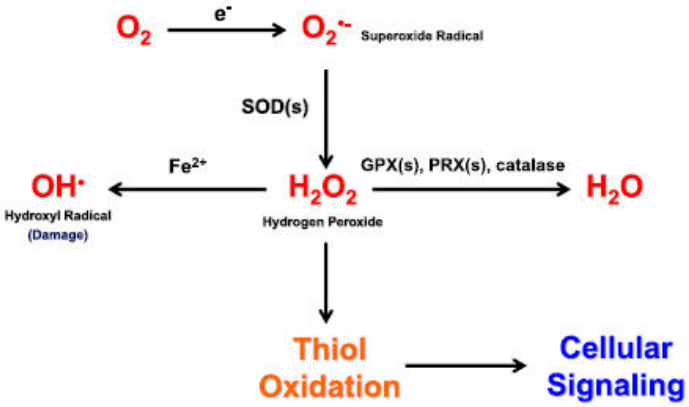

Figure 4.1A Production and interconversion of ROS *{Adapted from (Sullivan and Chandel, 2014)}*

4.1.2 ROS production by Complex-I attenuation:

Complex- I is one of the main site of ROS production during oxidative phosphorylation. During electron transfer through ETC, electrons get leaked at complex- which can reduce oxygen and give rise to superoxide anion (Kussmaul and Hirst, 2006) (Fig.4.1B). It has been suggested that iron-sulfur cluster N2 could be the site of electron leak (Genova et al., 2001). In addition, the N2-SQNf region (Ohnishi et al., 2005) ubisemiquinone (SQNf) (Lambert and Brand, 2004) and iron-sulfur cluster N1a (Kushnareva et al., 2002) have also been proposed to be electron donors to oxygen. It has been found that defective complex-I produces more ROS (Raha and Robinson, 2000) than the normal one. This suggests the crucial role played by structural modifications of the enzymes in ROS production.

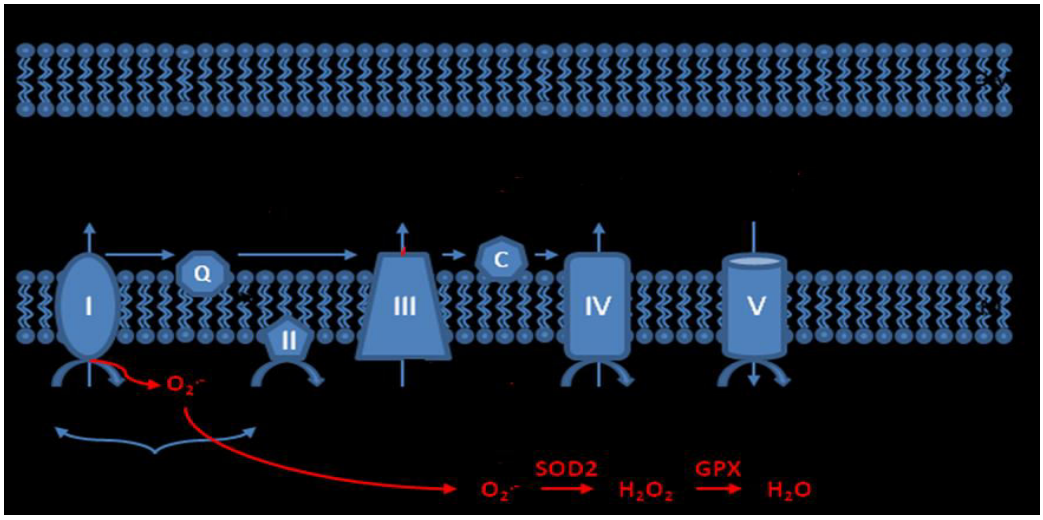

Fig. 4.1B Generation of ROS at complex-I of ETC

4.1.3 Reporters for ROS detection:

Fluorescent probes are routinely used for ROS detection in biological systems. The most common of them include DHE (Dihydroethidium) and DCFDA. DCFDA is more specific for the detection of peroxide ions whereas DHE is more suitable for superoxide ions detection. MitoSOX is a modified DHE analog which is specifically used for the detection of superoxide ions generated by mitochondria in contrast to DHE which detects cytoplasmic O^{2-} but not mitochondrial $O^{2-\cdot}$

GstD GFP reporter is a fly line used for live monitoring of antioxidant response. *GstD GFP* reporter activity is shown to induce when flies are exposed to various oxidants including paraquat, diethyl maleate, a glutathione depleting agent, and hydrogen peroxide, a bonafide oxidant. Therefore, this reporter construct is responsive to diverse oxidative stressors.

We used mitoSOX because of more selectivity in the detection of mitochondrial generated O^{2-} and *gstD GFP* reporter line to check the status of ROS levels in the embryos by knocking down nuclear genes encoding complex-I components of ETC.

4.2 Results

4.2.1 Elevated ROS levels in the mesoderm derivatives of knockdown embryos:

First of all, the possibility that attenuation of complex-I activity leads to an increase in ROS levels was explored. Elevated ROS levels were examined in *TwistGal4/+; UAS ND42dsRNA/+* and *TwistGal4/+; UAS ND75dsRNA/+* background using mitoSOX which specifically detects mitochondrial generated superoxide ions. Staining with mitoSOX revealed that the majority of mesodermal cells are positive for mitoSOX in *TwistGal4/+; UAS ND42dsRNA/+* (Fig.4.2 B) *and TwistGal4/+; UAS ND75dsRNA/+* (Fig.4.2 B) knockdown embryos at stage 13 of embryonic development compared to control embryos (Fig 4.2A) confirming the mitochondrial origin of ROS.

Glutathione-S- transferase D1-GFP (*gstD* GFP) reporter construct has been previously shown to be *in vivo* sensor for ROS (Bohmann, 2008). ROS activity was detected in the mesodermal population using *gst*D GFP construct in *TwistGal4/+; UAS ND42dsRNA/+* (Fig.4.2E) *and TwistGal4/+; UAS ND75dsRNA/+* (Fig.4.2F) knockdown embryos at stage 13 of embryonic development compared to control embryos (Fig 4.2D).

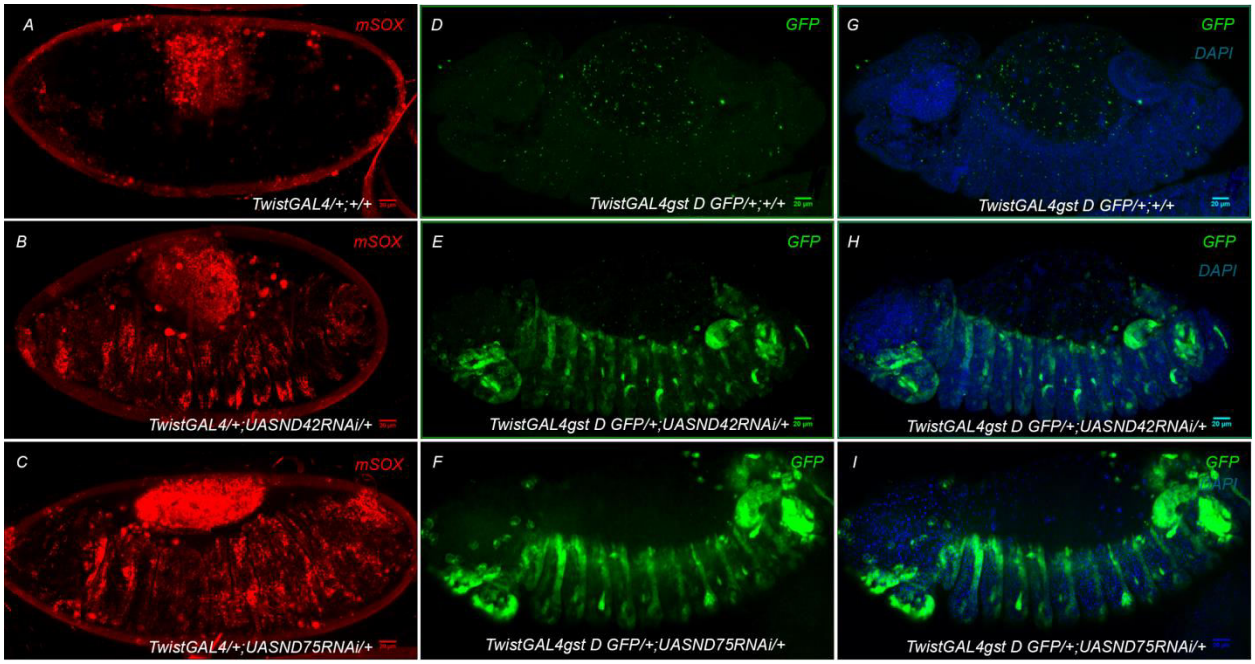

Fig. 4.2 Elevated ROS levels in cardiogenic mesoderm observed at stage 13 of embryonic development. Wild type stage 13 *Drosophila* embryo stained negative for mitoSOX red except in the amnioserosa region **(A)** MitoSOX red stain can be seen in certain regions in each hemisegment of stage 13 *ND42* and *ND75* knockdown embryos **(B, C)** Wild type stage 13 Drosophila embryo negative for gst D GFP expression (D); merged with DAPI (G). *ND42*

and *ND75* knockdown embryos show *gstD GFP* expression in each hemisegment at stage 13 of embryonic development **(E, F),** with DAPI **(H, I).**

4.2.2 Co-localization of Twist expressing and high gst D GFP expressing mesodermal cells at stage 10 of embryonic development:

Twist expression initiates at stage 10 of embryonic development in mesodermal progenitors and continues to express until stage 13 of embryonic development. Since *Twist Gal4* is used to derive *UAS ND42dsRNA* and *UAS ND75dsRNA*, it can be expected that ROS levels are increased in *Twist* expressing mesodermal cells.

Co-immunostaining with *Twist* antibody and anti-GFP antibody in *TwistGal4gstD GFP/+; UAS ND42dsRNA/+* and *TwistGal4gstD GFP/+; UAS ND75dsRNA/+* background revealed that at stage 10 of embryonic development when *gst*D GFP expression initiates in knockdown embryos, *Twist* expression overlaps exactly with *gst*D GFP expression confirming that ROS levels are increased in *Twist* expressing mesodermal cells in *TwistGal4/+; UAS ND42dsRNA/+* (Fig.4.3D,E,F) *and TwistGal4/+; UAS ND75dsRNA/+* (Fig.4.3G,H,I) knockdown embryos at stage 10 of embryonic development compared to control embryos (Fig 4.3A,B,C)

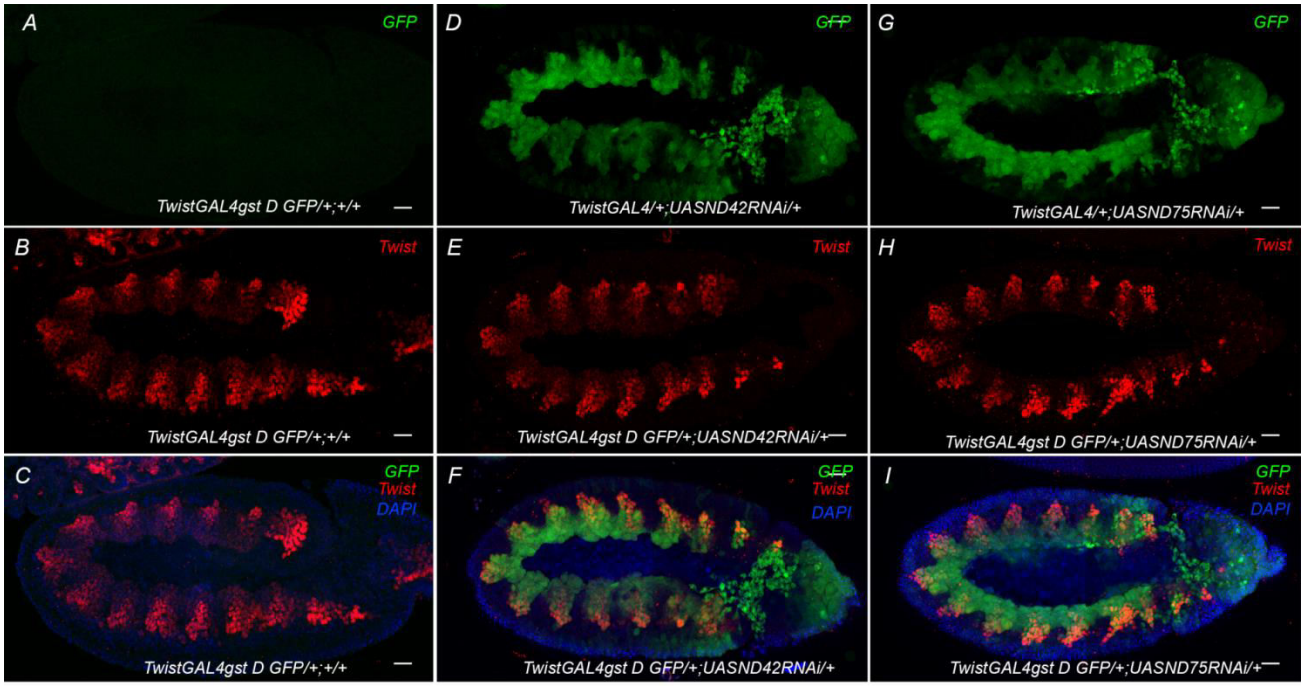

Fig. 4.3 Increase in ROS levels specifically in Twist expressing mesodermal cells. Wild type stage 10 *Drosophila* embryo stained negative for *gstD GFP* **(A).** *Twist* expression in the mesodermal progenitors at stage 10 of embryonic development in wild type embryo **(B),** merged with DAPI (**C**). *ND42* knockdown embryo shows *gstD GFP* expression in each hemisegment **(D**), co-immunostained with *Twist* antibody **(E).** Merged image shows co-localization of *gstD GFP* and *Twist* expression in the mesoderma cells (**F).** *ND75* knockdown embryo shows *gstD GFP* expression in each hemisegment (**G**), co-immunostained with *Twist* antibody **(H).** Merged image shows co-localization of *gstD GFP* and *Twist* expression in the mesoderma cells **(I)** in knockdown embryos.

4.2.3 Modest change in ATP levels of complex-I knockdown embryos:

ATP assay revealed modest change in ATP levels of *DaGal4/+;UAS ND42dsRNA/+ and DaGal4/+; UAS ND75dsRNA* /+knockdown embryos compared to control embryos. In case of *DaGal4/+; UAS ND42dsRNA/+* embryos, there was 16% drop in ATP levels compared to control whereas in case of *DaGal/+; UAS ND75dsRNA/+* embryos, there was 12% drop in ATP levels (Fig.4.4)

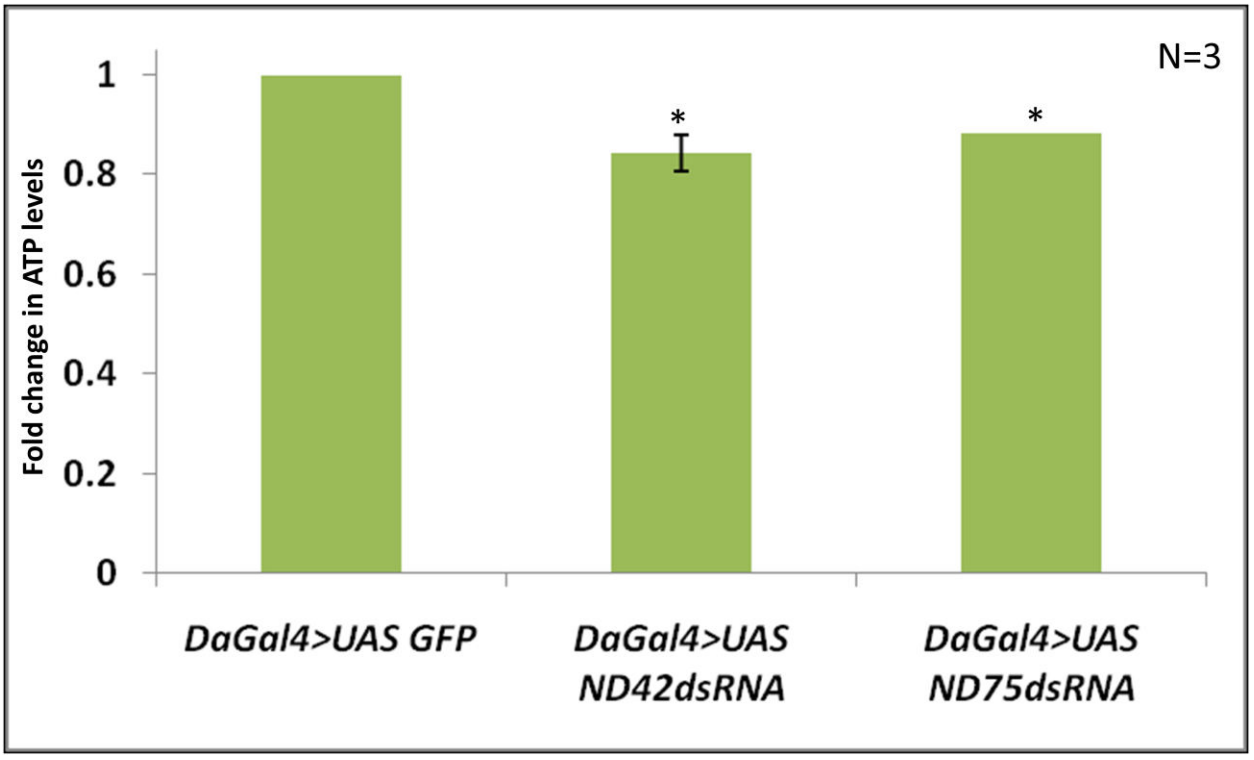

Fig. 4.4 ATP levels are not reduced significantly in *ND42* and *ND75* knockdown embryos.

4.2.4 Exploring the possibility of ROS as the key signal for structural and functional defects in cardiac tube caused by attenuation of complex-I activity of ETC:

In the process of uncovering the link between cues and effectors of cardiac dysfunction, ROS levels were found to be increased specifically in the *Twist* expressing mesodermal progenitors. To establish ROS is the key signal used by the cell having the perturbed mitochondrial function to ultimately affect cardiac function, we performed genetic manipulations i.e. over-expressing SOD in the complex-I knockdown background to scavenge superoxide ions and looked at structural and functional aspects of the cardiac tube for any change.

4.2.5 Overexpression of Superoxide dismutase 2 significantly restores the survival rate of ND42/75 knockdown embryos:

Quantitative analysis of rescue in terms of rate of hatching by scavenging superoxide Ions

Superoxide dismutase 2 (SOD2) specifically scavenges the superoxide ions generated during the mitochondrial electron transport chain. *SOD2* was over expressed in *TwistGal4/+; UAS ND42dsRNA/+ and TwistGal4/+; UAS ND75dsRNA/+* knockdown embryos. Lethality assay was done at 29 degrees the hatching rate of embryos was calculated. It was found that by over-expressing *SOD2* in *TwistGal4/+; UAS ND42dsRNA/+* background, around 54 % of embryos hatched, a significant rescue in comparison to 20% embryos hatched in *TwistGal4/+; UAS ND42dsRNA/+* progeny. A similar trend was observed by overexpressing *SOD2* in *TwistGal4/+; UAS ND75dsRNA/+* background, where average 57% embryos were hatched compared to only 21% embryos hatched in *TwistGal4/+; UAS ND75dsRNA/+* progeny, thus showing a significant rescue (Fig. 4.5A).

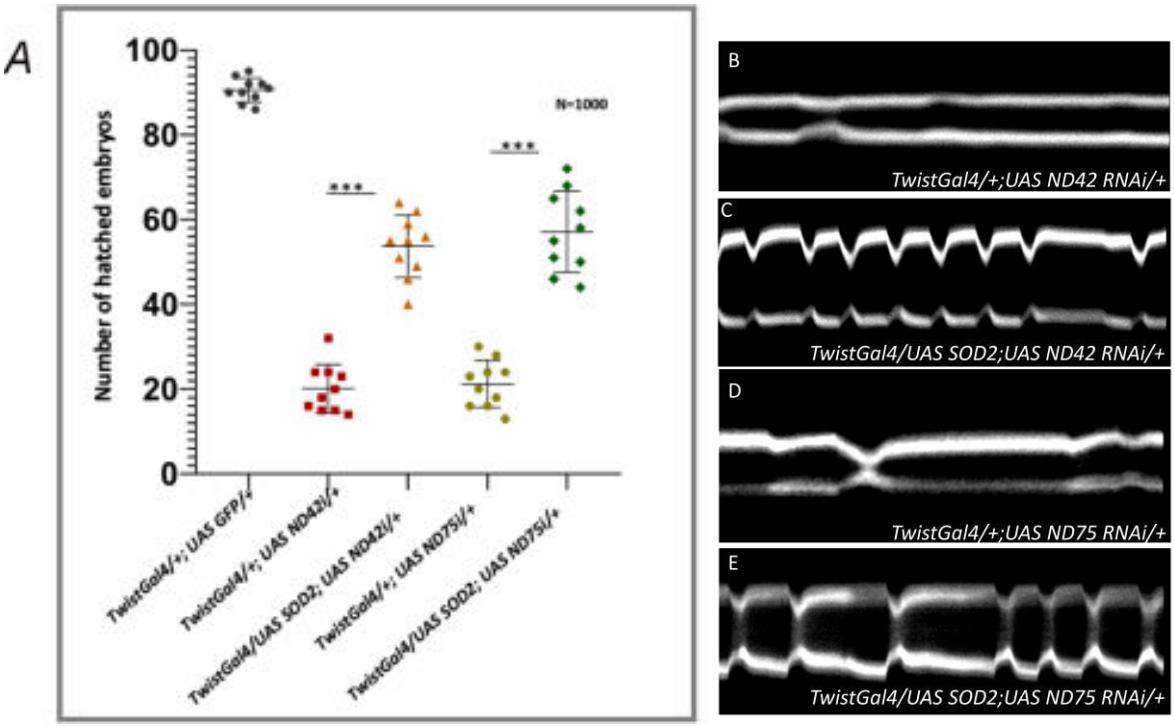
A
100
80
60
40
20
0
Number of hatched embryos
N=1000
***
***
TwistGal4/+; UAS GFP/+
TwistGal4/+; UAS ND42i/+
TwistGal4/UAS SOD2; UAS ND42i/+
TwistGal4/+; UAS ND75i/+
TwistGal4/UAS SOD2; UAS ND75i/+
B
TwistGal4/+;UAS ND42 RNAi/+
C
TwistGal4/UAS SOD2;UAS ND42 RNAi/+
D
TwistGal4/+;UAS ND75 RNAi/+
E
TwistGal4/UAS SOD2;UAS ND75 RNAi/+

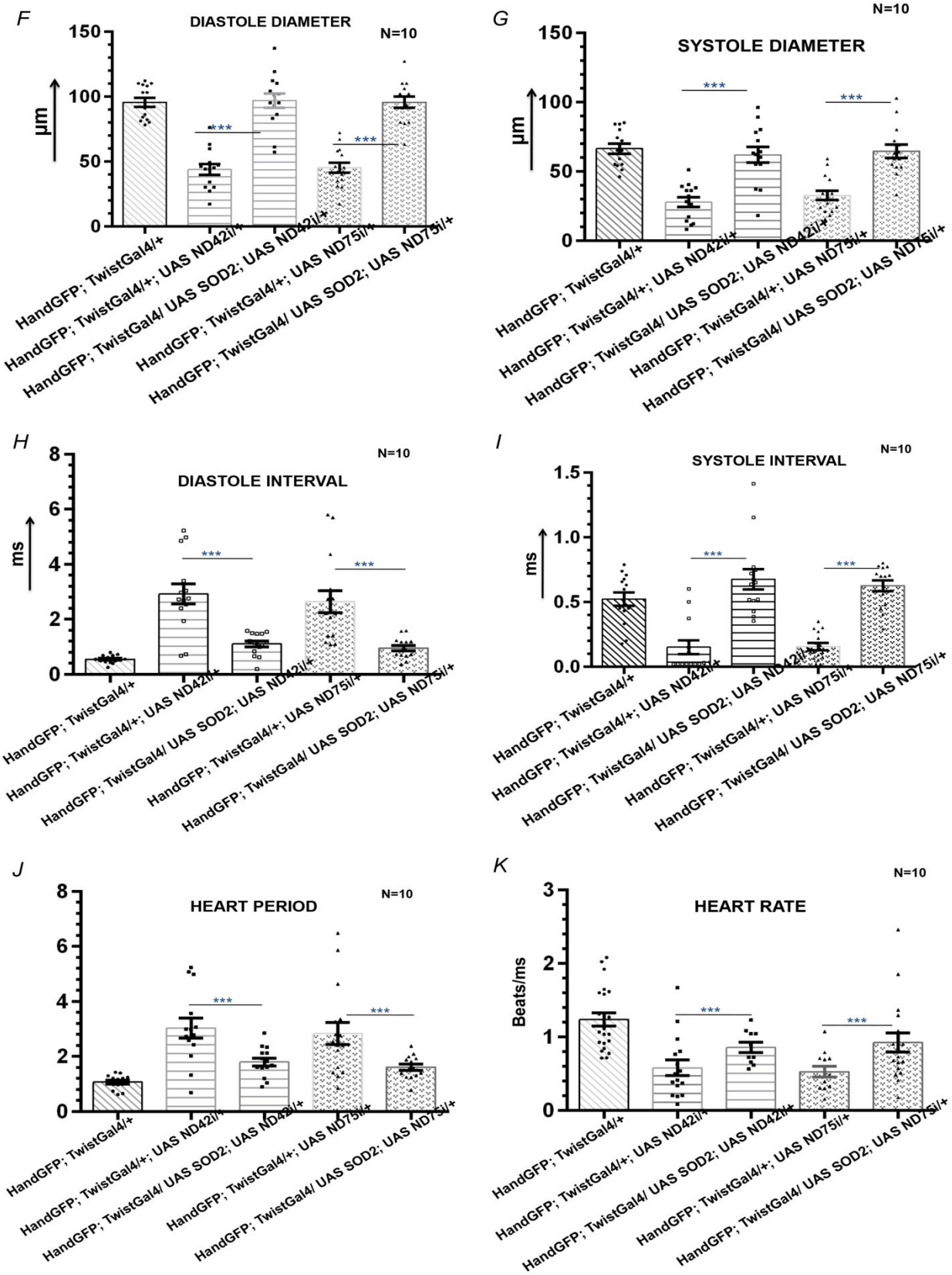
F
DIASTOLE DIAMETER
N=10
µm
150
100
50
0
***
***
HandGFP; TwistGal4/+
HandGFP; TwistGal4/+; UAS ND42i/+
HandGFP; TwistGal4/ UAS SOD2; UAS ND42i/+
HandGFP; TwistGal4/+; UAS ND75i/+
HandGFP; TwistGal4/ UAS SOD2; UAS ND75i/+
G
N=10
SYSTOLE DIAMETER
µm
150
100
50
0
***
***
HandGFP; TwistGal4/+
HandGFP; TwistGal4/+; UAS ND42i/+
HandGFP; TwistGal4/ UAS SOD2; UAS ND42i/+
HandGFP; TwistGal4/+; UAS ND75i/+
HandGFP; TwistGal4/ UAS SOD2; UAS ND75i/+
H
N=10
DIASTOLE INTERVAL
ms
8
6
4
2
0
***
***
HandGFP; TwistGal4/+
HandGFP; TwistGal4/+; UAS ND42i/+
HandGFP; TwistGal4/ UAS SOD2; UAS ND42i/+
HandGFP; TwistGal4/+; UAS ND75i/+
HandGFP; TwistGal4/ UAS SOD2; UAS ND75i/+
I
N=10
SYSTOLE INTERVAL
ms
1.5
1.0
0.5
0.0
***
***
HandGFP; TwistGal4/+
HandGFP; TwistGal4/+; UAS ND42i/+
HandGFP; TwistGal4/ UAS SOD2; UAS ND42i/+
HandGFP; TwistGal4/+; UAS ND75i/+
HandGFP; TwistGal4/ UAS SOD2; UAS ND75i/+
J
N=10
HEART PERIOD
8
6
4
2
0
***
***
HandGFP; TwistGal4/+
HandGFP; TwistGal4/+; UAS ND42i/+
HandGFP; TwistGal4/ UAS SOD2; UAS ND42i/+
HandGFP; TwistGal4/+; UAS ND75i/+
HandGFP; TwistGal4/ UAS SOD2; UAS ND75i/+
K
N=10
HEART RATE
Beats/ms
3
2
1
0
***
***
HandGFP; TwistGal4/+
HandGFP; TwistGal4/+; UAS ND42i/+
HandGFP; TwistGal4/ UAS SOD2; UAS ND42i/+
HandGFP; TwistGal4/+; UAS ND75i/+
HandGFP; TwistGal4/ UAS SOD2; UAS ND75i/+

Fig.4.5. Scavenging superoxide ions rescues embryonic lethality and restores functionality of the cardiac **tube:** Statistical analysis of hatching rate of embryos revealed significant rescue in *SOD2* overexpression background in *ND42* and *ND75* knockdown embryos compared to their knockdown counterparts. (n=1000) **(A)** . B, C, D, E M-mode of TwiGal4> UAS *SOD2*; UAS *ND42* RNAi and TwiGal4> UAS *SOD2*; UAS *ND75* RNAi shows more movements of heart wall with time as compared to M-mode in *ND42* and *ND75* knockdown embryos (**B-E).** Quantization of cardiac parameters with SOHA revealed significant rescue in heart rate, heart period, systole-diastole interval and systole-diastole diameters by scavenging superoxide ions from the developing mesoderm **(F-K)**

4.2.6 Scavenging ROS rescues the cardiac functionality to a significant level:

The alteration in the rhythmicity of the cardiac tube beating pattern observed in the case of *ND42/ND75* knockdown embryos can be rescued by over-expressing *SOD2* in the knockdown background.

Cardiac tube of stage 17 embryos from *HandGFP; TwistGAL4/UAS SOD2; UAS ND42 dsRNA/+* and *HandGFP*; *TwistGAL4/UAS SOD2; UAS ND75 dsRNA/+* was observed for beating patterns and the cardiac parameters were quantified using SOHA software.

M-mode patterns of these 2 genotypes show a significant restoration to the normal M-mode patterns observed in the case of control embryos (Fig. 4.5 B-E).

4.2.6a Heart period of stage 17 knockdown embryos in SOD2 overexpression background:

As reported previously, the heart period is increased to around 3 fold in *ND42*/*ND75* knockdown embryos compared to the control. Interestingly, by over-expressing *SOD2* in *ND42*/*ND75* knockdown embryos, the heart period is significantly reduced. In the case of *HandGFP; TwistGAL4/UAS SOD2; UAS ND42 dsRNA/+* embryos, the heart period is 8.98 milliseconds which is a significant reduction from the heart period of 15.15 milliseconds in *ND42* knockdown embryos (Fig. 4.5J).

In case of *HandGFP*; *TwistGAL4/UAS SOD2; UAS ND75 dsRNA/+* embryos, the heart period is 8.06 milliseconds which is a significant reduction from the heart period of 14.64 milliseconds in *ND75* knockdown embryos (Fig. 4.5J).

4.2.6b Diastolic interval is reduced in the knockdown embryos by over-expression of SOD2:

By knocking down *ND42*/*ND75*from the developing mesoderm, diastolic interval is increased to approximately 7 folds. By scavenging superoxide ions specifically from the mesoderm population, DI is reduced significantly in *ND42* (1.10 ms) and *ND75* knockdown embryos (0.95 ms) compared to *HandGFP;TwistGal4/+; UAS ND42dsRNA/+* (2.92ms) and *HandGFP;TwistGal4/+; UAS ND75dsRNA/+* embryos (2.63ms) (Fig. 4.5H).

4.2.6c Systolic interval is increased in knockdown embryos by over-expression of SOD2 in twist expressing mesoderm population:

Systolic interval was reportedly reduced drastically by knocking down *ND42* (SI=0.15ms) and *ND75* (SI=0.15ms) using *TwistGal4* as a driver by around 4 folds compared to control (SI=0.52ms). Over-expressing *SOD2* in *Twist* specific manner leads to a significant increase in SI in *ND42* (SI=0.67ms) and *ND75* knockdown embryos (SI=0.6m1s) (Fig. 4.5I).

4.2.6d Systolic and diastolic diameters are restored to normal by scavenging superoxide ions:

The systolic diameter in *HandGFP*; *TwistGAL4/UAS SOD2; UAS ND42 dsRNA/+* and *HandGFP*; *TwistGAL4/UAS SOD2; UAS ND75 dsRNA/+* embryos was increased significantly to 61.87 microns and 64.57 microns respectively compared to SD of 27.77 microns and 32.65 microns in Twi> *ND42*i and Twi>*ND75*i embryos respectively.
Diastolic diameter of *HandGFP*; *TwistGAL4/UAS SOD2; UAS ND42 dsRNA/+* and *HandGFP*; *TwistGAL4/UAS SOD2; UAS ND75 dsRNA/+* was increased significantly to 96.83 microns and 95.52 microns respectively compared to DD of 43.73 microns and 45.19 microns in *HandGFP*; *TwistGAL4/+; UAS ND42 dsRNA/+* and *HandGFP*; *TwistGAL4/+;UAS ND75 dsRNA/+* embryos respectively (Fig. 4.5F, G)

4.2.7 Rescue in lumen constriction by scavenging ROS:

The diameter of lumen was measured in *SOD2* overexpression in the background of *ND42* and *ND75* knockdown embryos respectively. Lumen diameter was significantly restored when compared to lumen diameter in wild type embryos. In case of *ND42* knockdown embryos, *SOD2* overexpression regained lumen diameter from 1.5 um (Fig.4.6C) to 2.22 um in aorta region (Fig. 4.6E) and 2.69um (Fig.4.6F) from 1.95um in heart proper (Fig.4.6D). A similar trend was observed in *ND75* knockdown embryos in *SOD2* overexpression background where lumen diameter was increased from 1.55 um (Fig.4.6G) to 2.07 um (Fig.4.6I) in aorta and 2.42um (Fig.4.6J) from 1.93 um in heart proper (Fig. 4.6H).

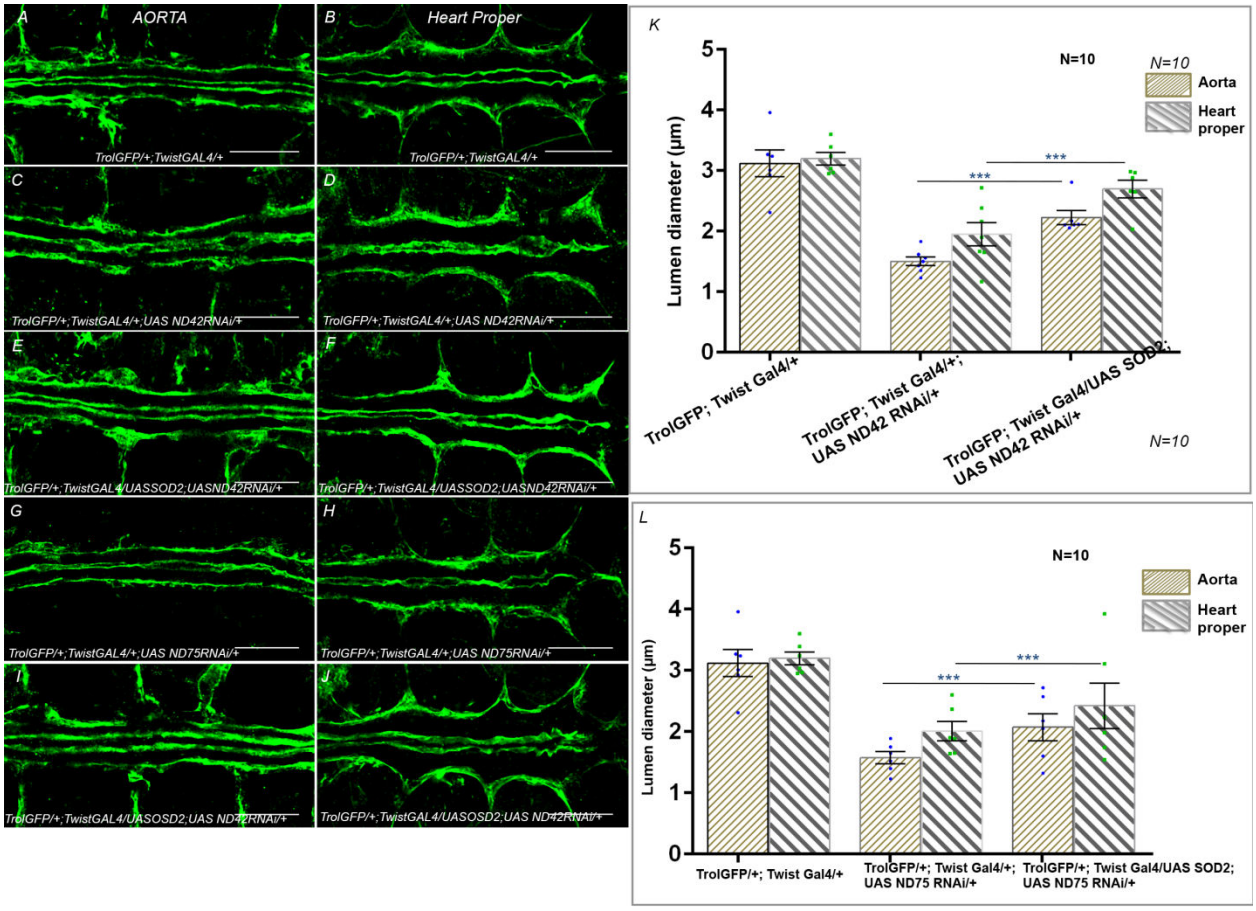

Fig. 4.6 Significant restoration of luminal diameter by scavenging superoxide ions from developing mesoderm: TrolGFP expression in the Aorta region **(A)** and Heart Proper (**B**) of wild type stage 16 embryonic heart. Knockdown of *ND42* and *ND75* from the developing mesoderm leads to constriction of lumen on aorta as well as heart proper regions (**C, D, G, H**). Overexpression of *SOD2* in the background of *ND42* and *ND75* knockdown evidently restores lumen diameter towards normal in the aorta **(E, I)**as well as heart proper region. (F, J) Statistical analysis revealed a significant rescue in lumen diameter in *SOD2* backgrounds compared to their knockdown counterparts **(K, L).**

4.2.8 Transcriptional upregulation of Pericardin is rescued by scavenging superoxide ions:

High *Pericardin* levels observed in complex-I knockdown embryos (Fig.4.7B,D) were decreased in *SOD2* over-expression background (Fig. 4.7C,E) as revealed by *Pericardin* immunostaining. *Pericardin* was much more restricted outside the lumen of the cardiac tube and *Pericardin* expression resembles closer to control embryos.

qRT PCR of *TwistGAL4/UAS SOD2; UAS ND42 dsRNA/+* knockdown embryos in revealed that *Pericardin* transcript levels were reduced significantly compared to ND42 and ND75 knockdown embryos (Fig. 4.7 G) .A similar trend was shown by *TwistGAL4/UAS SOD2; UAS ND75 dsRNA/+* embryos where *Pericardin* transcript levels were reduced compared to high levels as observed in *ND75* knockdown embryos. (Fig. 4.7H).

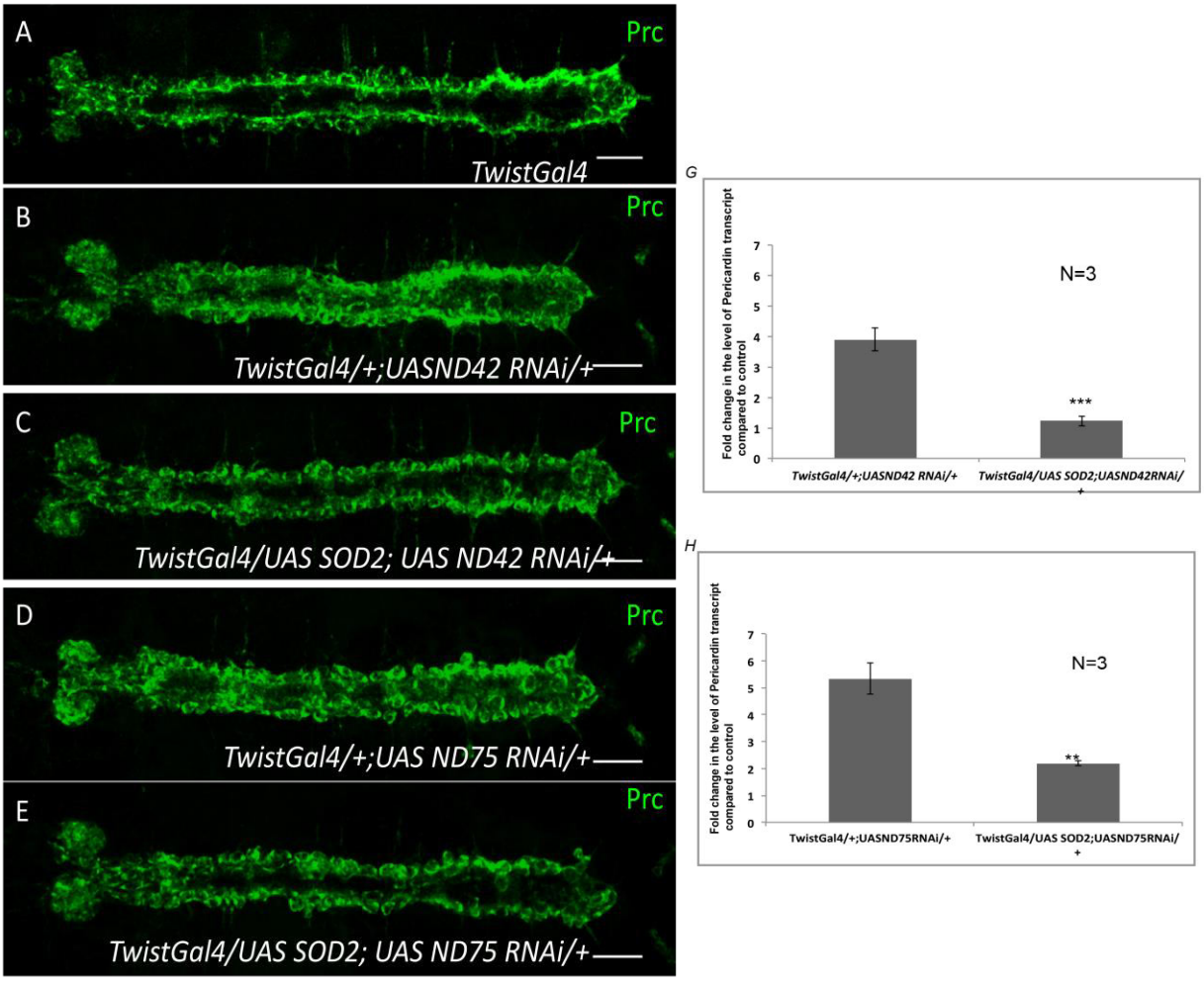

Fig.4.7. Increased Pericardin expression is rescued by overexpressing SOD2: Wild type stage 16 Drosophila embryonic heart immunostained for *Pericardin*, located at the boundaries of cardiac tube (A). Knockdown of *ND42* and *ND75* using *Twist*gal4 leads to increased and mislocalized *Pericardin* expression (B-D). Overexpression of *SOD2* in the knockdown backgrounds leads to the reduction and restriction of *Pericardin* expression on the cardiac tube boundaries (C-E). *Pericardin* transcript levels are significantly restored to normal in *TwistGAL4/UAS SOD2; UAS ND42 dsRNA/+* and *TwistGAL4/UAS SOD2; UAS ND75 dsRNA/+* embryos as revealed by qRT PCR (G-H).

4.2.8 Reduction in mitoSOX and gstD GFP levels by overexpression of SOD2:

At stage 13 of embryonic development, mitoSOX staining was performed to analyze superoxide levels in *SOD2* over expression background in complex-I knockdown embryos. It was found that elevated mSOX levels observed in the mesodermal derivatives of *TwistGal4/+;UAS ND42dsRNA/+(*Fig. 4.8B) and *TwistGal4/+;UAS ND75dsRNA/+* (Fig.4.8D)embryos were declined to insignificant mSOX levels in *SOD2* overexpression background (Fig. 4.8 C,E).
GstD GFP levels were significantly reduced to low levels in *ND42* (Fig.4.6I) as well as *ND75* knockdown embryos (Fig. 4.8K) in SOD 2 overexpression background compared to *TwistGal4/+;UAS ND42dsRNA/+(*Fig. 4.8H) and *TwistGal4/+;UAS ND75dsRNA/+* (Fig.4.8J)embryos.These results established that overexpression of *SOD2* is able to rescue elevated mitoSOX and *gstD GFP* levels.

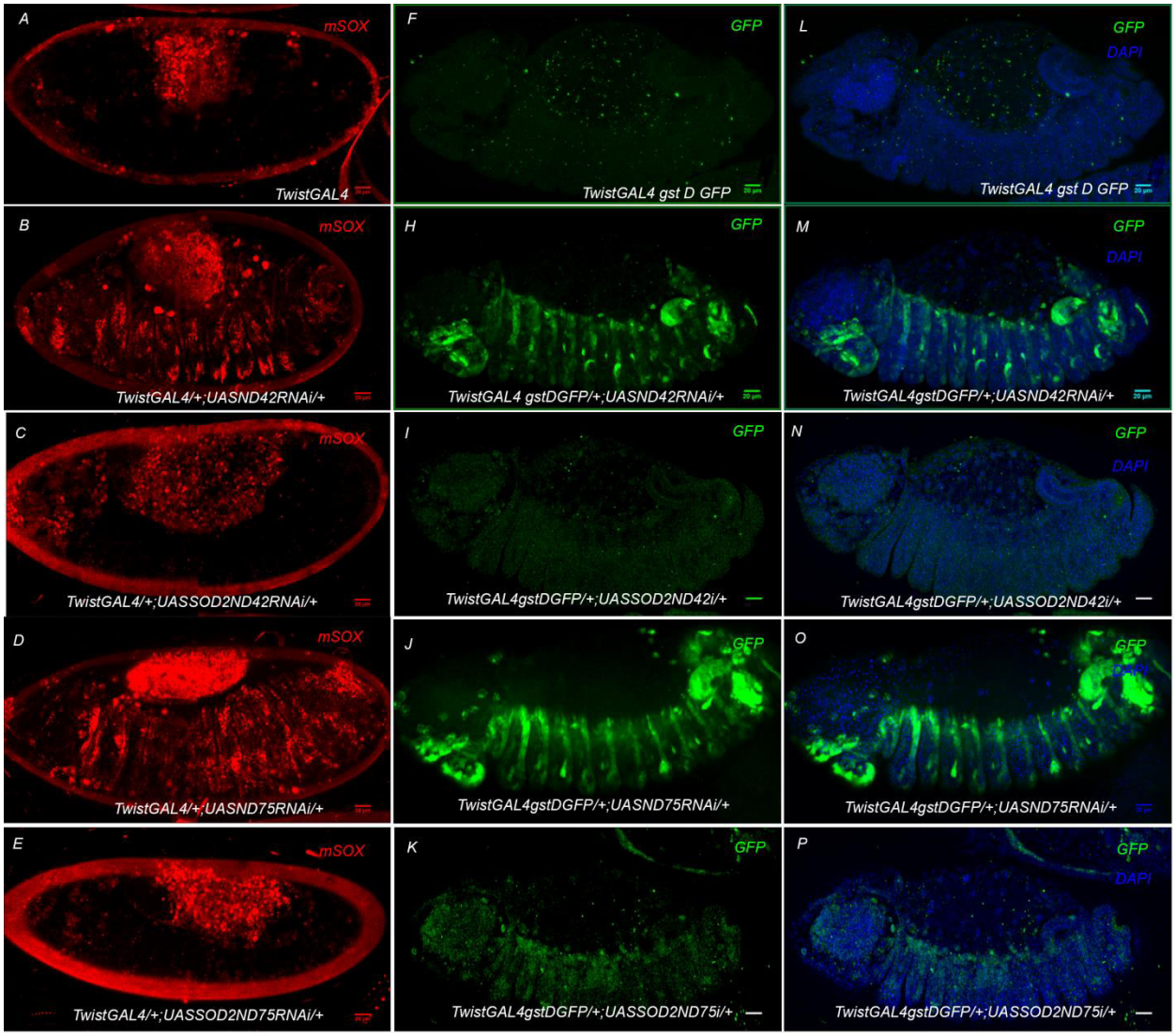

Fig.4.8. High ROS is scavenged from the cardiogenic mesoderm by overexpressing superoxide dismutase: Wild type stage 13 embryo stained for mitoSOX red **(A).** Mitosox staining can be located in each hemisegment in *ND42* and *ND75* knockdown embryos (**B, D**). Over-expression of *SOD2* in the background of *ND42* and *ND75* knockdown is able to scavenge high ROS levels as suggested by insignificant mitoSOX stain in these embryos (**C, E**). Wild type stage 13 embryos negative for *gstD GFP* expression (F, L). *ND42* and *ND75* knockdown embryos show a high level of *gstD GFP* expression in each hemisegment (**H, J**). Overexpression of *SOD2* in these knockdown backgrounds leads to a significant reduction in *gstD GFP* levels in each hemisegment **(I, K).**

4.2.9 Alteration in cell fate specification of cardioblasts:

Drosophila embryonic heart tube is comprised of total 104 cardioblasts spanning from abdominal segment A8 to thoracic segments T1 where it opens into the brain. At T2, the heart tube is flanked by the ring gland and at T3 by the lymph gland (Frasch et al, 2010).There are

mainly two cell types that make the cardiac tube. One type is myogenic in nature and expresses *Tinman*. They are called Generic cardioblasts. The second type is the inflow tracts that express *Seven up* and are known as ostial cardioblasts (Paululat A., 2012). Cardiogenesis in Drosophila is well explored in terms of the origin of different cell types and the signaling pathways regulating cell type specification spatially and temporally (Lovato TL, 2016). So while analyzing certain cardiac phenotypes, this information provides important cues on which cell signaling pathways are probably affected, thereby linking causal and effector molecules.

In wild type embryos at stage 16 of embryonic development, the cardiac tube has a 4+2 pattern in each hemisegment (4 *Tinman* positive cardioblasts+2 *Seven up* positive cardioblasts) as reported previously (Frasch et al, 2010) and evident from co-immunostaining for *Tinman* and *Seven up* GFP. By knocking down *ND42*/*ND75* from the developing mesoderm using *Twist*Gal4 as a driver, *Seven up* GFP revealed a random increase in the number of *Seven up* positive cardioblasts (Fig.4.9D, G). Co-immunostaining with *Tinman* and *Seven up* revealed a corresponding reduction in *Tinman* positive cardio blasts (Fig. 4.9 F, I) .These observations imply that a myogenic tentative *Tinman* expressing cardioblast has started expressing an ostial marker *Seven up*, and thus has changed its cell fate.

We tracked down this phenotype down the stages of heart tube formation and cell specifications. *Tinman* expression starts in the developing mesoderm from stage 9. At stage 11, *Seven up* expression begins in a subset of cardiac progenitors. These progenitors are initially both *Tinman* and *Seven up* positive but at stage 12; they lose *Tinman* expression and retain *Seven up* only (Lo et al, 2001)

In *ND42*/75 knockdown embryos, *Seven up* expression is normal at stage 11. At stage 12 also, the total number of cells expressing *Seven up* is unchanged when compared to wild type embryos (Fig.4.10). However at stage 13, when normal 4+2 pattern of *Tinman* + *Seven up* positive cells is found in control embryos, in *ND42*/*ND75* knockdown embryos, there were some *Tinman* positive cells that shows a very low level of *Seven up* expression too, suggesting the onset of 2+4 instead of 4+2 pattern of cardioblasts initiates at stage 13 (Fig. 4.11).

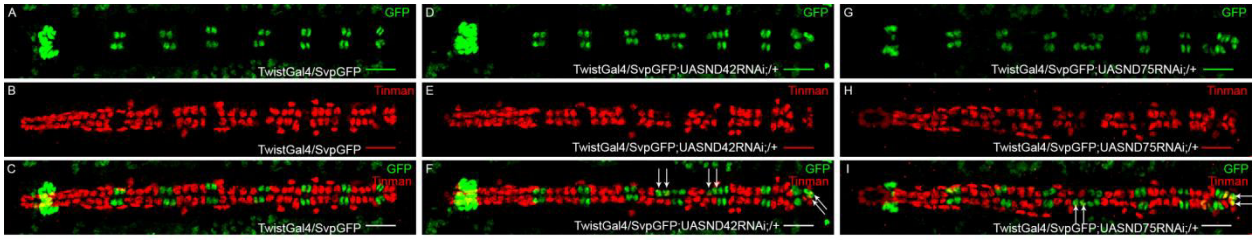

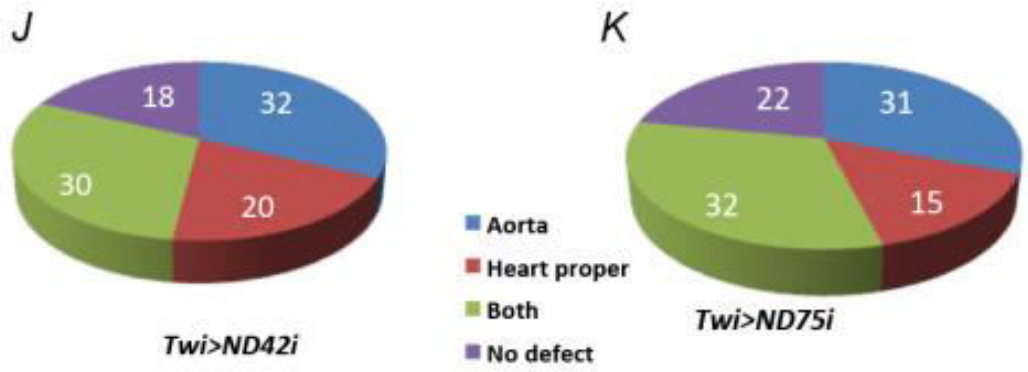

Fig.4.9.Cellular characterization of the cardiac tube revealed alteration in cell fate specification in complex-I knockdown embryos Wild type stage 16 Drosophila embryonic heart stained for *Seven up*GFP expressed in ring gland and two cardioblasts per hemisegment (A). *Tinman* is expressed in 4 cardioblasts per hemisegment in wild type stage 16 embryos (B). Co-immunostaining of *Tinman* and *Seven up* showed the 4+2 pattern of *Tinman+Seven up* cardioblasts in each hemisegment (C). In *ND42* and *ND75* knockdown embryos, there is an increase in *Seven up* positive cardioblasts in certain segments (D, G). Reduction in *Tinman* positive cardioblasts in some segments in *ND42* and *ND75* knockdown embryos (E, H). Co-immunostaining of *Tinman* and *Seven up* revealed an increase in *Seven up* positive cardioblasts correspond to reduced *Tinman* positive cardioblasts (F, I). There are some cardioblasts which co-express *Tinman* and *Seven up*. Quantization of cell fate defect with respect to its prevalence in aorta and heart proper regions of the cardiac tube (J, K).

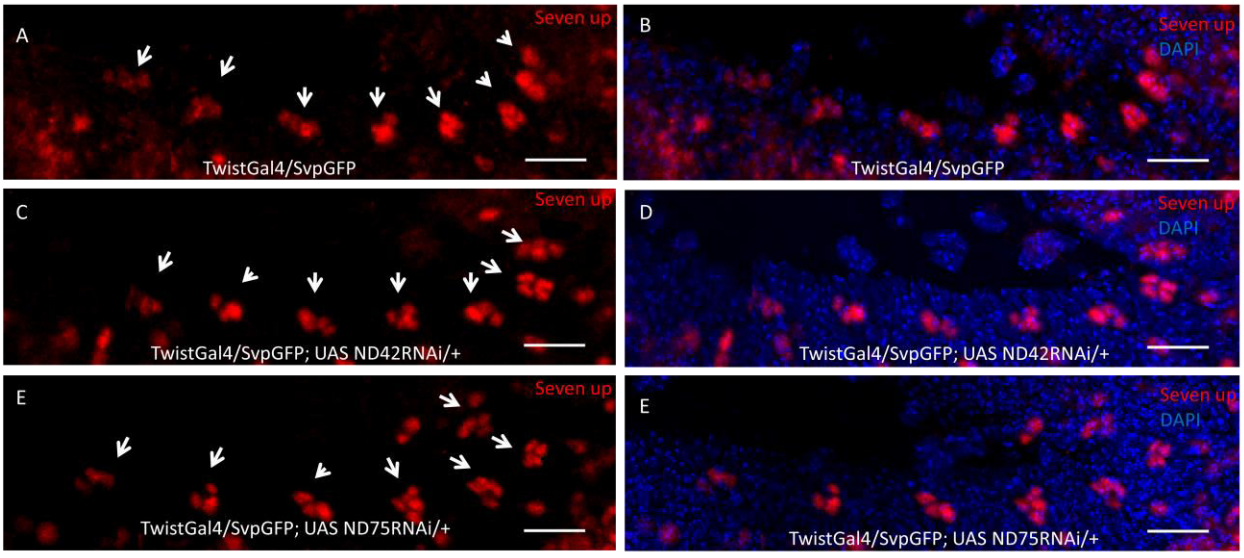

Fig.4.10 No change in number of seven up positive cardioblasts at stage 12 of embryonic development. Wild type stage 12 Drosophila embryonic hearts stained for *Seven up*GFP which is expressed in a subset of cardiac progenitores per hemisegment. Due to rapid movments and divisions at this stage, number of *Seven up* positive cells is not uniform in all the hemisegments. A range between 2 to 4 *Seven up* positive cardioblasts can be seen depending

on whether asymmetric division leading to 2 *Seven up* positive cardioblasts and 2 *Seven up* positive pericardial cells has taken place or not. (A) merged with DAPI (B). *Seven up* positive cardiac progenitors do not increase in number more than 4 in any of the hemisegment indicating no ectopic *Seven up* expression in any of the cardioblasts in *ND42* knockdown embryos (C) merged with DAPI (D) No ectopic *Seven up* expression in cardiac progenitors in *ND75* knockdown embryos at stage 12 of embryonic development (E) merged with DAPI (F).

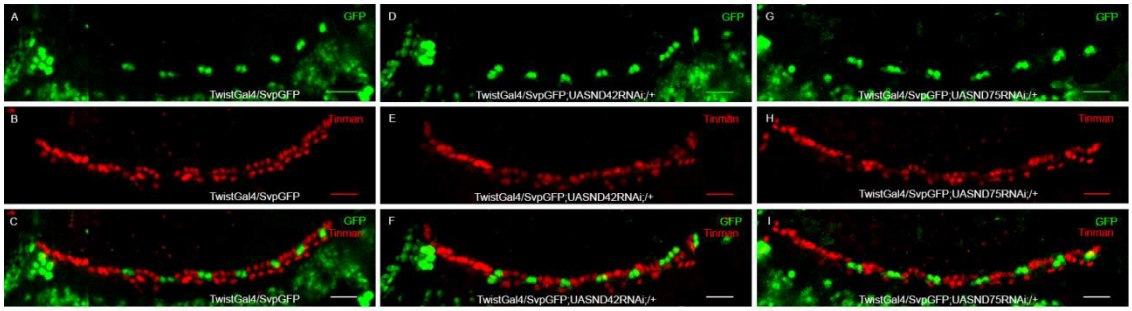

Fig. 4.11 Alteration in cell fate specification initiates at stage 13 of embryonic development: Wild type stage 13 Drosophila embryo stained for *Seven up* GFP, marking two cardioblasts per hemisegment **(A)** and *Tinman*, marking 4 cardioblasts per hemisegment **(B**) Co-immunostaining of *Tinman* and *Seven up*GFP reveals 4+2 pattern of these two subpopulations **(C).** In *ND42* and *ND75* knockdown embryos, reduction in *Tinman* positive cardioblasts is accompanied by an increase in number of *Seven up* positive cardioblasts (**D,E,F)**There are some cells which are positive for both *Tinman* and *Seven up*, although expression of *Tinman* is lowered compared to neighboring cells, suggesting fate change event has been initiated in these cells. (**G, H, I)**

4.2.10 Quantitative analysis of region-specific fate specification defects in knockdown embryos:

Since the cell type alteration defect is very random in terms of change in different parts of the cardiac tube, we quantified this phenotype with respect to following criteria:

a) Number of embryos with defect in the aorta region only

b) Number of embryos with defect in heart proper region only

c) Number of embryos with defect in both the aorta and heart proper region

d) Number of embryos with no defect.

Out of the total 100 embryos analyzed for both *ND42* and *ND75* knockdown, the distribution of phenotype is shown with the pie chart. (Fig. 4.7 J, K).

In case of *TwistGal4/+; UAS ND42dsRNA/+,* it was found that out of 100 embryos analyzed, 18 embryos show no cell fate alteration defect either in aorta or heart proper region. 32 embryos

exhibit defects in Aorta only whereas 20 embryo exhibit defects in Heart proper region. 30 embryos exhibit severe defects i.e. in these embryos, cell fate specification defects were observed in aorta as well as heart proper regions (Fig.4.7J). In case of *TwistGal4/+; UAS ND75dsRNA/+,* it was found that out of 100 embryos analyzed, 22 embryos show no cell fate alteration defect either in aorta or heart proper region. 31 embryos exhibit defects in Aorta only whereas 15 embryo exhibit defects in Heart proper region. 32 embryos exhibit severe defects i.e. in these embryos, cell fate specification defects were observed in aorta as well as heart proper regions (Fig.4.7K)

4.2.11 High level of ROS in the developing cardiogenic mesoderm is responsible for alteration in cell fate specification:

In order to investigate whether increased ROS levels in the cardiogenic mesoderm was responsible for alteration in cell fate specification observed from stage 13 of embryonic development onwards, *Tinman* vs *Seven up* subpopulations were observed in *TwistGAL4/UAS SOD2; UAS ND42 dsRNA/+* and *TwistGAL4/UAS SOD2; UAS ND75 dsRNA/+* knockdown embryos.

As described previously , knocking down *ND42* from the developing mesoderm result in increase in number of *Seven up* positive cardioblasts (Fig. 4.12D) in the cardiac tube of stage 16 *Drosophila* embryo compared to control(Fig. 4.12A). In these embryos, there is a simultaneous reduction in number of *Tinman* positive cardioblasts (Fig. 4.12E).By scavenging ROS by over expressing *super-oxide dismutase 2 (SOD2)* in these knockdown embryos lead to restoration of normal 4+2 pattern of *Tinman* vs *Seven up* cardioblasts as shown by co-immunostaining for *Tinman* and *Seven up* (Fig.4.12 G, H, I).

Knocking down *ND75* from the developing mesoderm also result in increase in number of *Seven up* positive cardioblasts (Fig. 4.12J) in the cardiac tube of stage 16 *Drosophila* embryo compared to control(Fig. 4.12A). In these embryos, there is a simultaneous reduction in number of *Tinman* positive cardioblasts (Fig. 4.12K).By scavenging ROS by over expressing super-oxide dismutase 2 (*SOD2*) in these knockdown embryos lead to restoration of normal 4+2 pattern of *Tinman* vs *Seven up* cardioblasts as shown by co-immunostaining for *Tinman* and *Seven up* (Fig.4.12 M, N, O).

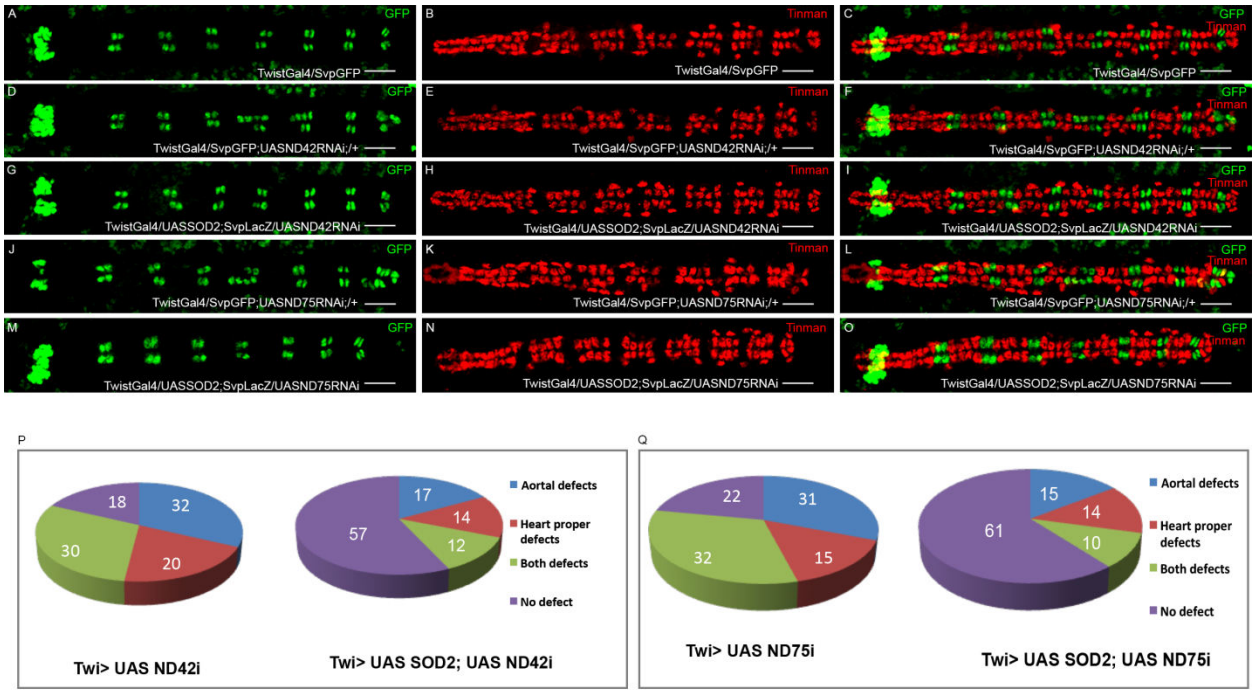

Fig. 4.12. Overexpression of SOD2 is able to reverse cell fate specification defects in complex-I knockdown embryos. *Seven up*(**A),** *Tinman* **(B**) and co-expression of *Tinman* and *Seven up* (**C)** in wild type stage 16 Drosophila embryonic heart. In *ND42* and *ND75* knockdown embryos, reduction in *Tinman* positive cardioblasts is complemented by an increase in *Seven up* positive cardioblasts (**F, L).** Overexpression of *SOD2* in *ND42* and *ND75* knockdown backgrounds lead to the significant restoration of the normal 4+2 pattern of *Tinman*+ *Seven up* cardioblasts. **(I, O**). Quantitative analysis of region-specific defects shows significant rescue in the number of defective embryos in *SOD2* overexpression background (**P, Q).**

4.2.12 No change in the total number of pericardial cells in ND42 and ND75 knockdown embryos:

Cardioblasts are flanked by pericardial cells which act as nephrocytes in *Drosophila* (Kowalevsky et al, 1889). In *ND42* and *ND75* knockdown embryos, the expression of *Pericardin* which is secreted by pericardial cells was increased compared to control. Our previous results also established an increase in *Pericardin* transcript levels in *ND42* and *ND75* knockdown embryos. However, whether there are any changes in the number of pericardial cells remained unanswered. *Zfh1(zinc finger homeodomain 1)* marks all the pericardial cell populations as well as the lymph gland (Sellin et al, 2009). In order to precisely calculate pericardial subpopulations and to eliminate lymph gland cells, co-immunostaining with *Zfh1* and *Pericardin* was done since

lymph gland cells do not express *Pericardin*. Quantitative analysis revealed no change in the total number of pericardial cells in *ND42* (Fig. 4.13E) and *ND75* knockdown embryos (Fig.4.13H) compared to control (Fig.4.13J)

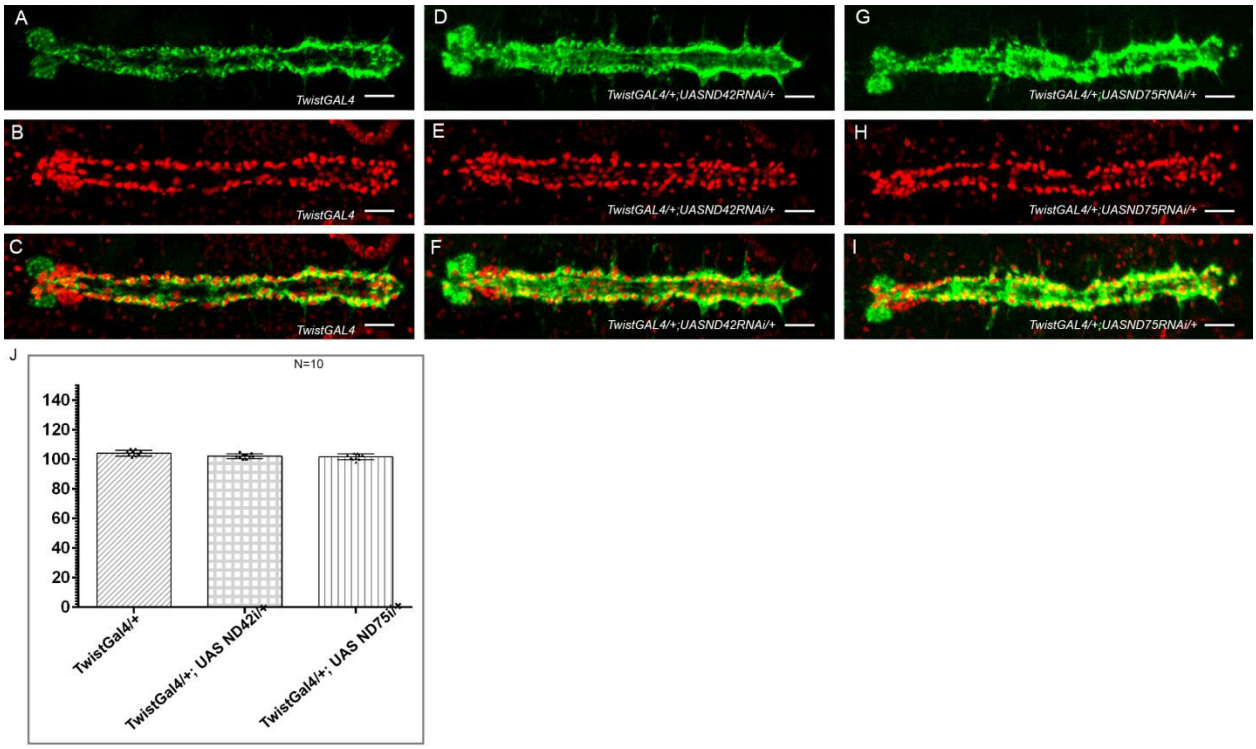

Fig. 4.13 Pericardial cell number is not affected in complex-I knockdown embryos. Wild type stage 16 Drosophila embryo stained for *Pericardin* **(A)** and *Zfh1* **(B, C)**. Merged image shows *Pericardin* surrounding the pericardial cells. In *ND42* and *ND75* knockdown embryos, *Pericardin* expression is increased and mislocalized towards the lumen of the cardiac tube. (**D, G**) However no apparent change in alignment or number of pericardial cells as revealed by *zfh1* immunostaining(**E, H**). Quantization of *Pericardin* secreting *zfh1* positive pericardial cells revealed no significant change in the total number of pericardial cells in knockdown embryos compared to control (**J).**

4.2.13 Increased and mislocalized pericardin in ND42 loss of function embryos:

Since all the studies were accomplished in knockdown embryos, the mutant analysis was done in support of RNAi analysis. P{EP}ND-42^{G4500}/TM6C,Sb fly line from BDSC was used for *ND42* mutant analysis. The P{EP} element contains UAS regulatory sequence and Hsp70 promoter sequence at its 3'end. The P{EP} element typicallt inserts at the 5'end of the gene , resulting in over- or mis-expression of the endogenous gene in the presence of Gal4 driver. These misexpression elements are reportedly not that strong (Rorth, 1996). Since any other *ND42* loss

of function allele was not commercially available, this line was used for mutant analysis. TM6C, Sb balancer was replaced by *KrGFP,TM3Sb* balancer so that homozygous embryos could be screened out.

Hatching rate of GFP negative homozygous embryos from synchronized collections of *ND-42*^{G4500}*/KrGFP,TM3Sb* was calculated. Embryonic lethality assay revealed 20% lethality in loss of function homozygous embryos (Fig.4.14A'). Immunostaining with *Pericardin* revealed a varying degree of increase in *Pericardin* expression (Fig. 4.14B, C) compared to control (Fig. 4.14A). Quantification of increased *Pericardin* phenotype revealed that in average 26 percent homozygous *ND42* loss of function mutant embryos, *Pericardin* expression mimics the *ND42* knockdown phenotype (Fig. 4.14).

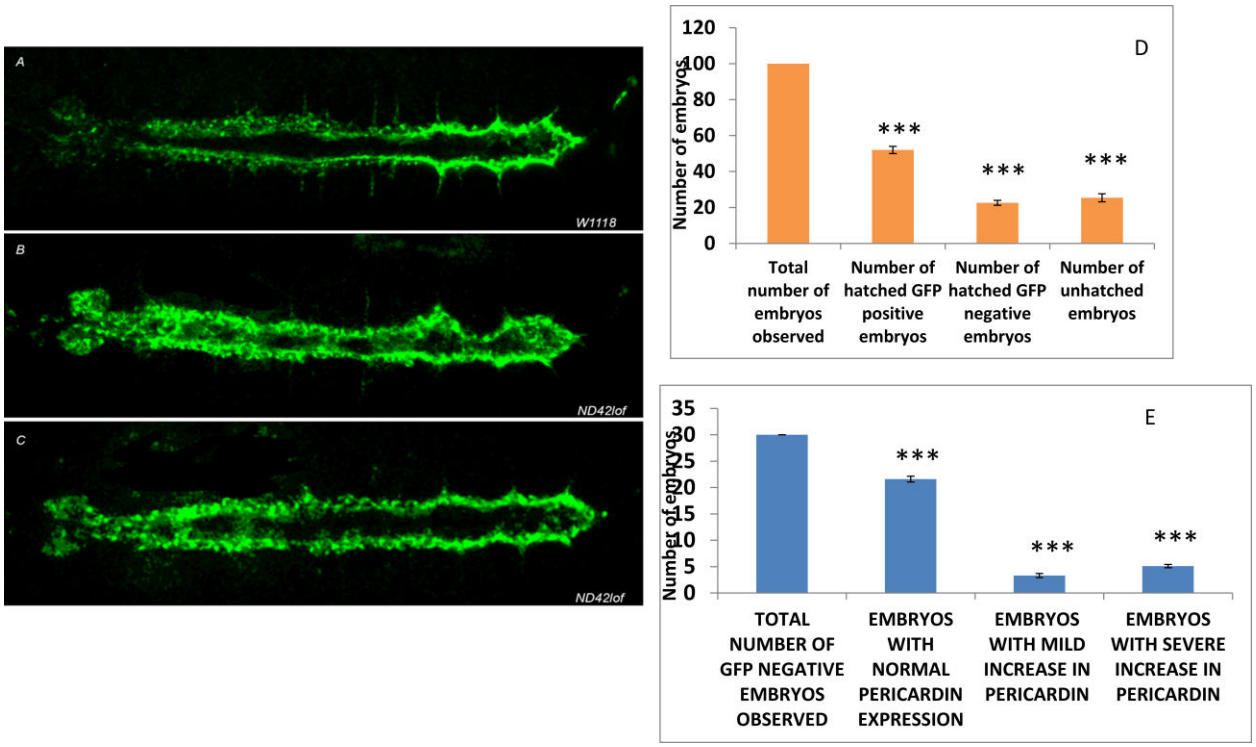

Fig.4.14 Pericardin expression in stage 16 embryonic heart at the boundaries of the cardiac tube Varying degrees of increased and mislocalized *Pericardin* towards lumen in *ND42* loss of function homozygous embryos (B, C) compred to wild type embryo at stage 16 of embryonic development (A). Quantization of homozygous mutant embryos in terms of null, less severe and more severe *Pericardin* phenotype (D). Quantization of number of GFP positive heterozygous *ND42* lof mutant embryos and GFP negative homozygous *ND42* lof mutant embryos that are hatched (E).

4.2.14. Gal4 titration in SOD2 over expression background in ND42/ND75 knockdown embryos is not responsible for rescue in cardiac phenotypes:

In order to show that rescue in cardiac phenotype in *HandGFP; TwistGAL4/UAS SOD2; UAS ND42 dsRNA/+* and *HandGFP; TwistGAL4/UAS SOD2; UAS ND75 dsRNA/+* embryos is not due to Gal4 titration, cardiac tube of stage 17 embryos from *HandGFP; TwistGAL4/UAS lacZ; UAS ND42 dsRNA/+* and *HandGFP; TwistGAL4/UAS lacZ; UAS ND75 dsRNA/+* was observed for beating patterns and the cardiac parameters were quantified using SOHA software.

Co-immunostaing with GFP and β-galactosidase antibody in *HandGFP; TwistGAL4/UAS lacZ; UAS ND42 dsRNA/+* and *HandGFP; TwistGAL4/UAS lacZ; UAS ND75 dsRNA/+*embryos confirmed the presence of lacZ insert and *Hand*GFP in these lines (Fig. 4.15 A, B)

It was found that M-mode pattern (Fig.4.15 B-F) as well as different cardiac parameters i.e. Heart Period, Heart rate, Diastole interval, Systole interval, Diastole diameter and Systole diameter were showing the same trend of cardiac dysfunction as that of *HandGFP; TwistGAL4/+; UAS ND42 dsRNA/+* and *HandGFP; TwistGAL4/+; UAS ND75 dsRNA/+* embryos (Fig.4.15)

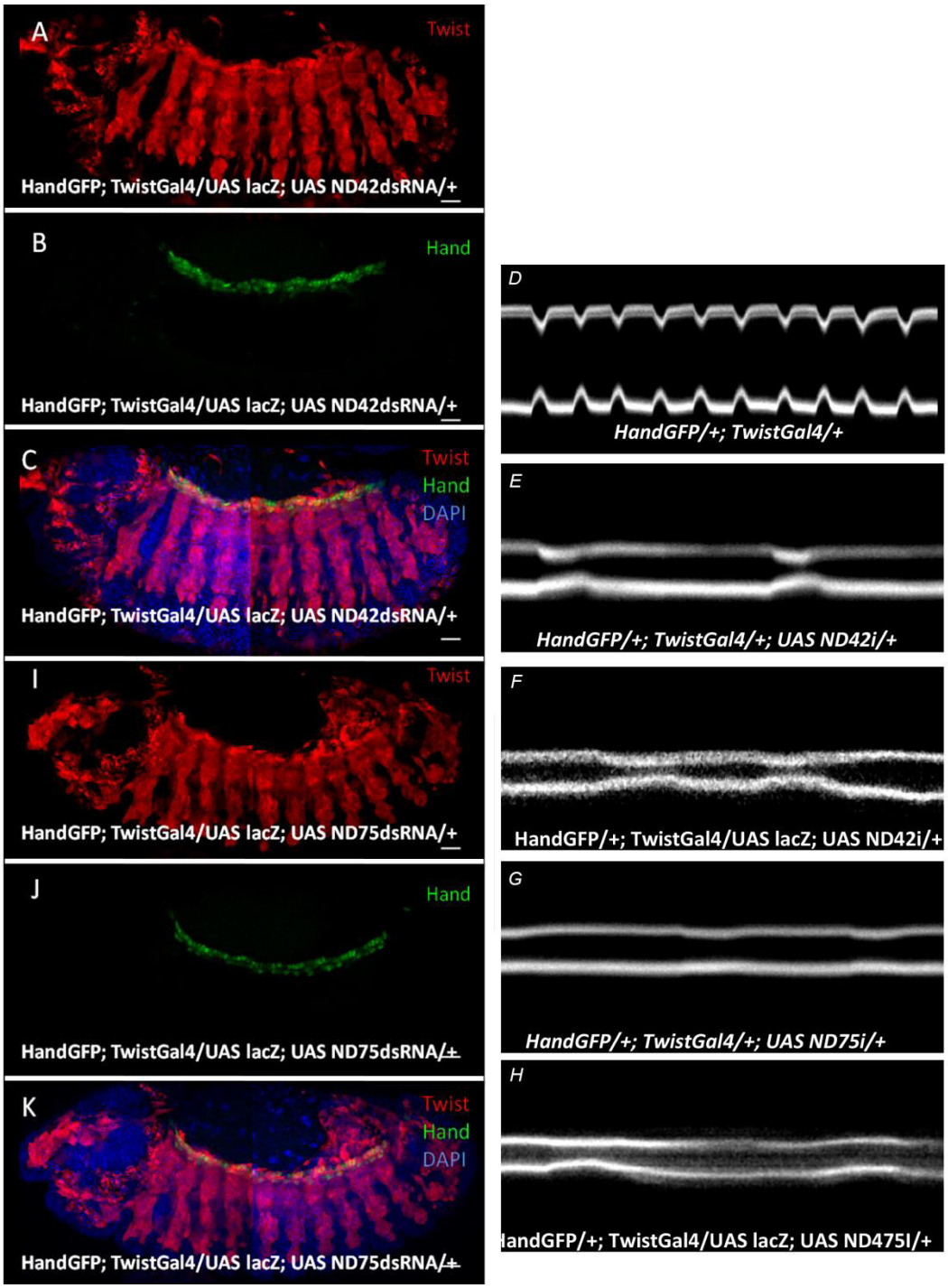

Fig.4.15. Overepxression of LacZ in ND42 and ND75 knockdown embryos does not rescue cardiac phenotypes :UAS lacz driven by *Hand*GFP, *Twist*Gal4 in *ND42* and*ND75* background is shown, β-gal staining in the *Twist* expression pattern (red) (A,I) and *Hand* expression (green) in stage *16 Drosophila* embryo (B,J), merged with DAPI (C,K), M-mode patterns of *Hand*GFP; *Twist*Gal4 (B), *Hand*GFP; TwisGAL4/+; UAS *ND42* dsRNA/+ **(C),** *Hand*GFP, *Twist*Gal4/ UAS lacZ; UAS *ND42*ds RNA/+ (D), *Hand*GFP; TwisGAL4/+ UAS *ND75* dsRNA/+ (E), *Hand*GFP;*Twist*Gal4/UAS lacZ; UAS *ND75* dsRNA/+ (F).

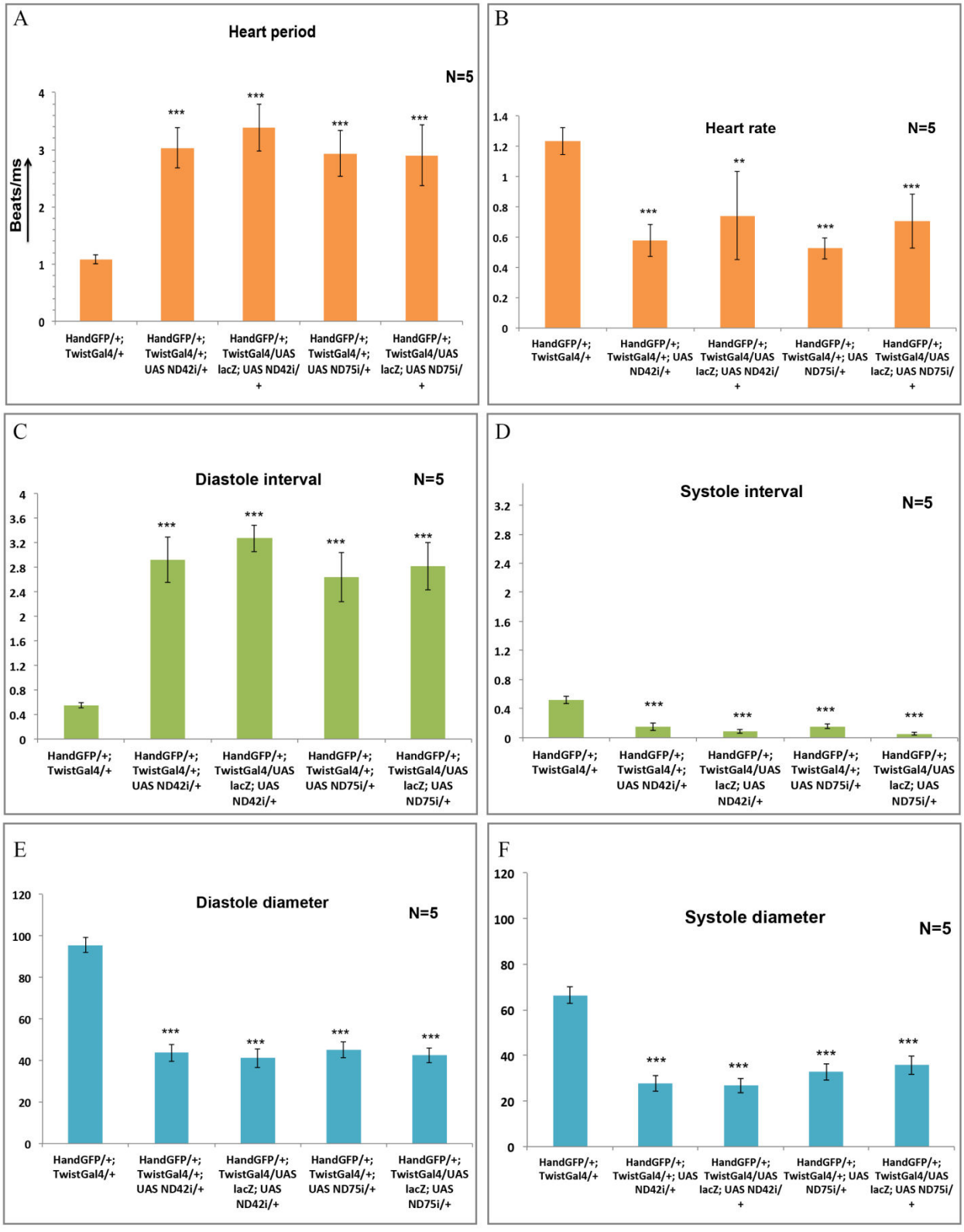

Fig 4.16 SOHA analysis of ND42/ND75 knockdown embryos in lacZ over expression background:

Quantization of cardiac parameters with SOHA revealed similar trend of altered heart rate, heart period, systole-diastole interval and systole-diastole diameters in complex-I knockdown embryos in lacZ over expression background (**A-F)**

4.3 DISCUSSION

In this study, I have investigated the outcome of attenuating complex- of ETC from the developing cardiogenic mesoderm and underlying mediators of retrograde response elicited by mitochondrial dysfunction.

Complex- I is the entry point of most of the electrons in the ETC (Koopman et al., 2010; Sharma et al., 2009). There are two major outcomes reported when complex-I function is attenuated. The first and foremost outcome is the decline in ATP levels since a majority of the substrates i.e. electrons are not entering into the ETC in this scenario. Surprisingly, we observed a modest decrease in ATP levels in ND42 and ND75 knockdown embryos compared to wild type embryos. This may happen because complex-I is not the sole entry point of electron to enter in ETC. It has been reported that in these conditions, electrons can go through complex-II into the ETC to replenish ATP production.

The second outcome of hampered complex-I is an increase in ROS levels due to more free electrons available which react with molecular oxygen to form superoxide ions (Drose et al., 2016; Fato et al., 2008). Superoxide ions further react with water to form peroxide ions. Two ROS reporters were used in this study. Mitosox Red permeates live cells and selectively targets mitochondria (Benov et al., 1998; Zielonka and Kalyanaraman, 2010). This dye is rapidly oxidized by superoxide ions specifically and is highly fluorescent upon binding to nucleic acids. *gstD GFP* reports superoxide as well as peroxide ions (Sykiotis and Bohmann, 2008).MitoSOX and *gstD GFP* revealed elevation in ROS levels in the developing mesoderm population in knockdown embryos.

The next objective of this study was to investigate whether superoxide dismutase can scavenge excessive ROS in the developing cardiogenic mesoderm. Superoxide dismutases are the set of enzymes that function to detoxify reactive oxygen species. The genetic ablation of *SOD2*, a manganese- containing superoxide dismutase, which is principal scavenger of mitochondria superoxide has been shown to negatively affect the survival of diverse organisms e.g. yeast (O'Brien et al., 2004; Unlu and Koc, 2007), *Drosophila (Duttaroy et al., 2003; Kirby et al.,*

2002) and mice (Lebovitz et al., 1996; Li et al., 1995). *SOD2* mutant strains have been shown to exhibit neonatal mortality (Lebovitz et al., 1996; Li et al., 1995).*SOD2* null-mutants of *Drosophila* also exhibit adult mortality within a day of pupal eclosion (Duttaroy et al., 2003).

By scavenging high ROS in knockdown embryos, the phenotype of altered cell identity was significantly rescued in knockdown embryos. It implied that high ROS levels were responsible for change in cell fate specification during cardiogenic mesoderm formation. This was quite an interesting discovery since it showed high ROS levels can interfere with specification programs and can change the fate of a particular cell to another cell.

Significant rescue of lumen diameter by scavenging ROS by overexpression of superoxide dismutase in the knockdown embryos is an intriguing observation. As previously reported, signaling through *Slit/ Robo* pathway mediates shape change and lumen formation of heart cells (Kramer et al., 2001; Wong et al., 2002).During cardiogenesis, embryos lacking *Slit* and *Robo* function have expanded E-cadherin and b-catenin localization into the presumptive luminal domain thereby preventing lumen encapsulation (Medioni et al., 2008; Qian et al., 2005; Santiago-Martinez et al., 2006). In mutants lacking either *Slit* or both *Robo* and *Robo*2 receptors, the cardioblasts remain rounded and come into contact along most of their opposing surfaces, including the presumptive luminal domain, thereby blocking lumen formation (Medioni et al., 2008). Our results suggest that ROS levels may be regulating *Slit*/*Robo* signaling; however, more investigation in this area is required.

Expression of *Pericardin*, a type IV collagen-like protein is highly increased in the cardiac tube of knockdown embryos. This phenotype is very similar to changes in ECM components associated with cardiac hypertrophy and cardiac fibrosis (Berk et al, 2007). ROS has been previously shown to be involved in cardiac hypertrophy induced by angiotensin II, endothelin 1, norepinephrine, tumor necrosis factor α or pulsatile mechanical stretch and has been shown to be inhibited by antioxidants (Cave et al., 2005). In this study, increased and mislocalized *Pericardin* in the cardiac tube has been scavenged by over expressing superoxide dismutase, thereby providing evident role of ROS as a causal factor for affecting ECM component *Pericardin*.

The above-mentioned result that high ROS levels can directly alter the choice of fate a cell adopts is a groundbreaking finding. It has improved our understanding of the impact of retrograde signaling by mitochondria to regulate nuclear gene expression. There is a significant

amount of research claiming the signaling pathways regulated by ROS (Zhnag et al, 2016); however, there are still very few reports which prove that the metabolic status of a cell can alter the course of fate it is going to take.

Tinman and *Seven up* positive cells are two different kinds of cardioblast populations with very different functions. *Tinman* positive cardioblasts are myocardioblasts which function as heart muscles and facilitate heart pumping. On the other *Hand*, *Seven up* positive cardioblasts are non-muscle cells that act as inflow tracts for hemolymph. Our finding implies that by sensing oxidative stress, a cascade of events started in the cardioblast to force it to adopt a completely different fate.

This finding adds a new aspect to the regulation of cardiogenesis. Apart from the key signaling pathways known to regulate cell fate specifications during cardiogenesis, reactive oxygen species have emerged out to be a key signal that has the capability to change course of events leading to altered cell fate of cardioblasts.

Implication of mitochondrial signaling in cell lineage specification and cardiogenesis has been shown by relatively fewer reports. Hom et al, 2011 has demonstrated that modulators of Mptp closure (mitochondrial permeability transition pores) promote mitochondrial maturation and cardiomyocyte differentiation in the mouse embryo (Folmes et al., 2012). In sea urchin embryos, oral-aboral axis specification has been shown to be entrained by mitochondrial distribution and redox state (Coffman and Davidson, 2001). The present study has added a new aspect to this field by showing that mitochondrial perturbations can directly hit the developmental programs and can reinforce the nuclear decisions to change the cell fate. Deciphering mechanisms underlying mitochondrial signaling in heart development may refine research on stem cell specification for regenerative applications thereby offer implications for cardiac pathology.

Chapter 5

High ROS levels in the mesoderm cause severe cell number reduction in the embryonic lymph gland

5.1 Introduction:

Drosophila and vertebrate hematopoiesis share several similarities in terms of genetic mechanisms and transcriptional factors involved(Evans and Banerjee, 2003).Similarly, *Drosophila* shares significant similarities with vertebrates in terms of developmental programs involved in cardiogenic mesoderm specifications(Mandal et al., 2004).

5.1a Development and characterization of *Drosophila* embryonic lymph gland:

Formation of blood cells i.e. hematopoiesis in *Drosophila* has three phases that serve to provide blood cells in embryonic, larval and adult stages of the Drosophila life cycle(Lebestky et al., 2000, Ghosh et al, 2015). In *Drosophila*, blood cells are termed as hemocytes. They play significant roles in development and immunity (Franc et al., 1996; Manaka et al., 2004; Kurant et al., 2004). They secrete and remodel ECM components critical for morphogenesis and selectively remove dead cells and debris(Llanes, 1975; Murray et al., 1995; Tepass et al., 1994).They also monitor and regulate the environment for pathogens and signaling to the larval fat body which is the major source of antimicrobial peptide production(Agaisse et al., 2003; Hetru et al., 2003; Tzou et al., 2002).

In Drosophila, three types of terminally differentiated hemocytes have been reported: plasmatocytes, crystal cells, and lamellocytes (Krzemien et al., 2007, Lebestky et al. 2003; Jung et al., 2005). Among them, plasmatocytes are the most prominent population of hemocytes (around 90-95 % of the entire population) and the majority of the left ones are crystal cells. Lamellocytes are very few in normal conditions but can be induced in large numbers during the immune challenge(Ramet et al., 2002; Sorrentino et al., 2002).

The first phase of hematopoiesis occurs during embryonic development when the head mesoderm gives rise to hemocytes which subsequently migrate throughout the embryo (Tepass et al., 1994). The second phase of hematopoiesis is initiated in a specialized organ, the lymph gland which is formed during embryogenesis and persists through the onset of metamorphosis(Rugendorff et al., 1994). The third phase of hematopoiesis occurs in the dorsal abdominal hemocyte clusters of the adult fly (Ghosh et al, 2015).

Hematopoietic development in *Drosophila* and vertebrates have a striking similarity with respect to signaling pathways and transcription factors involved in regulating proliferation, differentiation and lineage commitment. Another key similarity between *Drosophila* and vertebrate hematopiesis is the presence of hemangioblasts; a common precursor for hematopoietic and endothelial cell (Mandal et al., 2005; Choi K et al., 1998).

5.1b Development of the embryonic lymph gland:

During mid-embryogenesis, lymph gland originates from dorsal thoracic mesoderm as reportedly shown by the expression of zinc-finger protein odd-skipped. Three thoracic odd positive clusters coalesced to form the lymph gland(Mandal et al., 2007; Rugendorff et al., 1994). At stage 16 of embryonic development; lymph gland is a paired cluster of 20 prohemocytes flanking the aorta at T3 segment (Fig.5.1). All the prohemocytes constituting the lymph gland express serpent (Lebestky et al., 2000). These prohemocytes proliferate but do not differentiate during the embryonic stages. The proliferation of hemocytes in the embryo follows a fixed program of four mitotic divisions like the rest of the majority of the mesodermal population at specific times(Beer et al., 1987; Klapper et al., 1998; Tepass et al., 1994). These prohemocytes then proliferate subsequently during larval stages.

Prohemocytes constituting embryonic lymph glands are cells 4-6 um in diameter with a little cytoplasmic volume and a few defining characteristics(Ramet et al., 2002; Rehorn et al., 1996). They express GATA factor Serpent. Serpent plays a central role in committing mesodermal cells to hemocyte fate.

The embryonic lymph gland is comprised of two subpopulations, one is *antennapedia* and serpent positive population of cells constituting the Posterior Signaling Centre (PSC) or niche

and the other is serpent positive *antennapedia* negative cell population, constituting the primary lobe of the lymph gland. Further diversification of primary lobe of the lymph gland into cortical zone that house differentiated blood cells and medullary zone that contain stem- like progenitors, takes place during larval stages.

Recent report by Dey NS et al., 2016 has evidenced the presence of transient Notch expressing hematopoietic stem cells (HSCs) in the first instar larval lymph gland which give rise to progenitor cells. These HSCs shows similarities with mammalian AGM HSCs as they use BMP/dpp as a niche signal for their maintenance

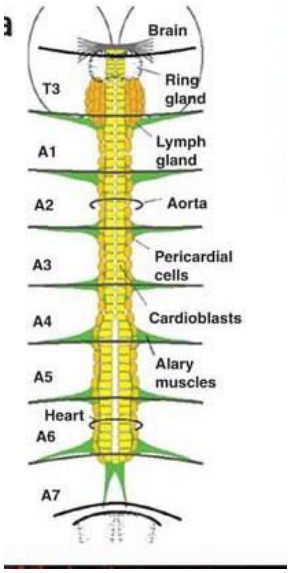

Figure 5.1: Schematic showing the structure and position of the lymph gland and dorsal vessel (Mandal, 2004)

5.1c Signaling cascades involved in the formation and functioning of embryonic lymph gland

The lymph gland progenitors originate from cardiogenic mesoderm (Mandal et al., 2007). Specifications of the cardiogenic mesoderm require the input of FGF (Beiman et al., 1996), Dpp (Frasch, 1995)and Wg(Wu et al., 1995) signaling from the overlying ectoderm. It has been shown that the antagonistic relationship between *Tinman* or *Pannier* expression in cardioblasts and *Srp* expression in lymph gland progenitors is responsible for the differentiation of cardiovascular and blood cell lineages. Notch signaling has been reported to be responsible for this differentiation. In the thoracic cardiogenic mesoderm, Notch antagonizes *tin* and *pnr* expression and promotes serpent expression, thereby favoring the development of lymph gland

progenitors(Mandal et al., 2007).Further studies have revealed that specification of blood progenitor fate is determined by convergence of Notch and MAPK signaling(Grigorian et al., 2011).

Studies have further explored how notch becomes active in the subset of cells that become blood progenitors. It has been shown that cardiogenic clusters are formed in each of the segments which are defined by high expression levels of *Delta* (Dl), *Lethal of scute* (L'sc) and activated MAPK. The default fate of all cardiogenic cells is cardioblasts(Mandal et al., 2004).Delta triggers Notch activity, which is required for specification of blood progenitors in thoracic cardiogenic clusters and nephrocytes in abdominal cardiogenic clusters, respectively (Fig.5.2). MAPK signaling maintains high levels of Dl in the cardiogenic clusters, and localizes Dl expression toward a dorsal subset of cells within these clusters, which will become cardioblasts. Dl stimulates Notch activity in the surrounding cells, which triggers the blood progenitor fate in the cells of thoracic segments and nephrocyte fate in cells of abdominal segments.

Four consecutive segments are shown in Fig. 5.2. T2 and T3 are the thoracic segments whereas A1 and A2 are the abdominal segments. At stage 11 of embryonic development, *delta* positive cardiogenic clusters as well as *even-skipped* positive pre-pericardial cells are present both in thoracic and abdominal segments .Following mitosis, each of the high *delta* cardiogenic clusters gives rise to two cardiobalsts whereas in abdominal segments, each high *delta* cluster gives rise to 3 cardiobalsts. However, only two cells out of three maintain high *delta* and *tin.* Third cell downregulates these geens and express *seven up*. (Ward and Skeath, 2000). *Seven up* positive cells divide once and form anterior and posterior pair in each segment. During germ band retraction, anterior and posterior *seven up* positive cells in adjacent segements come together to form a pair. The dorsal sibling of this pair becomes a cardioblast whereas ventral sibling becomes a pericardial cell (Ward and Skeath, 2000). In this way, the characteristic pattern of four *tinman/Delta* positive and two *seven up* positive cardioblasts in the abdominal dorsal vessel is generated.

The cardiogenic cluster in thoracic segment gives rise to 8-10 pairs of *seven up* negative blood progenitors. A significant fraction of these blood progenitors are the siblings of cardioblasts similar to abdominal segments (Mandal et al., 2004). Although cardiogenic cluster of stage 12 embryos is almost of same as that in abdominal segments , however , the fraction of cells that

undergo fourth round of division are considerably higher, which accounts for more blood progenitors per segment in thoracic segments (Grigorian et al., 2011).

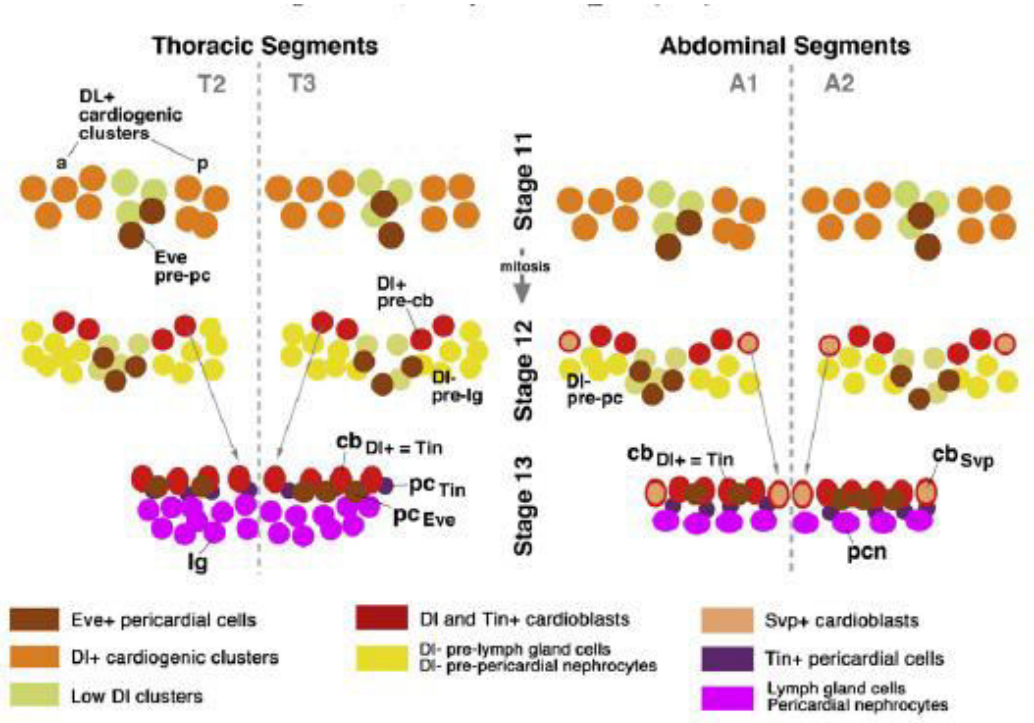

Figure 5.2: Schematic depiction of specification of different cell fates in the cardiogenic mesoderm. Two adjacent thoracic and abdominal segments are shown from stage 11 to stage 13. Different colored spheres denote different type of cells of cardiogenic mesoderm {Taken from (Grigorian et al., 2011)}

5.1d Formation of Posterior Signaling Center (Niche):

Posterior signaling centre or Niche is located in the posterior part of the lymph gland and is composed of about 30 cells as observed in late third instar of *Drosophila* larvae (Jung et al., 2005). During embryogenesis, specification of PSC requires function of *Collier (col)* gene. *Collier* is an ortholog of *early B-cell factor (ebf)* genes in mammals (Wang et al., 1993; Hagman et al., 1993; Daburon et al., 2008*). Col* mutant analysis have shown that PSC is required to maintain a pool of pluripotent hematopoietic progenitors in lymph gland (Krzemien et al., 2007; Mondal et al., 2011). This function of hematopoietic niche is similar to CSH niche in vertebrates.

Therefore, Drosophila PSC is a preferred model to study in vivo cellular and molecular mechanisms involved in the formation of hematopoietic niche.

5.1d1Signaling pathways involved in PSC function:

PSC is capable of releasing diffusible signals which in turn activate different signaling pathways in medullary zone and cortical zone of the lymph gland. Two most well characterized niche signals are *Hedgehog (hh)* and ligand *PVF1* (*platelet-derived growth factor / vascular endothelial growth factor-like factor*). The loss of function in the PSC of *hh* or *pvf1* genes leads to premature differentiation of hematopoietic progenitors. However, the targets and cellular communications of these two signals are very different. Hh acts directly on the progenitors of the ZM and is necessary to maintain their pluripotent progenitor status (Mandal et al., 2007). PVF1 diffuses by exocytosis from the PSC and acts, *via* its PDGF / VEGFR receptor, in the differentiating haemocytes. It stimulates the secretion of ADGF-A (*adenosine deaminase-related growth factor-A*), an extracellular adenosine-modifying enzyme. This modification leads to the inactivation of the adenosine / AdoR (*adenosine*) in the cells of the medullary zone (MZ). The AdoR pathway positively regulates the activity of protein kinase A (PKA), promoting differentiation, while Hh signaling inhibits PKA activity in the MZ . The positive control of the PKA activity by the cells differentiating *via* the adenosine / AdoR pathway and negative by the PSC *via* the Hh pathway makes it possible to maintain the equilibrium between progenitors and differentiated cells (Mondal et al., 2011).

5.1d2 Regulation of PSC:

The number of cells in the PSC is regulated by *Dpp* signaling in *Drosophila. Dpp* pathway is specifically activated in the PSC by binding of *Dpp* to its *Tkv* and *Wit* receptors (Pennetier et al., 2011). It has been shown that genetic activation of *dpp* signaling in PSC results in dramatic increase in the number of PSC cells. These results suggested that *Dpp* pathway regulates proliferation of PSC cells. On the pther hand, wingless signaling has been shown to positively regulate the size of PSC (Gilgenkrantz et al., 2011). These results suggest that the ratio between Wg and Dpp signaling determines the size of PSC. (Sineko et al., 2009).

5.1d3 Regulation of hemocyte differentiation by PSC:

Inactivation of *Dpp* signaling in PSC induces both an increase in the number of PSC cells and a loss of hemocyte differentiation, indicating that control of PSC size is an essential parameter of hemocyte homeostasis in the PSC. The expression of *Hh* is, however, not affected under these conditions (Mandal et al., 2007) , which suggests that the increase in the number of cells in the PSC causes an increase in the amount of total *Hh* produced, which leads to the maintenance of all the cells (Pennetier et al., 2011). *Hh* expression in PSC cells is significantly decreased under conditions of Col function loss which suggest that Collier transcription factor coordinates the proliferation and signaling programs of hematopoietic niche cells, and that this coordination is an essential parameter of hematopoiesis.

5.1e Evidences for regulation of complex-I activity by PINK1:

Research in the past decade has accumulated evidences from various model systems for the role of PINK1 in regulating complex-I activity (Aerts et al., 2015b). Complex-I deficiency has been reported in PPINK1 deficient mice, flies as well as patients fibroblasts (Hoepken et al., 2007; Gautier et al., 2008; Grunewald et al., 2009; Morais et al., 2009; Abramov et al., 2011; Liu et al., 2011). The mechanistic basis of regulation of complex-I activity by Pink1 is provided by a recent study, indicating that complex-I subunit NdufA10 is phosphorylated in a PINK1-dpeendent manner (Morais et al., 2014). The phosphorylation of NdufA10 is required to regulate the ubiquinone reductase activity of complex-I. It has also been shown that phosphomimetic NdufA10 is able to rescue PINK1 deficient phenotypes in flies and patients fibroblasts (Morains et al., 2014). This rescue activity is because of restoration of complex-I activity. This is a very strong evidence for the critical role played by PINK1 in regulation of complex-I activity, prompting me to investigate hematopoietic defects, if any, in PINK1 mutant and knockdown embryos.

5.1e1 PINK1 Gene, Its Nature and role in development:

PINK1 (PTEN induced kinase) is mitochondrially targeted serine/threonine kinase which has been shown to protect cells from oxidative stress-induced apoptosis (Pridgeon JW., 2007). *PINK1* has been identified as Parkinson's disease (PD) associated gene (Abou-Sleiman et al., 2006). Mutations associated with PD are majorly found within the kinase domain. The domain of *PINK1* consists of MTS (Mitochondrial targeting sequence) with the cleavage site for

mitochondrial processing peptidase (MPP). The transmembrane domain contains presenilin associated rhomboid-like protease (PARL) cleavage site. The kinase domain of *PINK1* has two putative phosphorylation sites: Ser228 and Ser402 (Bedford et al., 2008).

5.1e2 Mitochondrial localization of PINK1:

PINK1 is imported into mitochondria through the TOM (Translocase of Outer Membrane) and TIM23 (Translocase of inner membrane) complexes at the outer and inner mitochondrial membrane, respectively, and its MTS is cleaved off by the mitochondrial processing peptidase located in the matrix. Subsequently, the inner mitochondrial

membrane protease presenilin-associated rhomboid-like protease (PARL) cleaves *PINK1* between amino acids Ala103 and Phe104 within the hydrophobic TMD (Deas et al., 2011; Greene et al., 2003; Jin et al., 2010; Meissner et al., 2011). The resulting 52 kDa N-terminally processed *PINK1* species is released to the cytosol, where it is rapidly degraded by the proteasome through the N-end rule pathway (Yamano and Youle, 2013).

PI NK1 influences several cellular processes:

1) *PINK1* has been reported to protect against oxidative stress by phosphorylating the mitochondrial chaperone tumor necrosis factor receptor-associated protein 1 (TRAP1)/heat shock protein 75 (Hsp75) (Pridgeon et al., 2007). *PINK1* co-localizes and interacts with TRAP1 in the mitochondrial intermembrane space. Upon phosphorylation, TRAP1 prevents cytochrome c release and H2O2 induced apoptosis by an unknown mechanism and the ability of *PINK1* to phosphorylate TRAP1 is impaired by kinase inactivating or PD associated mutations. Notably, in the absence of TRAP1, over-expression of wild type *PINK1* is unable to protect cells against oxidative stress-mediated apoptosis indicating that TRAP1 is essential for the pro-survival effects of *PINK1*(Pridgeon et al., 2007).

2) *PINK1* can modulate complex-I activity and hence regulate mitochondrial bioenergetics. There are ample evidence which suggest regulation of complex-I activity by *PINK1*(Aerts et al., 2015). In *PINK1* deficient mice, flies and patients fibroblasts, Complex-I deficiency has been reported (Gautier et al., 2008; Grunewald et al., 2009; Hoepken et al., 2007). A recent study provided mechanistic insight of complex-I regulation by *PINK1* indicating that complex-I subunit NdufA10 is phosphorylated in a *PINK1* dependent manner (Morais et al., 2009).

3) *PINK1* functions as a central mitophagy protein that can induce mitophagy in Parkin dependent as well as Parkin independent manner (Lazarou et al., 2012).

4) *PINK1* can protect against cell death in response to various stress conditions,

5) It promotes selective mitochondrial quality control via mitochondria-derived vesicles (MDV) to protect mitochondria against oxidative stress.

5.2 Results

5.2.1 Severe cell number reduction in embryonic lymph gland of complex-I knockdown embryos:

Lymph gland at Stage 16 of embryonic development is marked by *zfh1* antibody. In wild type embryos, each lobe of the lymph gland is constituted by an average of 22 cells. At this stage of lymph gland development, there are only two subpopulations: primary lobe marked by *zfh1* (Fig. 5.3A) and niche marked by *Antennapedia* (Fig.5.3B). It was found that in *ND42* knockdown embryos, the total number of cells constituting the lymph gland was decreased to an average of 10 cells per lobe (Fig.5.3E), whereas *Antennapedia* positive niche cells declined from average 5 in control to 3 per lobe in *ND42* knockdown embryos (Fig, 5.3F).

In *ND75* knockdown embryos, LG cell number was reduced to 11 per lobe (Fig.5.3I, 5.5J) whereas niche cell number was reduced to 3 per lobe (Fig. 5.3J, 5.5K).

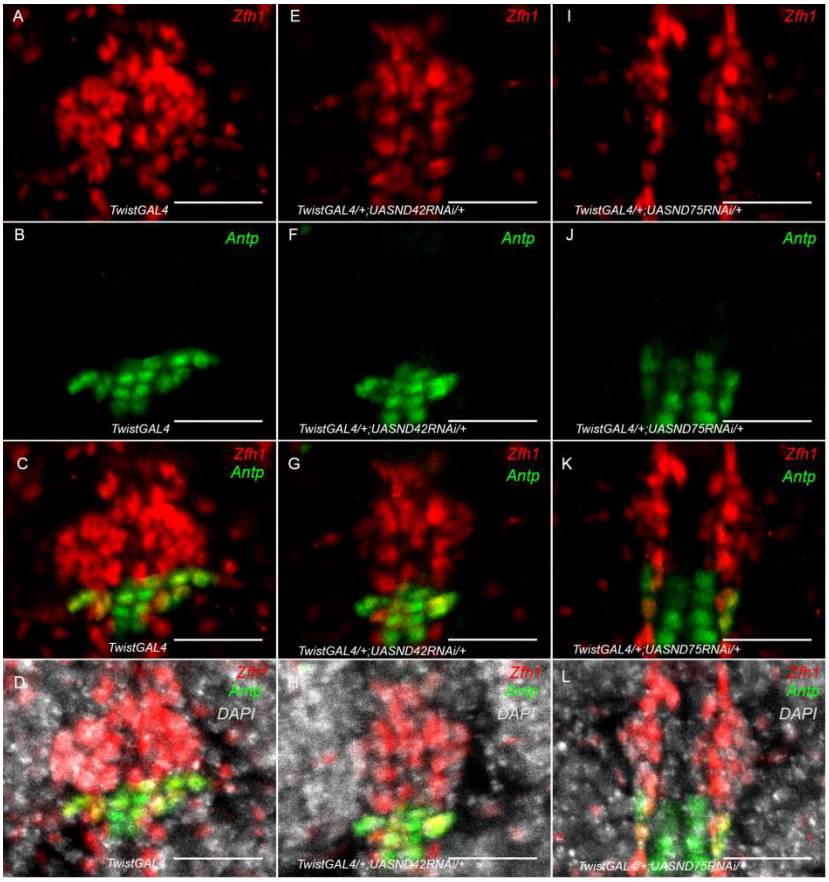

Fig. 5.3 Cell number in embryonic lymph gland is drastically reduced in complex-I knockdown embryos. Wild type stage 16 embryonic lymph gland marked with *zfh1*(**A**) Same embryo stained for *antennapedia* marking niche cells**(B)** Merged image of *zfh1* and *antennapedia*(*antp*) stained stage 16 embryonic lymph gland **(C)***Zfh1*, *antennapedia*, and DAPI stained merged image of wild type stage 16 embryonic lymph gland (**D**).Drastic reduction in the number of cells constituting the lymph gland in *ND42* (**E)** and *ND75*(**I**) knockdown embryo revealed by *zfh1* staining**.** Reduction in the number of *antp* positive niche cells in *ND42* and *ND75* knockdown embryos (**F,J**). **G,K, H, L** are the merged images of respective examples shown above.

5.2.2 High ROS levels in the developing cardiogenic mesoderm at stage 10 in complex-I knockdown embryos:

In the previous section, as it was noticed that knockdown of *ND42* and *ND75* lead to high ROS levels, therefore ROS levels were analyzed in *ND42* and *ND75* knockdown embryos at stage 10 of embryonic development since high ROS levels were observed in the knockdown embryo from stage 10 onwards.. Elevated *gstD GFP* levels were observed in the developing mesodermal populations of *ND42(Fig.5.4C and D)* and *ND75 (Fig.5.4E and F)* knockdown embryos compared to control (Fig. 5.4A and B).

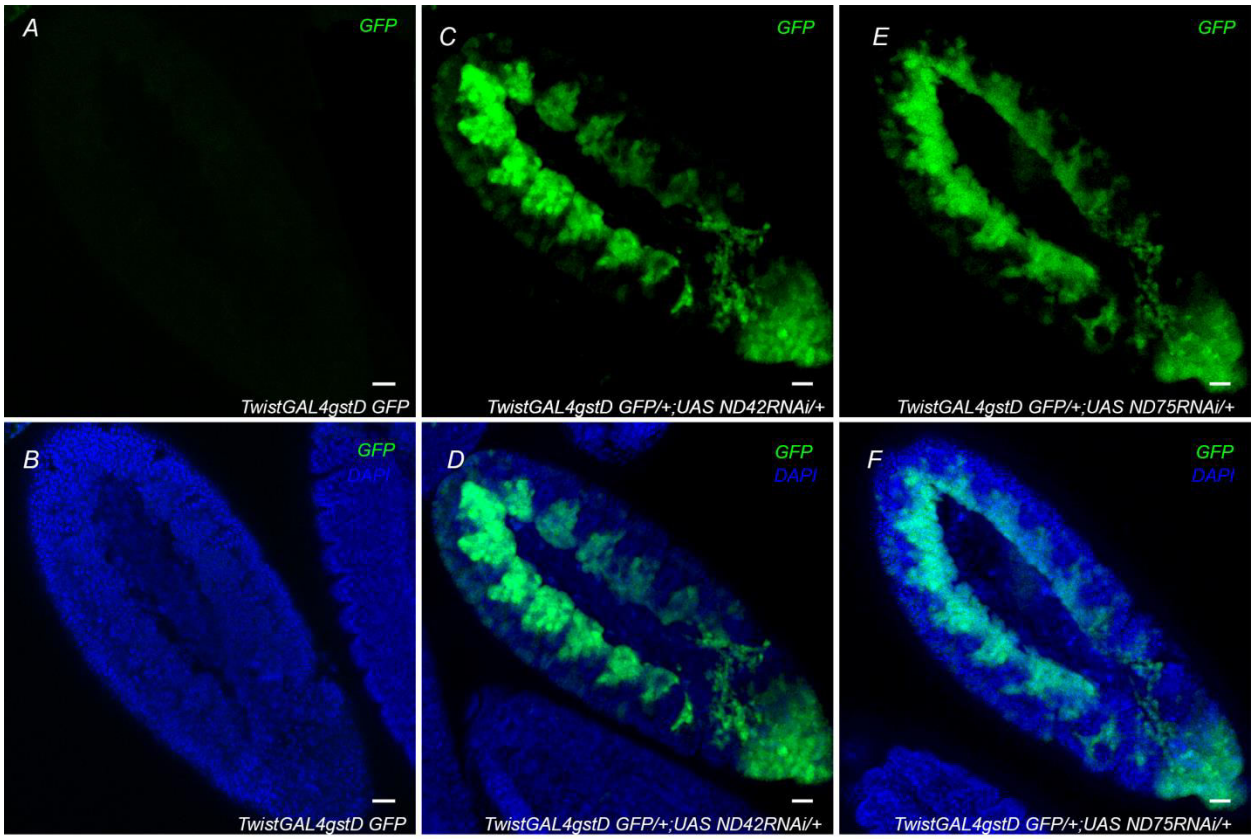

Fig. 5.4. Elevated ROS levels in the mesoderm population at stage 10 of embryonic development in complex-I knockdown embryos: Wild type stage 10 embryo negative for *gstD GFP* expression (A) counterstained with DAPI (B). *ND42* knockdown embryos showing gst D GFP expression in the developing mesoderm (C) counterstained with DAPI (D). *ND75* knockdown embryos exhibit a similar increase in gst DGFP levels in the developing mesoderm (E) merged image showing counterstaining with DAPI (F).

5.2.3 PINK1 mutant and RNAi knockdown embryos exhibit similar hematopoietic phenotype of complex-I knockdown embryos:

In *PINK1* B9 hemizygous embryos,co-immunostaining of *zfh1* and *antp* revealed a drastic reduction in the total number of lymph gland cells. It was found that total LG cell number was reduced to an average 10 cells/lobe (Fig.5.5I,)compared to 22 cells/lobe in control (Fig.5.5A). *Antennapedia* positive niche cell number was reduced to 3 per lobe (Fig.5.5J)compared to 5 per lobe in control embryos (Fig.5.5B). Similarly, in *Twist* Gal4> UAS *PINK1 RNAi* embryos, total LG cell number was reduced to 10 cells per lobe (Fig.5.5E)and antennapedia positive niche cell number was 3 cells per lobe (Fig. 5.5F) .

These results imply that *PINK1* knockdown has similar consequences on the lymph gland to those of *ND42* and *ND75* knockdown of complex-I of ETC.

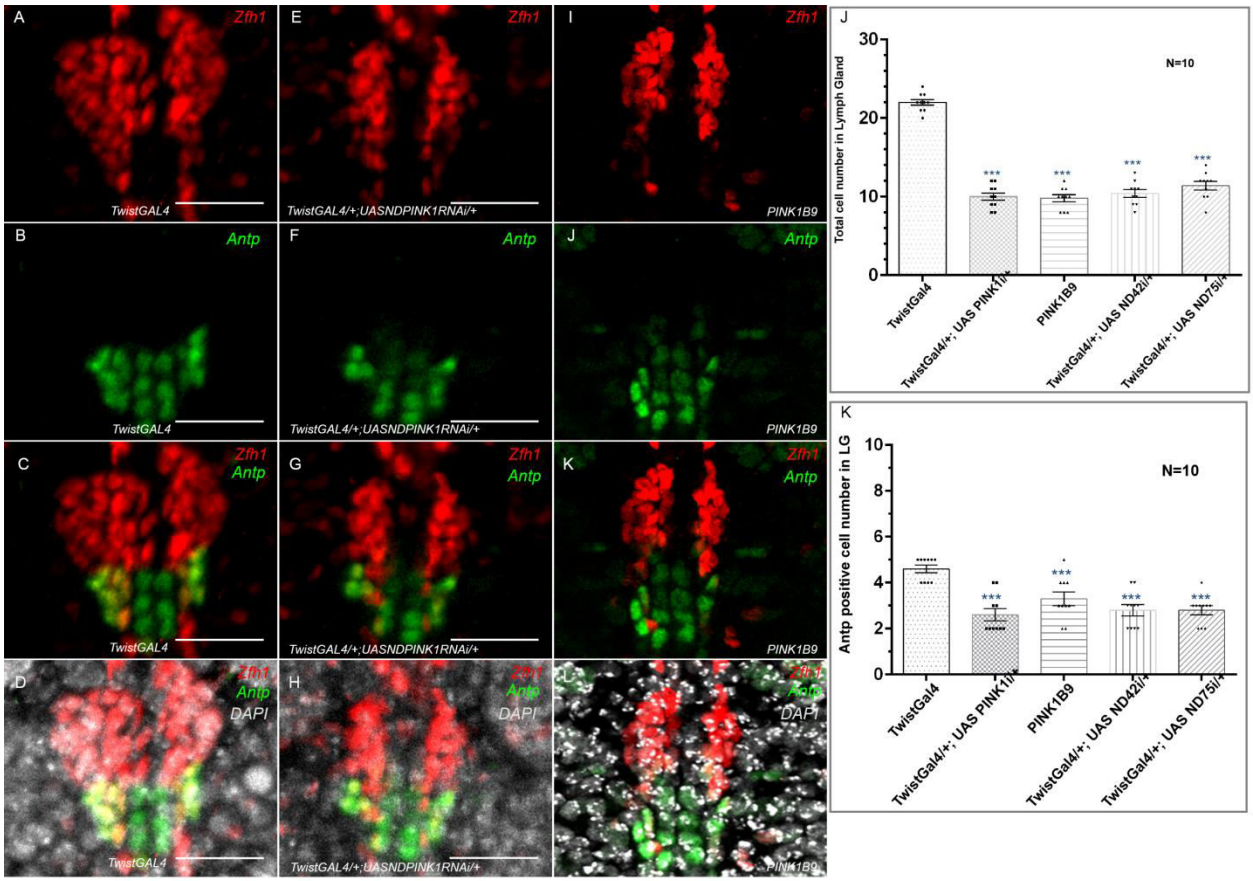

Fig. 5.5PINK1B9 and PINK1 knockdown embryos exhibit similar hematopoietic organ phenotype to that of complex-I knockdown embryos:**A,B,C,D** Wild type embryonic lymph gland marked with *zfh1* (red) *antp* (green) and DAPI (grey).**E,F,G,H***PINK1* knockdown embryonic lymph gland shows drastic reduction in total number of cells marked with *zfh1* (red)as well as reduction in number of *antp* positive niche cell number (green). A similar reduction can be seen in *PINK1*B9 mutant embryonic lymph gland **(I, J, K,L)**

5.2.4 High ROS levels in mesoderm population of PINK1 knockdown embryos at stage 10 of embryonic development:

In *PINK1* knockdown embryos, ROS levels were observed using *gstD GFP* reporter at stage 10 of embryonic development. ROS levels were found to be high in *PINK1* knockdown embryos (Fig. 5.6C and D)compared to same stage wild type embryos (Fig.5.6A and B). This result

suggests that knockdown of *PINK1* from mesoderm population using *Twist* Gal4 as a driver resulted in high ROS levels in the mesoderm

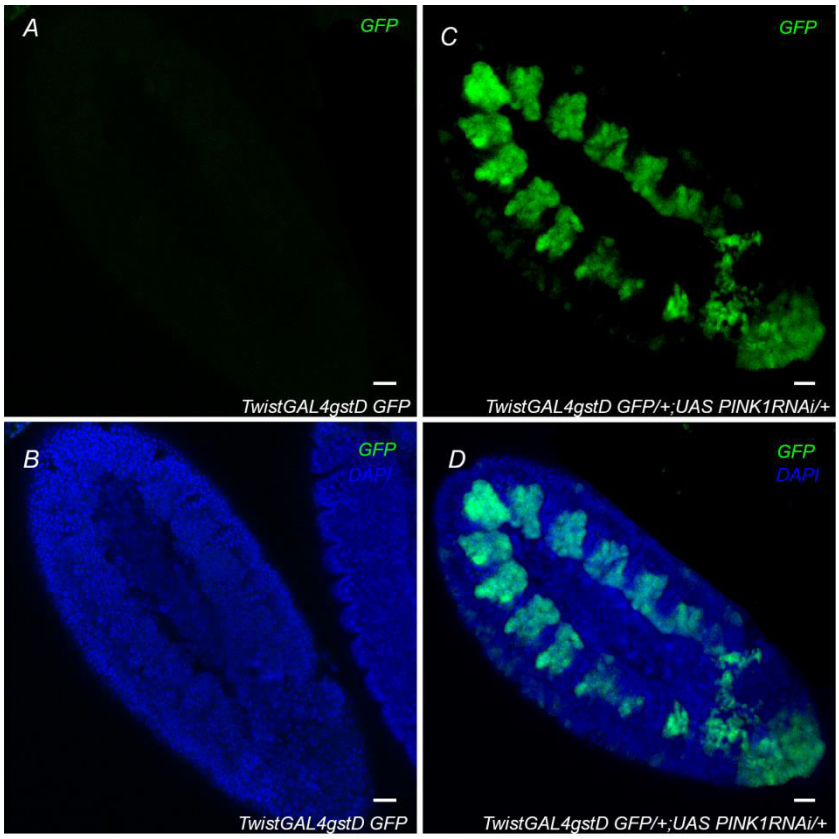

Fig. 5.6Elevated ROS levels in the developing mesoderm of PINK1 knockdown embryos Wild type stage 10 embryo negative for *gstD GFP* expression (**A**) counterstained with DAPI (**B**). *PINK1*knockdown embryos showing *gstD GFP* expression in the developing mesoderm (**C**) counterstained with DAPI

5.2.5 ROS levels are scavenged by overexpression of SOD2 in PINK1 and complex-I knockdown embryos

In order to determine a causal relationship between high ROS levels and the reduction in lymph gland cell number, ROS elvels were scavenged by over expressing superoxide dismutase (*SOD2*) in the *ND42* and *ND75* knockdown embryos. It was found that elevated gstD GFP levels observed in the mesoderm derivatives of *PINK1* (Fig.5.8E and F), *ND42* (Fig.5.7E and F) and *ND75* (Fig.5.7I and J) knockdown embryos were declined to very low levels in *SOD2* overexpression background. These results suggest that SOD2 is able to scavenge high ROS levels in the developing cardiogenic mesoderm of ND42 and ND75 knockodown embryos..

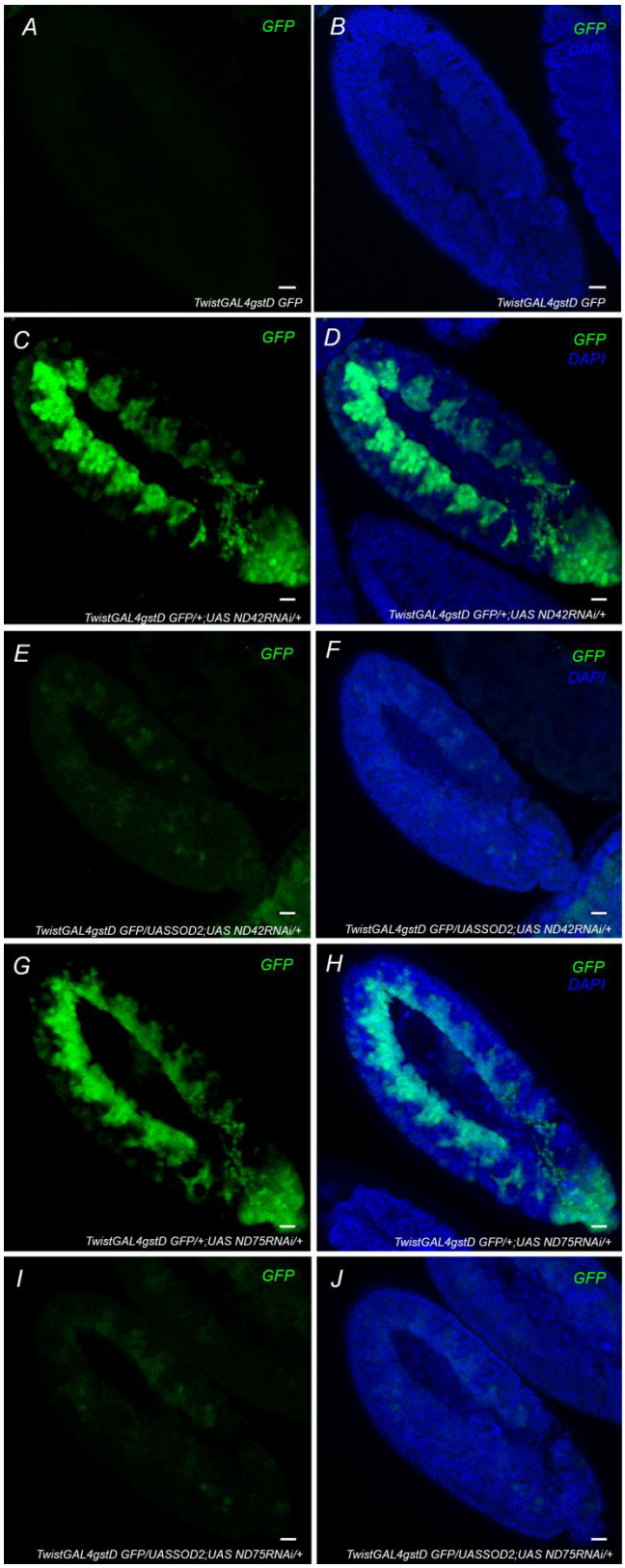

Fig. 5.7 SOD2 overexpression in the complex-I knockdown embryos is able to scavenge high ROS in the mesoderm population Wild type embryo showing negligible gst D GFP expression at stage 10 of embryonic

development (**A**) counterstained with DAPI (**B**). High level of ROS reported by gst D GFP in the mesodermal population of stage 10 embryo in *ND42*(**C**) and *ND75*(**G**) knockdown embryos; counterstained with DAPI (**D, H**). *SOD2* overexpression in *ND42* and *ND75* background results in a notable reduction in gst DGFP expression at stage 10 of embryonic development (**E, F, G, H)**

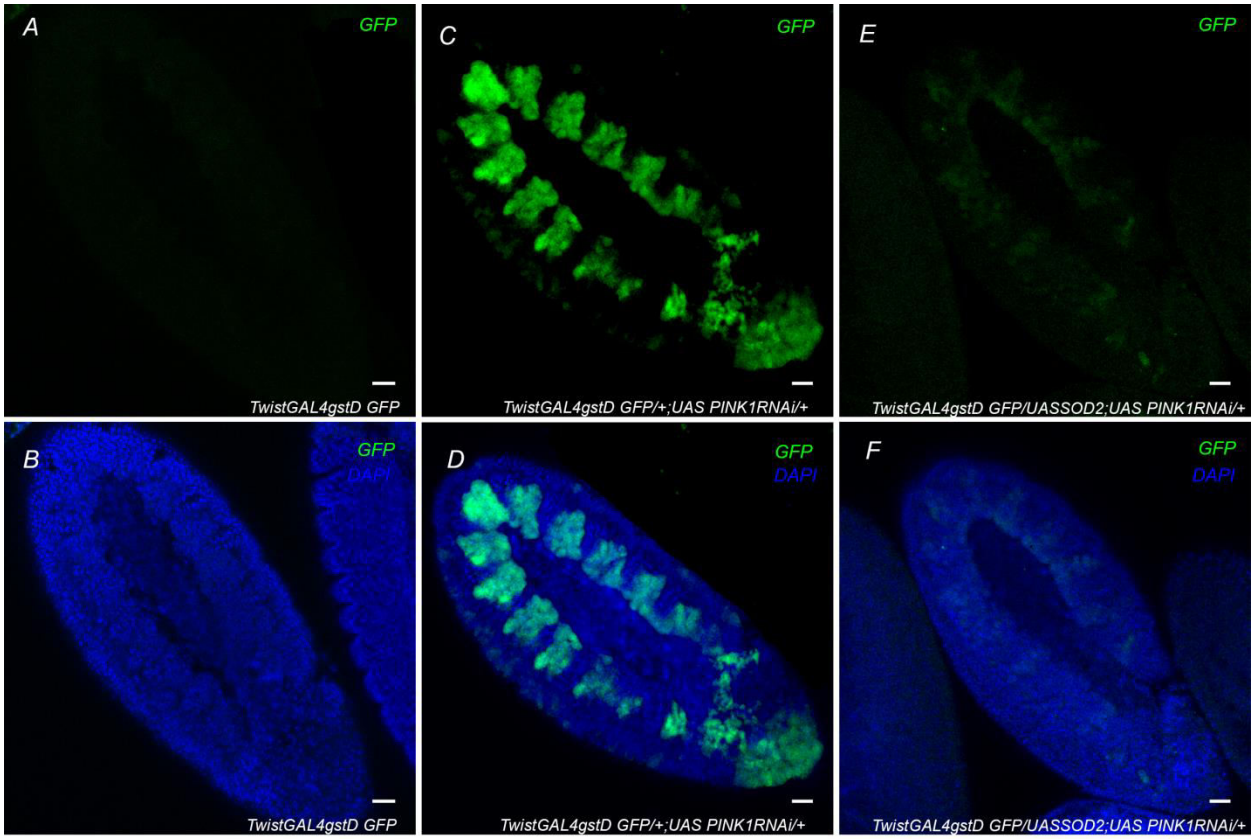

Fig. 5.8SOD2 overexpression in PINK1 knockdown embryos is able to scavenge high ROS in the mesoderm population.Wild type embryo showing negligible *gstD GFP* expression at stage 10 of embryonic development (**A**) counterstained with DAPI (**B**). High level of ROS reported by *gstD GFP* in the mesodermal population of stage 10 embryo in *PINK1*(**C**) knockdown embryos; counterstained with DAPI **(D)**. *SOD2* overexpression in *PINK1* knockdown background results in a notable reduction in gst DGFP expression at stage 10 of embryonic development **(E, F**).

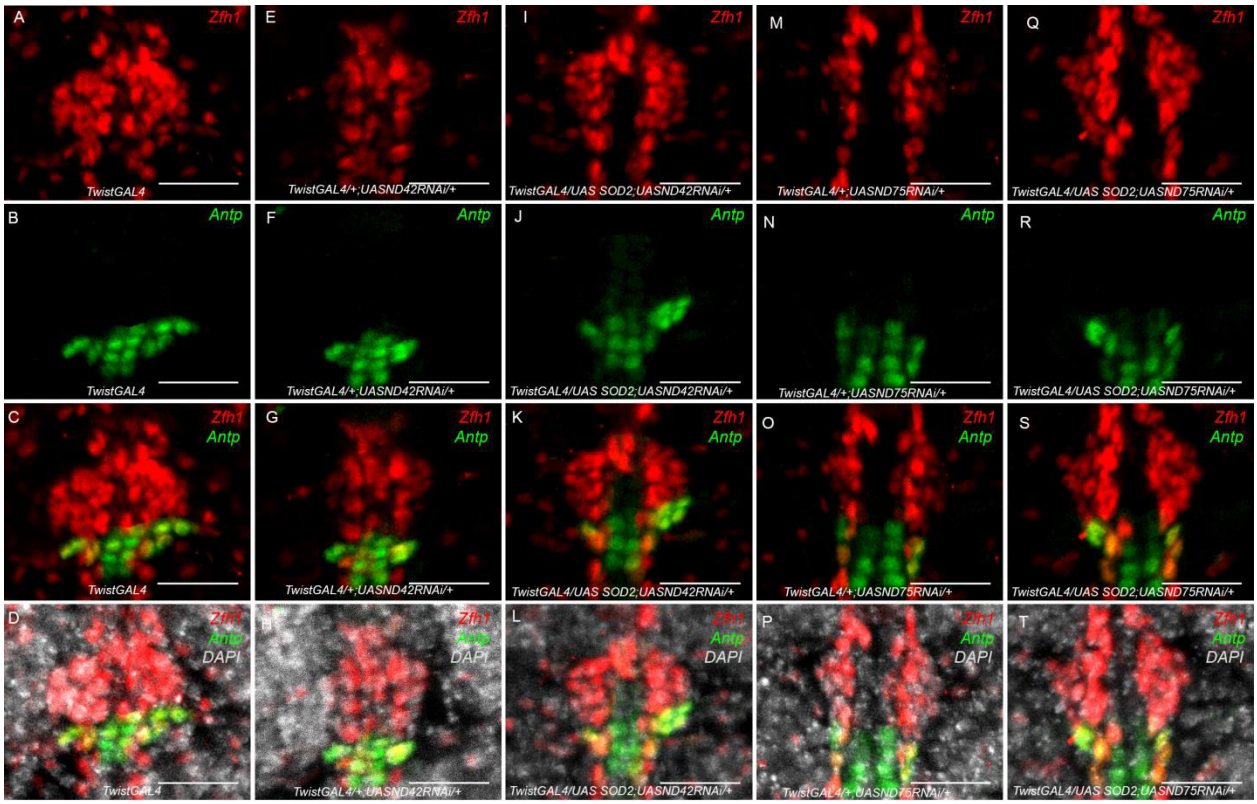

Fig. 5.9SOD2 overexpression in complex I knockdown embryos is able to rescue lymph gland phenotype Wild type embryonic lymph gland marked with *zfh1* (red) *antp* (green) and DAPI (grey) (**A, B, C, D**). *ND42* knockdown embryonic lymph gland shows a drastic reduction in total number of cells marked with *zfh1* (red)as well as reduction in the number of *antp* positive niche cell number (green) (**E, F, G, H**). Overexpression of *SOD2* in *ND42* knockdown embryos restore LG cell number (**I, J, K, L**). Similar restoration in LG cell number seen by overexpressing *SOD2* in *ND75* knockdown embryos (**Q, R, S, T**) compared to reduced cell number in *ND75* knockdown embryos **(M, N, O, P)**

5.2.6 Reduction in LG cell number is mediated through ROS in PINK1 and Complex-I knockdown embryos:

In order to investigate whether ROS is the key factor for reduction in LG cell number, superoxide dismutase (*SOD2*) was over expressed in Complex-I and *PINK1* knockdown embryos in. Co-immunostaining with *Zfh1* and *Antp* revealed that by scavenging high ROS using *SOD2* ,the total cell number in the lymph gland is significantly rescued by scavenging ROS from the mesoderm population in case of *ND42* (Fig.5.9I), *ND75* (Fig.5.9Q) and *PINK1* (Fig.5.10I) knockdown embryos. On the other *Hand*, *Antp* positive niche cell number did not show any

significant change in cell number in*SOD2* overexpression background of *ND42* (Fig.5.9J), *ND75* (Fig.5.9R) and *PINK1* (Fig.5.10J) knockdown embryos.

In case of *SOD2* overexpression in *ND42*, *ND75*, and *PINK1* knockdown embryos, average LG cell number per lobe was 15, 16 and 15 respectively compared to average 22 cells per lobe in control (Fig.5.10M). Whereas, niche cell number was average 3 per lobe in each of these three, which was similar to their knockdown counterparts (Fig. 5.10N).

These results suggest that ROS plays an important role in affecting LG cell number at stage 16 of embryonic development.

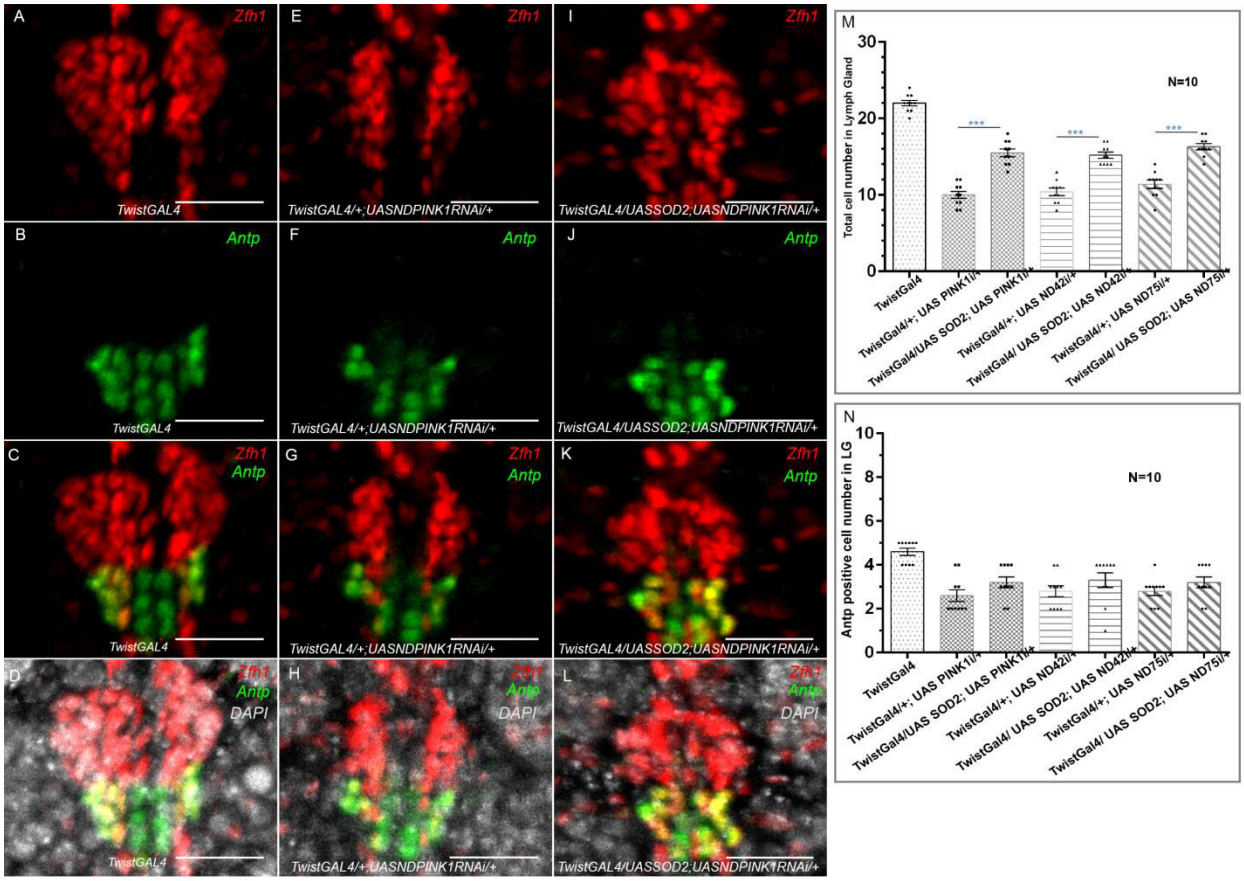

Fig. 5.10SOD2 overexpression in PINK1 knockdown embryos is able to rescue lymph gland phenotype Wild type embryonic lymph gland marked with *zfh1* (red) *antp* (green) and DAPI (grey) (**A, B, C, D**). *PINK1* knockdown embryonic lymph gland shows a drastic reduction in total number of cells marked with *zfh1* (red)as well as reduction in the number of *antp* positive niche cell number (green) (**E, F, G, H**). Overexpression of *SOD2* in *PINK1* knockdown embryos restore LG cell number (**I, J, K, L**).Statistical analysis of total LG cell number and niche cell numberrevealed that by overexpressing *SOD2* in complex-I and *PINK1* knockdown embryos, total cell number is significantly restored(**M),** however no significant change in niche cell number **(N).**

5.2.7 Discussion

This part of my study was the extension and further exploration of observations in the previous study. When we looked for a change in the total number of pericardial cells in complex-I knockdown embryos using *Zfh1*, one intriguing observation was a drastic reduction in the cell number of the lymph gland. Since we are knocking down complex-I components from the mesoderm population, it was quite obvious that all mesoderm derivatives would have affected in one way or another. Vascular and hematopoietic progenitors originate from cardiogenic mesoderm. These results suggest that both types of progenitors are affected by mitochondrial dysfunction in the developing mesodermal cells.

Mitochondria play an important role in regulating programmed cell death and cell proliferation (Wallace, 2008). Decreasein cell number of lymph gland in complex-I knockdown embryos can be either due to cell death or inadequate cell division at a certain point of lymph gland formation during embryonic development. . ROS generated during oxidative stress can play important role in early and late steps of apoptosis (Morgan et al., 2007). Studies on Drosophila eye imaginal disc have been performed to answer mechanistic basis of mitochondrial retrograde signaling for cell cycle regulation. It has been shown that disruption of complex-I of Electron Transport Chain specifically retards cell cycle during G1-S transition by using AMP and ROS at sublethal concentrations as independent signals (Owusu-Ansah et al., 2008). Alteration in oxidative phosphorylation due to mutation in gene encoding complex-I subunit ND5 has been shown to result in enhanced tumorigenesis through increased resistance to apoptosis (Sharma et al., 2011). Therefore based on these evidences, plus the observation that both lobes of the lymph gland show somewhat uniform reduction in total number of cells in knockdown embryos, possibility of proliferation defect at a certain point during LG formation is stronger than LG cells undergoing apoptosis.

Another interesting aspect opened from this study was that knocking down *PINK1* from developing mesoderm exhibit similar hematopoietic phenotype to those of complex-I knockdown embryos. Previous studies have already reported an association of *PINK1* with complex-I of ETC. *PINK1* has been shown to be involved in the phosphorylation of *ND42*; an accessory subunit of ETC. *PINK1* is a PTEN induced kinase; mutation of which has been shown to exhibit

Parkinson's disease-like phenotypes in *Drosophila* flies including loss of dopaminergic neurons and flight muscle degeneration (Clark et al., 2006; Park et al., 2005; Park et al., 2006).

In the present study, in *PINK1*B9 as well as *PINK1* knockdown embryos, high ROS levels are reported to be responsible for the reduction in lymph gland cell number. The lymph gland is formed from three thoracic prohemocyte clusters that are present in T1, T2, and T3 segments. These three clusters coalesce to form the lymph gland in the T3 segment (Mandal et al., 2004). There is possibility that reduction in cell number of lymph gland is because either one or all of these three prehemocytic clusters are not properly formed. This aspect need to be analyzed in future that whether reduction in LG cell number is due to proliferation defect or because of apoptosis.

HSCs are more sensitive to oxidative stress than their progeny, and oxidative damage to HSCs affect their self-renewal capability and can lead to their premature exhaustion via induction of HSC senescence and premature exhaustion (Ito et al., 2006; Ito et al., 2007; Tothova et al., 2007; Wang et al., 2010). In several pathological conditions such as the deletion of Bmi1, MDM2, and tuberous sclerosis complex-I, HSC defects have been associated with an increase in ROS levels (Park et al., 2003; Schuringa and Vellenga, 2010). It has already been shown that ROS can regulate HSC function in a concentration-dependent manner. Low and moderate levels of ROS are required for HSC proliferation, differentiation and mobilization (Juntilla et al., 2010; Kinder et al., 2010; Lewandowski et al., 2010). However, high levels of ROS have been shown to be toxic to HSCs both in vitro and in vivo (Ito et al., 2006; Ito et al., 2007; Miyamoto et al., 2007; Tothova et al., 2007; Wang et al., 2010). It has been reported that high levels of ROS in HSCs can lead to oxidative DNA damage and double-strand breaks (DSBs) (Pazhanisamy et al., 2011). It is well established that DSBs can activate ATM, Chk2, and p53 (Sancar et al., 2004; von Zglinicki et al., 2005). Activation of p53 induces p53 downstream targets, including the cell cycle inhibitors p21 and p16, and pro-apoptotic proteins Puma and Bax. p21 and p16 inhibit cyclin-dependent kinase (CDK) 2 and CDK4/6, respectively, to induce cell cycle arrest and senescence; whereas Puma and Bax can disrupt mitochondrial integrity to induce apoptosis. Alternatively, ROS can activate p38 mitogen-activated protein kinase (p38), which in turn induces HSC senescence by upregulating p16 and/or Arf (Ito et al., 2006).In *Drosophila*, a transient Notch expressing population of HSCs has been reported in the first instar larval lymph

gland (Dey et al., 2016). Since HSCs has been reported to be ROS sensitive, the lymph gland of complex-I knockdown embryos and *PINK1* mutant embryos can be further tracked to the first instar stage in order to observe status of HSCs. This investigation can provide important insight into how ROS is affecting the regulation of development and zonation of lymph gland.

6.CONCLUSION

The current study unravels an interesting role of ROS in regulating cell fate specification during cardiogenic mesoderm development. It is one of the first reports of its kind which is showing ROS targeting cell fate decisions in-vivo. Previously, it has been reported that ROS can affect differentiation programs but all of these studies were performed *in vitro*. One of the biggest achievements of this study is the establishment of a model system to study metabolic dysfunction induced CHDs. *Drosophila* embryonic heart has previously been explored extensively to investigate the role of various transcription factors and signaling pathways in cardiogenesis. However, metabolic perturbations were not induced during *Drosophila* embryonic development to study the effects of metabolic dysfunction on cardiogenesis.

Mitochondria have been only considered as a powerhouse of the cell for a very long time. By perturbing mitochondrial function in the developing mesoderm, an interesting finding that came into the light is that myogenic cardioblasts lost their identity to convert into non-myogenic, inflow valve forming cardioblasts. This finding implies that ROS is directly targeting the specification programs during cardioblast development. This can be the response to the oxidative stress generated inside a cell which pushes it towards different fate at that stage of development.

Previous reports suggest that ROS can have varied effects on cell processes depending on its level, different cocktail of ROS species, type of cell and the type of sensitized background(Finkel, 2011; Schieber and Chandel, 2014; Zhang et al., 2016). ROS regulates various processes in cell biology which includes cell division (Diebold and Chandel, 2016), cell elongation (Monshausen et al., 2007), cell differentiation (Owusu-Ansah and Banerjee, 2009; Sauer et al., 2001), cell migration (Hurd et al., 2012; Niethammer et al., 2009), senescence (Finkel, 2015) and cell death (Cross et al., 1987; Schieber and Chandel, 2014). This study clearly suggests that the spatiotemporal dynamics of ROS elevation is very critical to give an observable phenotype. While knocking down transcripts of nuclear genes encoding complex-I components of ETC with late Gal4 drivers in the mesoderm did not induce any cardiac defects, an early TwistGal4 driver did the trick.

Since we are knocking down complex-I components from the entire mesoderm, it is unrealistic to expect that it will only affect cardiogenesis. In synchrony with this fact, we found that the

lymph gland is severely affected in terms of reduction in cell number. The other mesoderm derivatives might have been affected too, although in this particular study we are only focusing on the effect on cardiogenesis and hematopoiesis since these two processes are very well explored in *Drosophila.*

This work has successfully established *Drosophila* embryonic heart as a model to study metabolic dysfunction induced CHDs. The critical role played by high ROS levels in inducing cell fate change has been explored. Given the high conservation of transcription factors and molecular mechanisms regulating cardiogenesis and hematopoiesis in *Drosophila* and vertebrates, the outcome of my thesis can open new doors in the field of metabolic regulation of developmental programs.

REFERENCES:

Benov, L., Sztejnberg, L., and Fridovich, I. (1998). Critical evaluation of the use of hydroethidine as a measure of superoxide anion radical. Free Radic Biol Med *25*, 826-831.

Bodmer, R., and Venkatesh, T.V. (1998). Heart development in Drosophila and vertebrates: conservation of molecular mechanisms. Developmental genetics *22*, 181-186.

Cave, A., Grieve, D., Johar, S., Zhang, M., and Shah, A.M. (2005). NADPH oxidase-derived reactive oxygen species in cardiac pathophysiology. Philos Trans R Soc Lond B Biol Sci *360*, 2327-2334.

Coffman, J.A., and Davidson, E.H. (2001). Oral-aboral axis specification in the sea urchin embryo. I. Axis entrainment by respiratory asymmetry. Developmental biology *230*, 18-28.

Cripps, R.M., and Olson, E.N. (2002). Control of cardiac development by an evolutionarily conserved transcriptional network. Developmental biology *246*, 14-28.

Cross, C.E., Halliwell, B., Borish, E.T., Pryor, W.A., Ames, B.N., Saul, R.L., McCord, J.M., and Harman, D. (1987). Oxygen radicals and human disease. Ann Intern Med *107*, 526-545.

Drose, S., Stepanova, A., and Galkin, A. (2016). Ischemic A/D transition of mitochondrial complex I and its role in ROS generation. Biochimica et biophysica acta *1857*, 946-957.

Duttaroy, A., Paul, A., Kundu, M., and Belton, A. (2003). A Sod2 null mutation confers severely reduced adult life span in Drosophila. Genetics *165*, 2295-2299.

Fato, R., Bergamini, C., Leoni, S., Strocchi, P., and Lenaz, G. (2008). Generation of reactive oxygen species by mitochondrial complex I: implications in neurodegeneration. Neurochem Res *33*, 2487-2501.

Folmes, C.D., Dzeja, P.P., Nelson, T.J., and Terzic, A. (2012). Mitochondria in control of cell fate. Circulation research *110*, 526-529.

Genova, M.L., Ventura, B., Giuliano, G., Bovina, C., Formiggini, G., Parenti Castelli, G., and Lenaz, G. (2001). The site of production of superoxide radical in mitochondrial Complex I is not a bound ubisemiquinone but presumably iron-sulfur cluster N2. FEBS letters *505*, 364-368.

Kirby, K., Hu, J., Hilliker, A.J., and Phillips, J.P. (2002). RNA interference-mediated silencing of Sod2 in Drosophila leads to early adult-onset mortality and elevated endogenous oxidative stress. Proceedings of the National Academy of Sciences of the United States of America *99*, 16162-16167.

Koopman, W.J., Nijtmans, L.G., Dieteren, C.E., Roestenberg, P., Valsecchi, F., Smeitink, J.A., and Willems, P.H. (2010). Mammalian mitochondrial complex I: biogenesis, regulation, and reactive oxygen species generation. Antioxidants & redox signaling *12*, 1431-1470.
Kramer, S.G., Kidd, T., Simpson, J.H., and Goodman, C.S. (2001). Switching repulsion to attraction: changing responses to slit during transition in mesoderm migration. Science *292*, 737-740.
Kushnareva, Y., Murphy, A.N., and Andreyev, A. (2002). Complex I-mediated reactive oxygen species generation: modulation by cytochrome c and NAD(P)+ oxidation-reduction state. Biochem J *368*, 545-553.
Kussmaul, L., and Hirst, J. (2006). The mechanism of superoxide production by NADH:ubiquinone oxidoreductase (complex I) from bovine heart mitochondria. Proceedings of the National Academy of Sciences of the United States of America *103*, 7607-7612.
Lambert, A.J., and Brand, M.D. (2004). Inhibitors of the quinone-binding site allow rapid superoxide production from mitochondrial NADH:ubiquinone oxidoreductase (complex I). The Journal of biological chemistry *279*, 39414-39420.
Lebovitz, R.M., Zhang, H., Vogel, H., Cartwright, J., Jr., Dionne, L., Lu, N., Huang, S., and Matzuk, M.M. (1996). Neurodegeneration, myocardial injury, and perinatal death in mitochondrial superoxide dismutase-deficient mice. Proceedings of the National Academy of Sciences of the United States of America *93*, 9782-9787.
Li, Y., Huang, T.T., Carlson, E.J., Melov, S., Ursell, P.C., Olson, J.L., Noble, L.J., Yoshimura, M.P., Berger, C., Chan, P.H.*, et al.* (1995). Dilated cardiomyopathy and neonatal lethality in mutant mice lacking manganese superoxide dismutase. Nature genetics *11*, 376-381.
Medioni, C., Astier, M., Zmojdzian, M., Jagla, K., and Semeriva, M. (2008). Genetic control of cell morphogenesis during Drosophila melanogaster cardiac tube formation. J Cell Biol *182*, 249-261.
O'Brien, K.M., Dirmeier, R., Engle, M., and Poyton, R.O. (2004). Mitochondrial protein oxidation in yeast mutants lacking manganese-(MnSOD) or copper- and zinc-containing superoxide dismutase (CuZnSOD): evidence that MnSOD and CuZnSOD have both unique and overlapping functions in protecting mitochondrial proteins from oxidative damage. The Journal of biological chemistry *279*, 51817-51827.

Ohnishi, S.T., Ohnishi, T., Muranaka, S., Fujita, H., Kimura, H., Uemura, K., Yoshida, K., and Utsumi, K. (2005). A possible site of superoxide generation in the complex I segment of rat heart mitochondria. J Bioenerg Biomembr *37*, 1-15.

Qian, L., Liu, J., and Bodmer, R. (2005). Slit and Robo control cardiac cell polarity and morphogenesis. Current biology : CB *15*, 2271-2278.

Raha, S., and Robinson, B.H. (2000). Mitochondria, oxygen free radicals, disease and ageing. Trends Biochem Sci *25*, 502-508.

Santiago-Martinez, E., Soplop, N.H., and Kramer, S.G. (2006). Lateral positioning at the dorsal midline: Slit and Roundabout receptors guide Drosophila heart cell migration. Proceedings of the National Academy of Sciences of the United States of America *103*, 12441-12446.

Sharma, L.K., Lu, J., and Bai, Y. (2009). Mitochondrial respiratory complex I: structure, function and implication in human diseases. Curr Med Chem *16*, 1266-1277.

Sullivan, L.B., and Chandel, N.S. (2014). Mitochondrial reactive oxygen species and cancer. Cancer Metab *2*, 17.

Sykiotis, G.P., and Bohmann, D. (2008). Keap1/Nrf2 signaling regulates oxidative stress tolerance and lifespan in Drosophila. Developmental cell *14*, 76-85.

Unlu, E.S., and Koc, A. (2007). Effects of deleting mitochondrial antioxidant genes on life span. Ann N Y Acad Sci *1100*, 505-509.

Wong, K., Park, H.T., Wu, J.Y., and Rao, Y. (2002). Slit proteins: molecular guidance cues for cells ranging from neurons to leukocytes. Curr Opin Genet Dev *12*, 583-591.

Zaffran, S., and Frasch, M. (2002). Early signals in cardiac development. Circulation research *91*, 457-469.

Zielonka, J., and Kalyanaraman, B. (2010). Hydroethidine- and MitoSOX-derived red fluorescence is not a reliable indicator of intracellular superoxide formation: another inconvenient truth. Free Radic Biol Med *48*, 983-1001.

Boulay, J.L., Dennefeld, C., and Alberga, A. (1987). The Drosophila developmental gene snail encodes a protein with nucleic acid binding fingers. Nature *330*, 395-398.

Brand, A.H., and Perrimon, N. (1993). Targeted gene expression as a means of altering cell fates and generating dominant phenotypes. Development *118*, 401-415.

Chartier, A., Zaffran, S., Astier, M., Semeriva, M., and Gratecos, D. (2002). Pericardin, a Drosophila type IV collagen-like protein is involved in the morphogenesis and maintenance of the heart epithelium during dorsal ectoderm closure. Development *129*, 3241-3253.

Chen, Y., Shi-wen, X., Eastwood, M., Black, C.M., Denton, C.P., Leask, A., and Abraham, D.J. (2006). Contribution of activin receptor-like kinase 5 (transforming growth factor beta receptor type I) signaling to the fibrotic phenotype of scleroderma fibroblasts. Arthritis and rheumatism *54*, 1309-1316.

Cripps, R.M., Black, B.L., Zhao, B., Lien, C.L., Schulz, R.A., and Olson, E.N. (1998). The myogenic regulatory gene Mef2 is a direct target for transcriptional activation by Twist during Drosophila myogenesis. Genes & development *12*, 422-434.

Duan, H., Skeath, J.B., and Nguyen, H.T. (2001). Drosophila Lame duck, a novel member of the Gli superfamily, acts as a key regulator of myogenesis by controlling fusion-competent myoblast development. Development *128*, 4489-4500.

Dunin-Borkowski, O.M., and Brown, N.H. (1995). Mammalian CD2 is an effective heterologous marker of the cell surface in Drosophila. Developmental biology *168*, 689-693.

Dykxhoorn, D.M., and Lieberman, J. (2005). The silent revolution: RNA interference as basic biology, research tool, and therapeutic. Annual review of medicine *56*, 401-423.

Fire, A., Xu, S., Montgomery, M.K., Kostas, S.A., Driver, S.E., and Mello, C.C. (1998). Potent and specific genetic interference by double-stranded RNA in Caenorhabditis elegans. Nature *391*, 806-811.

Fischer, J.A., Giniger, E., Maniatis, T., and Ptashne, M. (1988). GAL4 activates transcription in Drosophila. Nature *332*, 853-856.

Gajewski, K., Zhang, Q., Choi, C.Y., Fossett, N., Dang, A., Kim, Y.H., Kim, Y., and Schulz, R.A. (2001). Pannier is a transcriptional target and partner of Tinman during Drosophila cardiogenesis. Developmental biology *233*, 425-436.

Garcia-Diaz, L., Coserria, F., and Antinolo, G. (2013). Hypertrophic Cardiomyopathy due to Mitochondrial Disease: Prenatal Diagnosis, Management, and Outcome. Case reports in obstetrics and gynecology *2013*, 472356.

Grau, Y., Carteret, C., and Simpson, P. (1984). Mutations and Chromosomal Rearrangements Affecting the Expression of Snail, a Gene Involved in Embryonic Patterning in DROSOPHILA MELANOGASTER. Genetics *108*, 347-360.

Han, Z., Yi, P., Li, X., and Olson, E.N. (2006). Hand, an evolutionarily conserved bHLH transcription factor required for Drosophila cardiogenesis and hematopoiesis. Development *133*, 1175-1182.

Hirota, Y., Sawamoto, K., and Okano, H. (2002). tincar encodes a novel transmembrane protein expressed in the Tinman-expressing cardioblasts of Drosophila. Mech Dev *119 Suppl 1*, S279-283.

Juurlink, D.N. (2010). Rosiglitazone and the case for safety over certainty. Jama *304*, 469-471.

Juurlink, D.N., Gomes, T., Lipscombe, L.L., Austin, P.C., Hux, J.E., and Mamdani, M.M. (2009). Adverse cardiovascular events during treatment with pioglitazone and rosiglitazone: population based cohort study. Bmj *339*, b2942.

Karamanlidis, G., Nascimben, L., Couper, G.S., Shekar, P.S., del Monte, F., and Tian, R. (2010). Defective DNA replication impairs mitochondrial biogenesis in human failing hearts. Circulation research *106*, 1541-1548.

Leask, A., and Abraham, D.J. (2004). TGF-beta signaling and the fibrotic response. FASEB journal : official publication of the Federation of American Societies for Experimental Biology *18*, 816-827.

Lovato, T.L., Benjamin, A.R., and Cripps, R.M. (2005). Transcription of Myocyte enhancer factor-2 in adult Drosophila myoblasts is induced by the steroid hormone ecdysone. Developmental biology *288*, 612-621.

Massague, J. (1998). TGF-beta signal transduction. Annual review of biochemistry *67*, 753-791.

Na, J., Musselman, L.P., Pendse, J., Baranski, T.J., Bodmer, R., Ocorr, K., and Cagan, R. (2013). A Drosophila model of high sugar diet-induced cardiomyopathy. PLoS genetics *9*, e1003175.

Neubauer, S. (2007). The failing heart--an engine out of fuel. The New England journal of medicine *356*, 1140-1151.

Pogson, J.H., Ivatt, R.M., Sanchez-Martinez, A., Tufi, R., Wilson, E., Mortiboys, H., and Whitworth, A.J. (2014). The complex I subunit NDUFA10 selectively rescues Drosophila pink1 mutants through a mechanism independent of mitophagy. PLoS genetics *10*, e1004815.

Postigo, A.A., Ward, E., Skeath, J.B., and Dean, D.C. (1999). zfh-1, the Drosophila homologue of ZEB, is a transcriptional repressor that regulates somatic myogenesis. Molecular and cellular biology *19*, 7255-7263.

Purnomo, Y., Piccart, Y., Coenen, T., Prihadi, J.S., and Lijnen, P.J. (2013). Oxidative stress and transforming growth factor-beta1-induced cardiac fibrosis. Cardiovascular & hematological disorders drug targets *13*, 165-172.

Ranganayakulu, G., Zhao, B., Dokidis, A., Molkentin, J.D., Olson, E.N., and Schulz, R.A. (1995). A series of mutations in the D-MEF2 transcription factor reveal multiple functions in larval and adult myogenesis in Drosophila. Developmental biology *171*, 169-181.

Simpson, P. (1983). Maternal-Zygotic Gene Interactions during Formation of the Dorsoventral Pattern in Drosophila Embryos. Genetics *105*, 615-632.

Singh, S., Loke, Y.K., and Furberg, C.D. (2007). Long-term risk of cardiovascular events with rosiglitazone: a meta-analysis. Jama *298*, 1189-1195.

St Johnston, D. (2002). The art and design of genetic screens: Drosophila melanogaster. Nature reviews Genetics *3*, 176-188.

Tapanes-Castillo, A., and Baylies, M.K. (2004). Notch signaling patterns Drosophila mesodermal segments by regulating the bHLH transcription factor twist. Development *131*, 2359-2372.

Thisse, B., Stoetzel, C., Gorostiza-Thisse, C., and Perrin-Schmitt, F. (1988). Sequence of the twist gene and nuclear localization of its protein in endomesodermal cells of early Drosophila embryos. The EMBO journal *7*, 2175-2183.

Tian, J., An, X., and Niu, L. (2017). Myocardial fibrosis in congenital and pediatric heart disease. Experimental and therapeutic medicine *13*, 1660-1664.

Weber, K.T., and Brilla, C.G. (1991). Pathological hypertrophy and cardiac interstitium. Fibrosis and renin-angiotensin-aldosterone system. Circulation *83*, 1849-1865.

Wieschaus, E., Nusslein-Volhard, C., and Jurgens, G. (1984). Mutations affecting the pattern of the larval cuticle inDrosophila melanogaster : III. Zygotic loci on the X-chromosome and fourth chromosome. Wilehm Roux Arch Dev Biol *193*, 296-307.

Zhu, J., Vinothkumar, K.R., and Hirst, J. (2016). Structure of mammalian respiratory complex I. Nature *536*, 354-358.

Akasaka, T., Klinedinst, S., Ocorr, K., Bustamante, E.L., Kim, S.K., and Bodmer, R. (2006). The ATP-sensitive potassium (KATP) channel-encoded dSUR gene is required for *Drosophila* heart function and is regulated by *Tinman*. Proceedings of the National Academy of Sciences of the United States of America *103*, 11999-12004.

Alvarez, A.D., Shi, W., Wilson, B.A., and Skeath, J.B. (2003). pannier and pointedP2 act sequentially to regulate *Drosophila* heart development. Development *130*, 3015-3026.
Andree, B., Duprez, D., Vorbusch, B., Arnold, H.H., and Brand, T. (1998). BMP-2 induces ectopic expression of cardiac lineage markers and interferes with somite formation in chicken embryos. Mech Dev *70*, 119-131.
Ateghang, B., Wartenberg, M., Gassmann, M., and Sauer, H. (2006). Regulation of cardiotrophin-1 expression in mouse embryonic stem cells by HIF-1alpha and intracellular reactive oxygen species. Journal of cell science *119*, 1043-1052.
Bae, Y.S., Kang, S.W., Seo, M.S., Baines, I.C., Tekle, E., Chock, P.B., and Rhee, S.G. (1997). Epidermal growth factor (EGF)-induced generation of hydrogen peroxide. Role in EGF receptor-mediated tyrosine phosphorylation. The Journal of biological chemistry *272*, 217-221.
Balaban, R.S., Nemoto, S., and Finkel, T. (2005). Mitochondria, oxidants, and aging. Cell *120*, 483-495.
Bao, Z.Z., Bruneau, B.G., Seidman, J.G., Seidman, C.E., and Cepko, C.L. (1999). Regulation of chamber-specific gene expression in the developing heart by Irx4. Science *283*, 1161-1164.
Basson, C.T., Huang, T., Lin, R.C., Bachinsky, D.R., Weremowicz, S., Vaglio, A., Bruzzone, R., Quadrelli, R., Lerone, M., Romeo, G.*, et al.* (1999). Different TBX5 interactions in heart and limb defined by Holt-Oram syndrome mutations. Proceedings of the National Academy of Sciences of the United States of America *96*, 2919-2924.
Begemann, G., Michon, A.M., vd Voorn, L., Wepf, R., and Mlodzik, M. (1995). The *Drosophila* orphan nuclear receptor seven-up requires the Ras pathway for its function in photoreceptor determination. Development *121*, 225-235.
Beiman, M., Shilo, B.Z., and Volk, T. (1996). *Heartless*, a *Drosophila* FGF receptor homolog, is essential for cell migration and establishment of several mesodermal lineages. Genes & development *10*, 2993-3002.
Benhaourech, S., Drighil, A., and Hammiri, A.E. (2016). Congenital heart disease and Down syndrome: various aspects of a confirmed association. Cardiovasc J Afr *27*, 287-290.
Benit, P., Beugnot, R., Chretien, D., Giurgea, I., De Lonlay-Debeney, P., Issartel, J.P., Corral-Debrinski, M., Kerscher, S., Rus*tin*, P., Rotig, A.*, et al.* (2003). Mutant NDUFV2 subunit of mitochondrial complex I causes early onset hypertrophic cardiomyopathy and encephalopathy. Human mutation *21*, 582-586.

Bodmer, R. (1995). Heart development in *Drosophila* and its relationship to vertebrates. Trends Cardiovasc Med *5*, 21-28.

Bodmer, R., and Venkatesh, T.V. (1998). Heart development in *Drosophila* and vertebrates: conservation of molecular mechanisms. Developmental genetics *22*, 181-186.

Borkowski, O.M., Brown, N.H., and Bate, M. (1995). Anterior-posterior subdivision and the diversification of the mesoderm in *Drosophila*. Development *121*, 4183-4193.

Brunelle, J.K., Bell, E.L., Quesada, N.M., Vercauteren, K., Tiranti, V., Zeviani, M., Scarpulla, R.C., and C*Hand*el, N.S. (2005). Oxygen sensing requires mitochondrial ROS but not oxidative phosphorylation. Cell metabolism *1*, 409-414.

Buggisch, M., Ateghang, B., Ruhe, C., Strobel, C., Lange, S., Wartenberg, M., and Sauer, H. (2007). Stimulation of ES-cell-derived cardiomyogenesis and neonatal cardiac cell proliferation by reactive oxygen species and NADPH oxidase. Journal of cell science *120*, 885-894.

Bulua, A.C., Simon, A., Maddipati, R., Pelletier, M., Park, H., Kim, K.Y., Sack, M.N., Kastner, D.L., and Siegel, R.M. (2011). Mitochondrial reactive oxygen species promote production of proinflammatory cytokines and are elevated in TNFR1-associated periodic syndrome (TRAPS). The Journal of experimental medicine *208*, 519-533.

Burgoyne, J.R., Mongue-Din, H., Eaton, P., and Shah, A.M. (2012). Redox signaling in cardiac physiology and pathology. Circulation research *111*, 1091-1106.

Butow, R.A., and Avadhani, N.G. (2004). Mitochondrial signaling: the retrograde response. Molecular cell *14*, 1-15.

Cagin, U., Duncan, O.F., Gatt, A.P., Dionne, M.S., Sweeney, S.T., and Bateman, J.M. (2015). Mitochondrial retrograde signaling regulates neuronal function. Proceedings of the National Academy of Sciences of the United States of America *112*, E6000-6009.

Caricasole, A., Bruno, V., Cappuccio, I., Melchiorri, D., Copani, A., and Nicoletti, F. (2002). A novel rat gene encoding a Humanin-like peptide endowed with broad neuroprotective activity. FASEB journal : official publication of the Federation of American Societies for Experimental Biology *16*, 1331-1333.

Carmena, A., Buff, E., Halfon, M.S., Gisselbrecht, S., Jimenez, F., Baylies, M.K., and Michelson, A.M. (2002). Reciprocal regulatory interactions between the Notch and Ras signaling pathways in the *Drosophila* embryonic mesoderm. Developmental biology *244*, 226-242.

Chartier, A., Zaffran, S., Astier, M., Semeriva, M., and Gratecos, D. (2002). *Pericardin*, a *Drosophila* type IV collagen-like protein is involved in the morphogenesis and maintenance of the heart epithelium during dorsal ectoderm closure. Development *129*, 3241-3253.

Chen, C.T., Shih, Y.R., Kuo, T.K., Lee, O.K., and Wei, Y.H. (2008). Coordinated changes of mitochondrial biogenesis and antioxidant enzymes during osteogenic differentiation of human mesenchymal stem cells. Stem cells *26*, 960-968.

Cho, S.W., Park, J.S., Heo, H.J., Park, S.W., Song, S., Kim, I., Han, Y.M., Yamashita, J.K., Youm, J.B., Han, J.*, et al.* (2014). Dual modulation of the mitochondrial permeability transition pore and redox signaling synergistically promotes cardiomyocyte differentiation from pluripotent stem cells. Journal of the American Heart Association *3*, e000693.

Clavreul, N., Adachi, T., Pimental, D.R., Ido, Y., Schoneich, C., and Cohen, R.A. (2006). S-glutathiolation by peroxynitrite of p21ras at cysteine-118 mediates its direct activation and downstream signaling in endothelial cells. FASEB journal : official publication of the Federation of American Societies for Experimental Biology *20*, 518-520.

Copeland, J.M., Cho, J., Lo, T., Jr., Hur, J.H., Bahadorani, S., Arabyan, T., Rabie, J., Soh, J., and Walker, D.W. (2009). Extension of *Drosophila* life span by RNAi of the mitochondrial respiratory chain. Current biology : CB *19*, 1591-1598.

Cripps, R.M., Black, B.L., Zhao, B., Lien, C.L., Schulz, R.A., and Olson, E.N. (1998). The myogenic regulatory gene *Mef2* is a direct target for transcriptional activation by Twist during *Drosophila* myogenesis. Genes & development *12*, 422-434.

Cripps, R.M., and Olson, E.N. (2002). Control of cardiac development by an evolutionarily conserved transcriptional network. Developmental biology *246*, 14-28.

Cuesto, G., Enriquez-Barreto, L., Carames, C., Cantarero, M., Gasull, X., Sandi, C., Ferrus, A., Acebes, A., and Morales, M. (2011). Phosphoinositide-3-kinase activation controls synaptogenesis and spinogenesis in hippocampal neurons. J Neurosci *31*, 2721-2733.

Duan, H., Skeath, J.B., and Nguyen, H.T. (2001). *Drosophila* Lame duck, a novel member of the Gli superfamily, acts as a key regulator of myogenesis by controlling fusion-competent myoblast development. Development *128*, 4489-4500.

Durocher, D., Charron, F., Warren, R., Schwartz, R.J., and Nemer, M. (1997). The cardiac transcription factors Nkx2-5 and GATA-4 are mutual cofactors. The EMBO journal *16*, 5687-5696.

Fan, W., Lin, C.S., Potluri, P., Procaccio, V., and Wallace, D.C. (2012). mtDNA lineage analysis of mouse L-cell lines reveals the accumulation of multiple mtDNA mutants and intermolecular recombination. Genes & development *26*, 384-394.

Finsterer, J. (2009). Cardiogenetics, neurogenetics, and pathogenetics of left ventricular hypertrabeculation/noncompaction. Pediatric cardiology *30*, 659-681.

Formen*tin*i, L., Sanchez-Arago, M., Sanchez-Cenizo, L., and Cuezva, J.M. (2012). The mitochondrial ATPase inhibitory factor 1 triggers a ROS-mediated retrograde prosurvival and proliferative response. Molecular cell *45*, 731-742.

Frasch, M. (1995). Induction of visceral and cardiac mesoderm by ectodermal *Dpp* in the early *Drosophila* embryo. Nature *374*, 464-467.

Frei, C., Galloni, M., Hafen, E., and Edgar, B.A. (2005). The *Drosophila* mitochondrial ribosomal protein mRpL12 is required for Cyclin D/Cdk4-driven growth. The EMBO journal *24*, 623-634.

Gajewski, K., Zhang, Q., Choi, C.Y., Fossett, N., Dang, A., Kim, Y.H., Kim, Y., and Schulz, R.A. (2001). Pannier is a transcriptional target and partner of *Tinman* during *Drosophila* cardiogenesis. Developmental biology *233*, 425-436.

Gibson, K., Halliday, J.L., Kirby, D.M., Yaplito-Lee, J., Thorburn, D.R., and Boneh, A. (2008). Mitochondrial oxidative phosphorylation disorders presen*tin*g in neonates: clinical manifestations and enzymatic and molecular diagnoses. Pediatrics *122*, 1003-1008.

Giordano, F.J. (2005). Oxygen, oxidative stress, hypoxia, and heart failure. The Journal of clinical investigation *115*, 500-508.

Gisselbrecht, S., Skeath, J.B., Doe, C.Q., and Michelson, A.M. (1996). *Heartless* encodes a fibroblast growth factor receptor (DFR1/DFGF-R2) involved in the directional migration of early mesodermal cells in the *Drosophila* embryo. Genes & development *10*, 3003-3017.

Griffin, K.J., Stoller, J., Gibson, M., Chen, S., Yelon, D., Stainier, D.Y., and Kimelman, D. (2000). A conserved role for H15-related T-box transcription factors in zebrafish and *Drosophila* heart formation. Developmental biology *218*, 235-247.

Gryzik, T., and Muller, H.A. (2004). FGF8-like1 and FGF8-like2 encode putative ligands of the FGF receptor Htl and are required for mesoderm migration in the *Drosophila* gastrula. Current biology : CB *14*, 659-667.

Guzy, R.D., Hoyos, B., Robin, E., Chen, H., Liu, L., Mansfield, K.D., Simon, M.C., Hammerling, U., and Schumacker, P.T. (2005). Mitochondrial complex III is required for hypoxia-induced ROS production and cellular oxygen sensing. Cell metabolism *1*, 401-408.
Halfon, M.S., Carmena, A., Gisselbrecht, S., Sackerson, C.M., Jimenez, F., Baylies, M.K., and Michelson, A.M. (2000). Ras pathway specificity is determined by the integration of multiple signal-activated and tissue-restricted transcription factors. Cell *103*, 63-74.
Han, Z., and Bodmer, R. (2003). Myogenic cells fates are antagonized by Notch only in asymmetric lineages of the *Drosophila* heart, with or without cell division. Development *130*, 3039-3051.
Han, Z., and Olson, E.N. (2005). *Hand* is a direct target of *Tinman* and GATA factors during *Drosophila* cardiogenesis and hematopoiesis. Development *132*, 3525-3536.
Han, Z., Yi, P., Li, X., and Olson, E.N. (2006). *Hand*, an evolutionarily conserved bHLH transcription factor required for *Drosophila* cardiogenesis and hematopoiesis. Development *133*, 1175-1182.
Hartenstein, A.Y., Rugendorff, A., Tepass, U., and Hartenstein, V. (1992). The function of the neurogenic genes during epithelial development in the *Drosophila* embryo. Development *116*, 1203-1220.
Hashimoto, Y., Niikura, T., Tajima, H., Yasukawa, T., Sudo, H., Ito, Y., Kita, Y., Kawasumi, M., Kouyama, K., Doyu, M.*, et al.* (2001). A rescue factor abolishing neuronal cell death by a wide spectrum of familial Alzheimer's disease genes and Abeta. Proceedings of the National Academy of Sciences of the United States of America *98*, 6336-6341.
Hou, Y., Ouyang, X., Wan, R., Cheng, H., Mattson, M.P., and Cheng, A. (2012). Mitochondrial superoxide production negatively regulates neural progenitor proliferation and cerebral cortical development. Stem cells *30*, 2535-2547.
Imam, F., Sutherland, D., Huang, W., and Krasnow, M.A. (1999). stumps, a *Drosophila* gene required for fibroblast growth factor (FGF)-directed migrations of tracheal and mesodermal cells. Genetics *152*, 307-318.
Ingraham, C.A., Burwell, L.S., Skalska, J., Brookes, P.S., Howell, R.L., Sheu, S.S., and Pinkert, C.A. (2009). NDUFS4: creation of a mouse model mimicking a Complex I disorder. Mitochondrion *9*, 204-210.

Ito, K., Hirao, A., Arai, F., Takubo, K., Matsuoka, S., Miyamoto, K., Ohmura, M., Naka, K., Hosokawa, K., Ikeda, Y., *et al.* (2006). Reactive oxygen species act through p38 MAPK to limit the lifespan of hematopoietic stem cells. Nature medicine *12*, 446-451.

Jagla, K., Frasch, M., Jagla, T., Dretzen, G., Bellard, F., and Bellard, M. (1997). ladybird, a new component of the cardiogenic pathway in *Drosophila* required for diversification of heart precursors. Development *124*, 3471-3479.

Jang, Y.Y., and Sharkis, S.J. (2007). A low level of reactive oxygen species selects for primitive hematopoietic stem cells that may reside in the low-oxygenic niche. Blood *110*, 3056-3063.

Jiang, J., Kosman, D., Ip, Y.T., and Levine, M. (1991). The dorsal morphogen gradient regulates the mesoderm determinant twist in early *Drosophila* embryos. Genes & development *5*, 1881-1891.

Jiang, Y., and Evans, T. (1996). The Xenopus GATA-4/5/6 genes are associated with cardiac specification and can regulate cardiac-specific transcription during embryogenesis. Developmental biology *174*, 258-270.

Jordan-Alvarez, S., Fouquet, W., Sigrist, S.J., and Acebes, A. (2012). Presynaptic PI3K activity triggers the formation of glutamate receptors at neuromuscular terminals of *Drosophila*. Journal of cell science *125*, 3621-3629.

Kaelin, W.G., Jr. (2005). The concept of synthetic lethality in the context of anticancer therapy. Nature reviews Cancer *5*, 689-698.

Kasahara, A., Cipolat, S., Chen, Y., Dorn, G.W., 2nd, and Scorrano, L. (2013). Mitochondrial fusion directs cardiomyocyte differentiation via calcineurin and Notch signaling. Science *342*, 734-737.

Kerber, B., Fellert, S., and Hoch, M. (1998). Seven-up, the *Drosophila* homolog of the COUP-TF orphan receptors, controls cell proliferation in the insect kidney. Genes & development *12*, 1781-1786.

Kim, K., Kim, I.H., Lee, K.Y., Rhee, S.G., and Stadtman, E.R. (1988). The isolation and purification of a specific "protector" protein which inhibits enzyme inactivation by a thiol/Fe(III)/O2 mixed-function oxidation system. The Journal of biological chemistry *263*, 4704-4711.

Kirkinezos, I.G., and Moraes, C.T. (2001). Reactive oxygen species and mitochondrial diseases. Seminars in cell & developmental biology *12*, 449-457.

Klinedinst, S.L., and Bodmer, R. (2003). Gata factor Pannier is required to establish competence for heart progenitor formation. Development *130*, 3027-3038.
Knirr, S., and Frasch, M. (2001). Molecular integration of inductive and mesoderm-intrinsic inputs governs even-skipped enhancer activity in a subset of pericardial and dorsal muscle progenitors. Developmental biology *238*, 13-26.
Knock, G.A., and Ward, J.P. (2011). Redox regulation of protein kinases as a modulator of vascular function. Antioxidants & redox signaling *15*, 1531-1547.
Kohli, L., and Passegue, E. (2014). Surviving change: the metabolic journey of hematopoietic stem cells. Trends in cell biology *24*, 479-487.
Komuro, I., and Izumo, S. (1993). Csx: a murine homeobox-containing gene specifically expressed in the developing heart. Proceedings of the National Academy of Sciences of the United States of America *90*, 8145-8149.
Kramer, S., West, S.R., and Hiromi, Y. (1995). Cell fate control in the *Drosophila* re*tin*a by the orphan receptor seven-up: its role in the decisions mediated by the ras signaling pathway. Development *121*, 1361-1372.
Kramer, S.G., Kidd, T., Simpson, J.H., and Goodman, C.S. (2001). Switching repulsion to attraction: changing responses to slit during transition in mesoderm migration. Science *292*, 737-740.
Kremser, T., Gajewski, K., Schulz, R.A., and Renkawitz-Pohl, R. (1999). *Tinman* regulates the transcription of the beta3 tubulin gene (betaTub60D) in the dorsal vessel of *Drosophila*. Developmental biology *216*, 327-339.
Kumar, V., Zhang, M.X., Swank, M.W., Kunz, J., and Wu, G.Y. (2005). Regulation of dendritic morphogenesis by Ras-PI3K-Akt-mTOR and Ras-MAPK signaling pathways. J Neurosci *25*, 11288-11299.
Lander, H.M., Ogiste, J.S., Teng, K.K., and Novogrodsky, A. (1995). p21ras as a common signaling target of reactive free radicals and cellular redox stress. The Journal of biological chemistry *270*, 21195-21198.
Larsson, N.G., Wang, J., Wilhelmsson, H., Oldfors, A., Rus*tin*, P., Lewandoski, M., Barsh, G.S., and Clayton, D.A. (1998). Mitochondrial transcription factor A is necessary for mtDNA maintenance and embryogenesis in mice. Nature genetics *18*, 231-236.

Laverriere, A.C., MacNeill, C., Mueller, C., Poelmann, R.E., Burch, J.B., and Evans, T. (1994). GATA-4/5/6, a subfamily of three transcription factors transcribed in developing heart and gut. The Journal of biological chemistry *269*, 23177-23184.

Lawrence, P.A., Bodmer, R., and Vincent, J.P. (1995). Segmental patterning of heart precursors in *Drosophila*. Development *121*, 4303-4308.

Lee, H.H., and Frasch, M. (2000). Wingless effects mesoderm patterning and ectoderm segmentation events via induction of its downstream target sloppy paired. Development *127*, 5497-5508.

Lee, S.J., Hwang, A.B., and Kenyon, C. (2010). Inhibition of respiration extends C. elegans life span via reactive oxygen species that increase HIF-1 activity. Current biology : CB *20*, 2131-2136.

Lee, S.R., Kwon, K.S., Kim, S.R., and Rhee, S.G. (1998a). Reversible inactivation of protein-tyrosine phosphatase 1B in A431 cells stimulated with epidermal growth factor. The Journal of biological chemistry *273*, 15366-15372.

Lee, Y., Shioi, T., Kasahara, H., Jobe, S.M., Wiese, R.J., Markham, B.E., and Izumo, S. (1998b). The cardiac tissue-restricted homeobox protein Csx/Nkx2.5 physically associates with the zinc finger protein GATA4 and cooperatively activates atrial natriuretic factor gene expression. Molecular and cellular biology *18*, 3120-3129.

Lep*tin*, M. (1991). twist and snail as positive and negative regulators during *Drosophila* mesoderm development. Genes & development *5*, 1568-1576.

Lev, D., Nissenkorn, A., Leshinsky-Silver, E., Sadeh, M., Zeharia, A., Garty, B.Z., Blieden, L., Barash, V., and Lerman-Sagie, T. (2004). Clinical presentations of mitochondrial cardiomyopathies. Pediatric cardiology *25*, 443-450.

Li, Y., Hiroi, Y., Ngoy, S., Okamoto, R., Noma, K., Wang, C.Y., Wang, H.W., Zhou, Q., Radtke, F., Liao, R.*, et al.* (2011). Notch1 in bone marrow-derived cells mediates cardiac repair after myocardial infarction. Circulation *123*, 866-876.

Liao, X., and Butow, R.A. (1993). RTG1 and RTG2: two yeast genes required for a novel path of communication from mitochondria to the nucleus. Cell *72*, 61-71.

Liao, X.S., Small, W.C., Srere, P.A., and Butow, R.A. (1991). Intramitochondrial functions regulate nonmitochondrial citrate synthase (CIT2) expression in Saccharomyces cerevisiae. Molecular and cellular biology *11*, 38-46.

Liberatore, C.M., Searcy-Schrick, R.D., Vincent, E.B., and Yutzey, K.E. (2002). Nkx-2.5 gene induction in mice is mediated by a Smad consensus regulatory region. Developmental biology *244*, 243-256.

Liesa, M., Palacin, M., and Zorzano, A. (2009). Mitochondrial dynamics in mammalian health and disease. Physiological reviews *89*, 799-845.

Lim, H.Y., Wang, W., Chen, J., Ocorr, K., and Bodmer, R. (2014). ROS regulate cardiac function via a distinct paracrine mechanism. Cell reports *7*, 35-44.

Lindsley, R.C., Gill, J.G., Kyba, M., Murphy, T.L., and Murphy, K.M. (2006). Canonical Wnt signaling is required for development of embryonic stem cell-derived mesoderm. Development *133*, 3787-3796.

Lints, T.J., Parsons, L.M., Hartley, L., Lyons, I., and Harvey, R.P. (1993). Nkx-2.5: a novel murine homeobox gene expressed in early heart progenitor cells and their myogenic descendants. Development *119*, 419-431.

Liu, J., Wu, Q., He, D., Ma, T., Du, L., Dui, W., Guo, X., and Jiao, R. (2011). *Drosophila* sbo regulates lifespan through its function in the synthesis of coenzyme Q in vivo. Journal of genetics and genomics = Yi chuan xue bao *38*, 225-234.

Liu, Z., and Butow, R.A. (2006). Mitochondrial retrograde signaling. Annual review of genetics *40*, 159-185.

Lockwood, W.K., and Bodmer, R. (2002). The patterns of wingless, decapentaplegic, and *Tinman* position the *Drosophila* heart. Mech Dev *114*, 13-26.

Lovato, T.L., Benjamin, A.R., and Cripps, R.M. (2005). Transcription of Myocyte enhancer factor-2 in adult *Drosophila* myoblasts is induced by the steroid hormone ecdysone. Developmental biology *288*, 612-621.

Lovato, T.L., Sensibaugh, C.A., Swingle, K.L., Mar*tin*ez, M.M., and Cripps, R.M. (2015). The *Drosophila* Transcription Factors *Tinman* and Pannier Activate and Collaborate with Myocyte Enhancer Factor-2 to Promote Heart Cell Fate. PloS one *10*, e0132965.

Lowell, S., Benchoua, A., Heavey, B., and Smith, A.G. (2006). Notch promotes neural lineage entry by pluripotent embryonic stem cells. PLoS Biol *4*, e121.

Mandal, L., Banerjee, U., and Hartenstein, V. (2004). Evidence for a fruit fly hemangioblast and similarities between lymph-gland hematopoiesis in fruit fly and mammal aorta-gonadal-mesonephros mesoderm. Nature genetics *36*, 1019-1023.

Mansfield, K.D., Guzy, R.D., Pan, Y., Young, R.M., Cash, T.P., Schumacker, P.T., and Simon, M.C. (2005). Mitochondrial dysfunction resulting from loss of cytochrome c impairs cellular oxygen sensing and hypoxic HIF-alpha activation. Cell metabolism *1*, 393-399.

Mar*tin*-Pena, A., Acebes, A., Rodriguez, J.R., Sorribes, A., de Polavieja, G.G., Fernandez-Funez, P., and Ferrus, A. (2006). Age-independent synaptogenesis by phosphoinositide 3 kinase. J Neurosci *26*, 10199-10208.

Maryanovich, M., and Gross, A. (2013). A ROS rheostat for cell fate regulation. Trends in cell biology *23*, 129-134.

Mast, J.D., Tomalty, K.M., Vogel, H., and Clandinin, T.R. (2008). Reactive oxygen species act remotely to cause synapse loss in a *Drosophila* model of developmental mitochondrial encephalopathy. Development *135*, 2669-2679.

McFadden, D.G., Charite, J., Richardson, J.A., Srivastava, D., Firulli, A.B., and Olson, E.N. (2000). A GATA-dependent right ventricular enhancer controls d*HAND* transcription in the developing heart. Development *127*, 5331-5341.

Medioni, C., Astier, M., Zmojdzian, M., Jagla, K., and Semeriva, M. (2008). Genetic control of cell morphogenesis during *Drosophila* melanogaster cardiac tube formation. J Cell Biol *182*, 249-261.

Melkani, G.C., Trujillo, A.S., Ramos, R., Bodmer, R., Bernstein, S.I., and Ocorr, K. (2013). Hun*tin*gton's disease induced cardiac amyloidosis is reversed by modula*tin*g protein folding and oxidative stress pathways in the *Drosophila* heart. PLoS genetics *9*, e1004024.

Michelson, A.M., Gisselbrecht, S., Buff, E., and Skeath, J.B. (1998). Heartbroken is a specific downstream mediator of FGF receptor signalling in *Drosophila*. Development *125*, 4379-4389.

Migliaccio, E., Giorgio, M., Mele, S., Pelicci, G., Reboldi, P., Pandolfi, P.P., Lanfrancone, L., and Pelicci, P.G. (1999). The p66shc adaptor protein controls oxidative stress response and life span in mammals. Nature *402*, 309-313.

Milton, V.J., Jarrett, H.E., Gowers, K., Chalak, S., Briggs, L., Robinson, I.M., and Sweeney, S.T. (2011). Oxidative stress induces overgrowth of the *Drosophila* neuromuscular junction. Proceedings of the National Academy of Sciences of the United States of America *108*, 17521-17526.

Milton, V.J., and Sweeney, S.T. (2012). Oxidative stress in synapse development and function. Dev Neurobiol *72*, 100-110.

Monnier, V., Iche-Torres, M., Rera, M., Contremoulins, V., Guichard, C., Lalevee, N., Tricoire, H., and Perrin, L. (2012). dJun and Vri/dNFIL3 are major regulators of cardiac aging in *Drosophila*. PLoS genetics *8*, e1003081.

Muliyil, S., and Narasimha, M. (2014). Mitochondrial ROS regulates cytoskeletal and mitochondrial remodeling to tune cell and tissue dynamics in a model for wound healing. Developmental cell *28*, 239-252.

Mumm, J.S., and Kopan, R. (2000). Notch signaling: from the outside in. Developmental biology *228*, 151-165.

Nakahira, K., Haspel, J.A., Rathinam, V.A., Lee, S.J., Dolinay, T., Lam, H.C., Englert, J.A., Rabinovitch, M., Cernadas, M., Kim, H.P.*, et al.* (2011). Autophagy proteins regulate innate immune responses by inhibi*tin*g the release of mitochondrial DNA mediated by the NALP3 inflammasome. Nature immunology *12*, 222-230.

Niikura, T., Chiba, T., Aiso, S., Matsuoka, M., and Nishimoto, I. (2004). Humanin: after the discovery. Molecular neurobiology *30*, 327-340.

Nishioka, K., Vilarino-Guell, C., Cobb, S.A., Kachergus, J.M., Ross, O.A., Hentati, E., Hentati, F., and Farrer, M.J. (2010). Genetic variation of the mitochondrial complex I subunit NDUFV2 and Parkinson's disease. Parkinsonism Relat Disord *16*, 686-687.

Nooter, K., Overdevest, J., Dubbes, R., Koch, G., Bentvelzen, P., Zurcher, C., Coolen, J., and Calafat, J. (1978). Type-C oncovirus isolate from human leukemic bone marrow: further in vitro and in vivo characterization. International journal of cancer *21*, 27-34.

Owusu-Ansah, E., and Banerjee, U. (2009). Reactive oxygen species prime *Drosophila* haematopoietic progenitors for differentiation. Nature *461*, 537-541.

Owusu-Ansah, E., Song, W., and Perrimon, N. (2013). Muscle mitohormesis promotes longevity via systemic repression of insulin signaling. Cell *155*, 699-712.

Owusu-Ansah, E., Yavari, A., Mandal, S., and Banerjee, U. (2008). Distinct mitochondrial retrograde signals control the G1-S cell cycle checkpoint. Nature genetics *40*, 356-361.

Pan, D.J., Huang, J.D., and Courey, A.J. (1991). Functional analysis of the *Drosophila* twist promoter reveals a dorsal-binding ventral activator region. Genes & development *5*, 1892-1901.

Parikh, V.S., Morgan, M.M., Scott, R., Clements, L.S., and Butow, R.A. (1987). The mitochondrial genotype can influence nuclear gene expression in yeast. Science *235*, 576-580.

Park, M., Wu, X., Golden, K., Axelrod, J.D., and Bodmer, R. (1996). The wingless signaling pathway is directly involved in *Drosophila* heart development. Developmental biology *177*, 104-116.

Park, M., Yaich, L.E., and Bodmer, R. (1998). Mesodermal cell fate decisions in *Drosophila* are under the control of the lineage genes numb, Notch, and sanpodo. Mech Dev *75*, 117-126.

Peterson, C., Ailes, E., Riehle-Colarusso, T., Oster, M.E., Olney, R.S., Cassell, C.H., Fixler, D.E., Carmichael, S.L., Shaw, G.M., and Gilboa, S.M. (2014). Late detection of critical congenital heart disease among US infants: estimation of the potential impact of proposed universal screening using pulse oximetry. JAMA Pediatr *168*, 361-370.

Ponzielli, R., Astier, M., Chartier, A., Gallet, A., Therond, P., and Semeriva, M. (2002). Heart tube patterning in *Drosophila* requires integration of axial and segmental information provided by the Bithorax Complex genes and *hedgehog* signaling. Development *129*, 4509-4521.

Postigo, A.A., Ward, E., Skeath, J.B., and Dean, D.C. (1999). zfh-1, the *Drosophila* homologue of ZEB, is a transcriptional repressor that regulates somatic myogenesis. Molecular and cellular biology *19*, 7255-7263.

Puceat, M. (2005). Role of Rac-GTPase and reactive oxygen species in cardiac differentiation of stem cells. Antioxidants & redox signaling *7*, 1435-1439.

Qian, L., Liu, J., and Bodmer, R. (2005). Slit and Robo control cardiac cell polarity and morphogenesis. Current biology : CB *15*, 2271-2278.

Ranganayakulu, G., Elliott, D.A., Harvey, R.P., and Olson, E.N. (1998). Divergent roles for NK-2 class homeobox genes in cardiogenesis in flies and mice. Development *125*, 3037-3048.

Ranganayakulu, G., Zhao, B., Dokidis, A., Molken*tin*, J.D., Olson, E.N., and Schulz, R.A. (1995). A series of mutations in the D-*MEF2* transcription factor reveal multiple functions in larval and adult myogenesis in *Drosophila*. Developmental biology *171*, 169-181.

Raza, Q.S., Vanderploeg, J.L., and Jacobs, J.R. (2017). Matrix Metalloproteinases are required for membrane motility and lumenogenesis during *Drosophila* heart development. PloS one *12*, e0171905.

Reddy, V.M., Meyrick, B., Wong, J., Khoor, A., Liddicoat, J.R., Hanley, F.L., and Fineman, J.R. (1995). In utero placement of aortopulmonary shunts. A model of postnatal pulmonary hypertension with increased pulmonary blood flow in lambs. Circulation *92*, 606-613.

Reiling, J.H., and Hafen, E. (2004). The hypoxia-induced paralogs Scylla and Charybdis inhibit growth by down-regulating S6K activity upstream of TSC in *Drosophila*. Genes & development *18*, 2879-2892.
Reim, I., and Frasch, M. (2005). The *Dorsocross* T-box genes are key components of the regulatory network controlling early cardiogenesis in *Drosophila*. Development *132*, 4911-4925.
Reim, I., and Frasch, M. (2010). Genetic and genomic dissection of cardiogenesis in the *Drosophila* model. Pediatric cardiology *31*, 325-334.
Rossant, J., Ciruna, B., and Partanen, J. (1997). FGF signaling in mouse gastrulation and anteroposterior patterning. Cold Spring Harb Symp Quant Biol *62*, 127-133.
Roth, S., Stein, D., and Nusslein-Volhard, C. (1989). A gradient of nuclear localization of the dorsal protein determines dorsoventral pattern in the *Drosophila* embryo. Cell *59*, 1189-1202.
Rotstein, B., and Paululat, A. (2016). On the Morphology of the *Drosophila* Heart. J Cardiovasc Dev Dis *3*.
Rugendorff, A., Younossi-Hartenstein, A., and Hartenstein, V. (1994). Embryonic origin and differentiation of the *Drosophila* heart. Roux's archives of developmental biology : the official organ of the EDBO *203*, 266-280.
Rushlow, C.A., Han, K., Manley, J.L., and Levine, M. (1989). The graded distribution of the dorsal morphogen is initiated by selective nuclear transport in *Drosophila*. Cell *59*, 1165-1177.
Ryan, K.M., Hendren, J.D., Helander, L.A., and Cripps, R.M. (2007). The NK homeodomain transcription factor *Tinman* is a direct activator of seven-up in the *Drosophila* dorsal vessel. Developmental biology *302*, 694-702.
Salmeen, A., Andersen, J.N., Myers, M.P., Meng, T.C., Hinks, J.A., Tonks, N.K., and Barford, D. (2003). Redox regulation of protein tyrosine phosphatase 1B involves a sulphenyl-amide intermediate. Nature *423*, 769-773.
Santiago-Mar*tin*ez, E., Soplop, N.H., and Kramer, S.G. (2006). Lateral positioning at the dorsal midline: Slit and Roundabout receptors guide *Drosophila* heart cell migration. Proceedings of the National Academy of Sciences of the United States of America *103*, 12441-12446.
Sanyal, S., Sandstrom, D.J., Hoeffer, C.A., and Ramaswami, M. (2002). AP-1 functions upstream of CREB to control synaptic plasticity in *Drosophila*. Nature *416*, 870-874.

Sauer, H., Rahimi, G., Hescheler, J., and Wartenberg, M. (2000). Role of reactive oxygen species and phosphatidylinositol 3-kinase in cardiomyocyte differentiation of embryonic stem cells. FEBS letters *476*, 218-223.

Scherz-Shouval, R., Shvets, E., Fass, E., Shorer, H., Gil, L., and Elazar, Z. (2007). Reactive oxygen species are essential for autophagy and specifically regulate the activity of Atg4. The EMBO journal *26*, 1749-1760.

Scheubel, R.J., Tostlebe, M., Simm, A., Rohrbach, S., Prondzinsky, R., Gellerich, F.N., Silber, R.E., and Holtz, J. (2002). Dysfunction of mitochondrial respiratory chain complex I in human failing myocardium is not due to disturbed mitochondrial gene expression. Journal of the American College of Cardiology *40*, 2174-2181.

Schmelter, M., Ateghang, B., Helmig, S., Wartenberg, M., and Sauer, H. (2006). Embryonic stem cells utilize reactive oxygen species as transducers of mechanical strain-induced cardiovascular differentiation. FASEB journal : official publication of the Federation of American Societies for Experimental Biology *20*, 1182-1184.

Schroeder, T., Fraser, S.T., Ogawa, M., Nishikawa, S., Oka, C., Bornkamm, G.W., Nishikawa, S., Honjo, T., and Just, U. (2003). Recombination signal sequence-binding protein Jkappa alters mesodermal cell fate decisions by suppressing cardiomyogenesis. Proceedings of the National Academy of Sciences of the United States of America *100*, 4018-4023.

Schultheiss, T.M., Burch, J.B., and Lassar, A.B. (1997). A role for bone morphogenetic proteins in the induction of cardiac myogenesis. Genes & development *11*, 451-462.

Schwartz, R.J., and Olson, E.N. (1999). Building the heart piece by piece: modularity of cis-elements regulating Nkx2-5 transcription. Development *126*, 4187-4192.

Sellin, J., Drechsler, M., Nguyen, H.T., and Paululat, A. (2009). Antagonistic function of Lmd and *Zfh1* fine tunes cell fate decisions in the Twi and *Tin* positive mesoderm of *Drosophila* melanogaster. Developmental biology *326*, 444-455.

Sepulveda, J.L., Belaguli, N., Nigam, V., Chen, C.Y., Nemer, M., and Schwartz, R.J. (1998). GATA-4 and Nkx-2.5 coactivate Nkx-2 DNA binding targets: role for regulating early cardiac gene expression. Molecular and cellular biology *18*, 3405-3415.

Sharma, S., Aramburo, A., Rafikov, R., Sun, X., Kumar, S., Oishi, P.E., Datar, S.A., Raff, G., Xoinis, K., Kalkan, G.*, et al.* (2013). L-carni*tin*e preserves endothelial function in a lamb model of increased pulmonary blood flow. Pediatric research *74*, 39-47.

Shishido, E., Ono, N., Kojima, T., and Saigo, K. (1997). Requirements of DFR1/*Heartless*, a mesoderm-specific *Drosophila* FGF-receptor, for the formation of heart, visceral and somatic muscles, and ensheathing of longitudinal axon tracts in CNS. Development *124*, 2119-2128.
Somi, S., Buffing, A.A., Moorman, A.F., and Van Den Hoff, M.J. (2004). Dynamic patterns of expression of BMP isoforms 2, 4, 5, 6, and 7 during chicken heart development. Anat Rec A Discov Mol Cell Evol Biol *279*, 636-651.
Song, W., Owusu-Ansah, E., Hu, Y., Cheng, D., Ni, X., Zirin, J., and Perrimon, N. (2017). Activin signaling mediates muscle-to-adipose communication in a mitochondria dysfunction-associated obesity model. Proceedings of the National Academy of Sciences of the United States of America.
Srinivasan, V., Kriete, A., Sacan, A., and Jazwinski, S.M. (2010). Comparing the yeast retrograde response and NF-kappaB stress responses: implications for aging. Aging cell *9*, 933-941.
Srivastava, D., and Olson, E.N. (2000). A genetic blueprint for cardiac development. Nature *407*, 221-226.
Stathopoulos, A., Tam, B., Ronshaugen, M., Frasch, M., and Levine, M. (2004). *Pyramus* and *Thisbe*: FGF genes that pattern the mesoderm of *Drosophila* embryos. Genes & development *18*, 687-699.
Steward, R. (1989). Relocalization of the dorsal protein from the cytoplasm to the nucleus correlates with its function. Cell *59*, 1179-1188.
Sugden, P.H., and Clerk, A. (2006). Oxidative stress and growth-regulating intracellular signaling pathways in cardiac myocytes. Antioxidants & redox signaling *8*, 2111-2124.
Sundaresan, M., Yu, Z.X., Ferrans, V.J., Irani, K., and Finkel, T. (1995). Requirement for generation of H2O2 for platelet-derived growth factor signal transduction. Science *270*, 296-299.
Thisse, C., Perrin-Schmitt, F., Stoetzel, C., and Thisse, B. (1991). Sequence-specific transactivation of the *Drosophila* twist gene by the dorsal gene product. Cell *65*, 1191-1201.
Tormos, K.V., Anso, E., Hamanaka, R.B., Eisenbart, J., Joseph, J., Kalyanaraman, B., and C*Hand*el, N.S. (2011). Mitochondrial complex III ROS regulate adipocyte differentiation. Cell metabolism *14*, 537-544.

Torti, S.V., Akimoto, H., Lin, K., Billingham, M.E., and Torti, F.M. (1998). Selective inhibition of muscle gene expression by oxidative stress in cardiac cells. Journal of molecular and cellular cardiology *30*, 1173-1180.

Tsatmali, M., Walcott, E.C., and Crossin, K.L. (2005). Newborn neurons acquire high levels of reactive oxygen species and increased mitochondrial proteins upon differentiation from progenitors. Brain research *1040*, 137-150.

Vanderploeg, J., Vazquez Paz, L.L., MacMullin, A., and Jacobs, J.R. (2012). Integrins are required for cardioblast polarisation in *Drosophila*. BMC developmental biology *12*, 8.

Vincent, S., Wilson, R., Coelho, C., Affolter, M., and Lep*tin*, M. (1998). The *Drosophila* protein Dof is specifically required for FGF signaling. Molecular cell *2*, 515-525.

Volk, T., Wang, S., Rotstein, B., and Paululat, A. (2014). Matricellular proteins in development: perspectives from the *Drosophila* heart. Matrix Biol *37*, 162-166.

Wallace, D.C., and Fan, W. (2009). The pathophysiology of mitochondrial disease as modeled in the mouse. Genes & development *23*, 1714-1736.

Walton, N.M., Shin, R., Tajinda, K., Heusner, C.L., Kogan, J.H., Miyake, S., Chen, Q., Tamura, K., and Matsumoto, M. (2012). Adult neurogenesis transiently generates oxidative stress. PloS one *7*, e35264.

Wang, J., Tao, Y., Reim, I., Gajewski, K., Frasch, M., and Schulz, R.A. (2005). Expression, regulation, and requirement of the toll transmembrane protein during dorsal vessel formation in *Drosophila* melanogaster. Molecular and cellular biology *25*, 4200-4210.

Ward, E.J., and Skeath, J.B. (2000). Characterization of a novel subset of cardiac cells and their progenitors in the *Drosophila* embryo. Development *127*, 4959-4969.

Wilmes, A.C., Klinke, N., Rotstein, B., Meyer, H., and Paululat, A. (2018). Biosynthesis and assembly of the Collagen IV-like protein *Pericardin* in *Drosophila* melanogaster. Biol Open *7*.

Wisotzkey, R.G., Mehra, A., Sutherland, D.J., Dobens, L.L., Liu, X., Dohrmann, C., Attisano, L., and Raftery, L.A. (1998). Medea is a *Drosophila* Smad4 homolog that is differentially required to potentiate *DPP* responses. Development *125*, 1433-1445.

Wong, J.L., Creton, R., and Wessel, G.M. (2004). The oxidative burst at fertilization is dependent upon activation of the dual oxidase Udx1. Developmental cell *7*, 801-814.

Wong, K., Park, H.T., Wu, J.Y., and Rao, Y. (2002). Slit proteins: molecular guidance cues for cells ranging from neurons to leukocytes. Curr Opin Genet Dev *12*, 583-591.

Wren, C., Reinhardt, Z., and Khawaja, K. (2008). Twenty-year trends in diagnosis of life-threatening neonatal cardiovascular malformations. Archives of disease in childhood Fetal and neonatal edition *93*, F33-35.

Wu, J., Niu, J., Li, X., Wang, X., Guo, Z., and Zhang, F. (2014). TGF-beta1 induces senescence of bone marrow mesenchymal stem cells via increase of mitochondrial ROS production. BMC developmental biology *14*, 21.

Wu, X., Golden, K., and Bodmer, R. (1995). Heart development in *Drosophila* requires the segment polarity gene wingless. Developmental biology *169*, 619-628.

Xia, Y., Dobaczewski, M., Gonzalez-Quesada, C., Chen, W., Biernacka, A., Li, N., Lee, D.W., and Frangogiannis, N.G. (2011). Endogenous thrombospondin 1 protects the pressure-overloaded myocardium by modula*tin*g fibroblast phenotype and matrix metabolism. Hypertension *58*, 902-911.

Xu, X., Yin, Z., Hudson, J.B., Ferguson, E.L., and Frasch, M. (1998). Smad proteins act in combination with synergistic and antagonistic regulators to target *Dpp* responses to the *Drosophila* mesoderm. Genes & development *12*, 2354-2370.

Yakes, F.M., and Van Houten, B. (1997). Mitochondrial DNA damage is more extensive and persists longer than nuclear DNA damage in human cells following oxidative stress. Proceedings of the National Academy of Sciences of the United States of America *94*, 514-519.

Yamaguchi, T.P., Conlon, R.A., and Rossant, J. (1992). Expression of the fibroblast growth factor receptor FGFR-1/flg during gastrulation and segmentation in the mouse embryo. Developmental biology *152*, 75-88.

Yaplito-Lee, J., Weintraub, R., Jamsen, K., Chow, C.W., Thorburn, D.R., and Boneh, A. (2007). Cardiac manifestations in oxidative phosphorylation disorders of childhood. The Journal of pediatrics *150*, 407-411.

Yin, Z., and Frasch, M. (1998). Regulation and function of *Tinman* during dorsal mesoderm induction and heart specification in *Drosophila*. Developmental genetics *22*, 187-200.

Yin, Z., Xu, X.L., and Frasch, M. (1997). Regulation of the twist target gene *Tinman* by modular cis-regulatory elements during early mesoderm development. Development *124*, 4971-4982.

Zaffran, S., Astier, M., Gratecos, D., Guillen, A., and Semeriva, M. (1995). Cellular interactions during heart morphogenesis in the *Drosophila* embryo. Biology of the cell *84*, 13-24.

Zaffran, S., and Frasch, M. (2002). Early signals in cardiac development. Circulation research *91*, 457-469.

Zaffran, S., Reim, I., Qian, L., Lo, P.C., Bodmer, R., and Frasch, M. (2006). Cardioblast-intrinsic *Tinman* activity controls proper diversification and differentiation of myocardial cells in *Drosophila*. Development *133*, 4073-4083.

Zhao, W., Zhao, T., Chen, Y., Ahokas, R.A., and Sun, Y. (2008). Oxidative stress mediates cardiac fibrosis by enhancing transforming growth factor-beta1 in hypertensive rats. Molecular and cellular biochemistry *317*, 43-50.

Zhou, G., Dada, L.A., Wu, M., Kelly, A., Trejo, H., Zhou, Q., Varga, J., and Sznajder, J.I. (2009). Hypoxia-induced alveolar epithelial-mesenchymal transition requires mitochondrial ROS and hypoxia-inducible factor 1. American journal of physiology Lung cellular and molecular physiology *297*, L1120-1130.

Zhou, R., Yazdi, A.S., Menu, P., and Tschopp, J. (2011). A role for mitochondria in NLRP3 inflammasome activation. Nature *469*, 221-225.

Zwart, M.F., Randlett, O., Evers, J.F., and Landgraf, M. (2013). Dendritic growth gated by a steroid hormone receptor underlies increases in activity in the developing *Drosophila* locomotor system. Proceedings of the National Academy of Sciences of the United States of America *110*, E3878-3887.